The Norwegian College of Fishery Science, UiT The Arctic University of Norway

Expression of Secondary Metabolite Gene Clusters and Production of Secondary Metabolites in Three *Nostoc* strains Subjected to Deprivation on Nutrients and Competition.

Oda Sofie Bye Wilhelmsen

Master thesis in Marine Biotechnology (May 2019)
60 credits

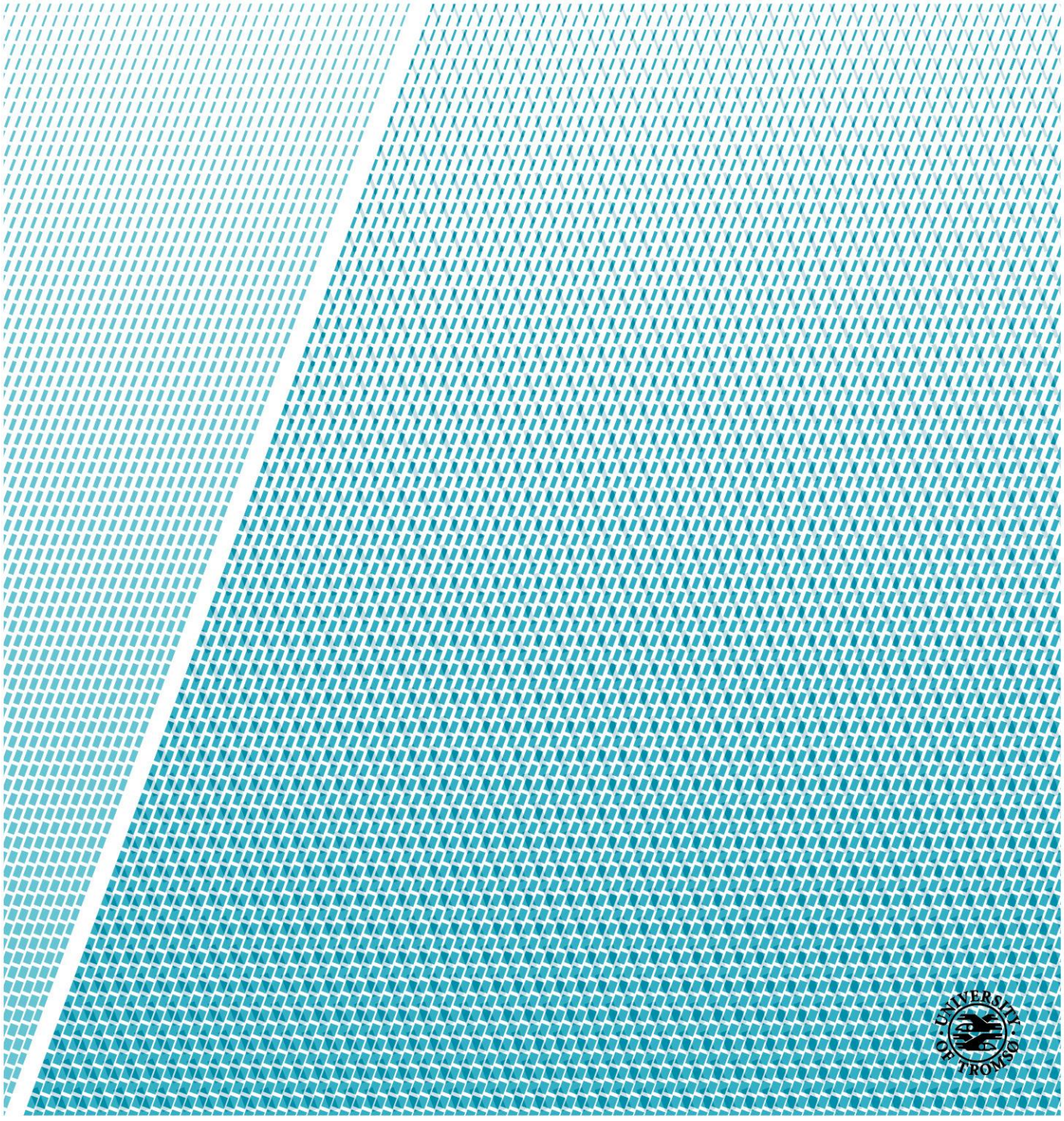

Acknowledgments

This master thesis was conducted at the Artic Marine Biology Institute in collaboration with Marbio, Norwegian College of Fisheries. The project lasted from January 2017 until June 2019 and concluded my master's degree in Marine Biotechnology at UiT The Arctic University of Norway. I would like to thank my supervisors: Anton Liaimer and Espen Hansen. Special thanks to Anton Liaimer who has been there for all my hurdles along the way. Thanks to Rigmor Reiersen and Bente Lindgård for all your technical support. To my significant other, family and friends, thanks for all your love and support. And finally, thanks to all my fellow students for five great years.

Tromsø, May 2019

Oda Sofie Bye Wilhelmsen

Abstract

Cyanobacteria are a unique source of natural products, where most of them are synthesized by non-ribosomal peptide synthase, polyketide synthase, or a hybrid of these pathways. The identification of such biosynthetic genes responsible for the production of secondary metabolites is still a relatively unexplored area, and it remains many natural products for which a biosynthetic origin is unknown. Secondary metabolites from marine cyanobacteria have gained much attention the last decades, however few comprehensive studies on secondary metabolites and their biosynthetic gene clusters from terrestrial cyanobacteria have been conducted.

Three terrestrial *Nostoc* spp. KVJ20, KVJ2, and KVJ10 were recently sequenced which allowed us to conduct genome-wide predictions by AntiSMASH of their potential to produce secondary metabolites. These strains were subjected to various cultivation conditions including nutrient limitations and competition. Gene expression analysis by RT-qPCR of predicted gene clusters and the production of secondary metabolites by UPLC-HR-MS were conducted. Analysis of gene expression patterns revealed higher expression of several NRPS, PKS and RiPP genes in nutrient-deprived media, as well as confirming the present known function of the housekeeping genes; *NifH*, *Gvp*C, and *PilT*. Most of the secondary metabolites found by UPLC-HR-MS were not identified, however a variety of Nostocyclopeptides, Suomilide/Banyaside-like peptides, Anabaenopeptins, as well as Aeruginosin, Hapalosin, and Nosperin were recorded from extracts of the respective strains. The results from this thesis give valuable knowledge for further cultivation of terrestrial cyanobacteria, with the purpose of awaking cryptic gene clusters and identifying novel secondary metabolites. We have also suggested conditions most suitable for enrichment for identified compounds.

Table of content

Abbreviations

Aer	Aeruginosin
Apt	Anabaenopeptin
AvaK	Akinete marker gene
cDNA	Complementary DNA
dNTP	Deoxyribonucleotide triphosphate
ESI	Electrospray ionization
FC	Fold Change
GvpC	Gas vesicle marker gene
Hap	Hapalosin
Hgl	Heterocyst glycolipids
KVJ10	*Nostoc* sp. KVJ10
KVJ2	*Nostoc* sp. KVJ2
KVJ20	*Nostoc* sp. KVJ20
Lan	Lanthipeptide
m/z	Mass-to-Charge
MDR	Multidrug-Resistant
Mvd	Microviridin
MQ	Milli-Q Ultrapure Water
NCBI	National Center for Biotechnology Information
Ncp	Nostocyclopeptide
Ngn	Nostoginin
NifH	Nitrogen fixation marker gene
NRPS	Non-ribosomal peptide synthases
Nsp	Nosperin
PilT	Twitching motility marker gene
PKS	Polyketide Synthases
qTOF	Quadrupole Time-of-Flight
RiPP	Post ribosomally and post-translationally produced peptides
RT	Retention time
RT-qPCR	Reverse transcriptase-quantitative polymerase chain reaction
S/B	Suomilide/Banyaside
Sid	Siderophore
TIC	Total Ion Chromatogram
UPLC-HR-MS	Ultra-Performance Liquid Chromatography-High resolution-Mass spectrometry
Val-Val	Valine-Valine bounds
n.d	Not detected

Introduction

A prokaryote with photosynthesis – The cyanobacteria

Among the oldest organism on the earth, we find the cyanobacteria. Fossils of these unique microorganisms have been dated back to between 1,8 billion and 2,5 billion years ago (Rasmussen et al., 2008; Schirrmeister et al., 2011), and today they are one of the largest and most significant group of bacteria inhabiting the earth.

The cyanobacteria have contributed to developing the earth as we know it, and their production of oxygen helped oxygenate the earth about 2.5 billion years ago and contributed to making the earth inhabitable for bigger organisms like ourselves. They completely altered the course of evolution by the development of aerobic respiration, thus giving life to more complex lifeforms (Soo et al., 2017).

A well-known theory supposes that in the late Proterozoic era or the early Cambrian Period the cyanobacteria began to occupy some eukaryote cells, making nutrient supplies for the eukaryote host in exchange for shelter. This is known as the endosymbiosis theory and supposes that the chloroplast in algae and plants originated from endosymbiotic cyanobacteria (Martin et al., 2015).

Cyanobacteria are often referred to as blue-green algae, and by eye resembles algae, but they are recognized as a major group of bacteria distinguished from other photosynthetic bacteria by their nature of their pigment system and by their performance of aerobic photosynthesis. Even though they, in fact, are not algae, they show some similar features with algae and plants by having chlorophyll *a* and photosynthesis which leads to the development of oxygen (Stanier et al., 1971).

Cyanobacteria consist of oxygenic photosynthetic prokaryote which has two photosystems (PSII and PSI), with H_2O as photo reductant in the photosynthesis. All known cyanobacteria are photoautotrophic, which use CO_2 as carbon source. The photopigments characteristic of cyanobacteria are chlorophyll a, phycobiliproteins (C-phycocyanin, *allo*-phycocyanin, and in some strains phycoerythrin), and in a variable array of carotenoids (O'Carra et al., 1980). Where chlorophyll *a* and phycobiliproteins are their primary photosynthetic pigments (Waterbury, 2006)

Morphology

Throughout their long evolutionary history, the cyanobacteria have diversified into a variety of species with various morphologies, niche habitats and having unique interactions with other organisms (Foster et al., 2011; Freeman & Thacker, 2011). Cyanobacteria are developmentally and morphologically one of the most diverse groups of Prokaryotes, including unicellular, surface-attached, filamentous colony- and mat-forming species (Castenholz et al., 2001)

They range from simple unicellular forms, that reproduce by binary fission to complex filamentous forms that possess a variety of highly differentiated cell types, some forms are even capable of true branching (Gugger & Hoffmann, 2004; Schirrmeister et al., 2011). The recognition of cyanobacteria is mainly based on differences in the structure and development of five large sub-groups. These sub-groups do not, for the most part, correspond precisely to major taxa now recognized by phycologists; the sub-groups are defined as section I-V, section I-II include the unicellular cyanobacteria, and III-V include filamentous cyanobacteria (Castenholz, 2015)

Members belonging to the section I form single cells and reproduce by binary fission or buddying and include members of the genus *Synechocystis*. Members belonging to section II either only reproduce by multiple fission, or by both binary fission and multiple fission, which gives rise to small daughter cells (baeocytes) and include members of the genus *Dermocarpa* and *Xenococcus* (Rippka et al., 1979).

While the filamentous cyanobacteria fill up section III, IV and section V, and they all consist of chains of cells called trichomes. In section III the trichrome is always composed of only vegetative cells, and division happens only on one plane for example, members of the genus *Spirulina* (Rippka et al., 1979). In section IV and V, the trichome will contain other specialized cells, like the heterocyst in the absence of combined nitrogen. The members of section IV divide on only one plane and include members of the genus *Nostoc*, *Anabaena* and *Cylindrospermum*. The members of section V divide on more than one plane and include members of the genus's *Fischerella* and *Chlorogloeopsis* (Rippka et al., 1979).

Nutrition

Cyanobacteria are photoautotrophic, using a photosynthetic apparatus that carries out oxygenic plantlike photosynthesis with chlorophyll *a* as the primary photosynthetic pigment, and phycobiliproteins as auxiliary light-harvesting pigments (Waterbury, 2006).

Cyanobacteria are also capable of mixotrophy, a process in which a variety of organic compounds, such as amino acids, that can not serve as sole carbon sources, are assimilated as a supplement to autotrophic CO_2 fixation (Chojnacka & Noworyta, 2004; Mitra & Flynn, 2010). Many free-living cyanobacteria can fix dinitrogen, which permits them to exploit habitats low in combined nitrogen. The nitrogenase enzyme system responsible for the fixation of dinitrogen, is sensitive to oxygen, hence some of the filamentous cyanobacteria (IV-V) has developed highly differentiated cells, known as heterocysts where the fixation takes place. Since the nitrogenase enzyme is sensitive to oxygen, the heterocysts also lack the ability to carry out oxygenic photosynthesis (Waterbury, 2006).

Since the cyanobacteria are photoautotrophs, they can be grown in simple mineral media, supplemented with essential nutrients to support cell growth, such as sources of nitrogen, phosphorus and trace elements (Waterbury, 2006). Because of their minimum demand of nutrients, cyanobacteria can inhabit several diverse environments included extreme ones (Liengen & Olsen, 1997; Pushkareva et al., 2018).

Habitats

In addition to inhabiting a diverse range of aquatic, terrestrial and marine habitats, cyanobacteria are also commonly found in more extreme environments; in Antarctica where they are found as cryptoendoliths in rocks (Blackhurst et al., 2005), in the dry desert (Potts & Friedmann, 1981), in thermophilic lakes (Steunou et al., 2006), as well as unlikely habitats for phototrophs, such as Lava Caves (Saw et al., 2013). Most cyanobacteria are mesophilic and live in environments where the temperature range from freezing temperatures to 40°C. However, their typical growth optimum is between 20 – 35°C and the maximum temperature for growth is typically below 45°C (Waterbury, 2006).

In addition to the diverse habitats occupied by free-living forms, both unicellular and filamentous cyanobacteria occur in symbioses with other prokaryotes, eukaryotic protist, metazoan and plants (Adams et al., 2013; Meeks, 1998). The cyanobacteria can inhabit different plant organs or tissues either intracellularly or externally (Santi et al., 2013). The ability of cyanobacteria to fix dinitrogen often plays an important role in these associations

(Meeks, 1998), where the plant acquires reduced nitrogen (N) from the cyanobacterial N_2-fixation, whereas the cyanobacteria have shelter and are supplied with reduced carbon and other nutrients from the host (Rai et al., 2000). When nitrogen-fixation bacteria enter a symbiotic relation, both their morphology and their physiology changes dramatically. These changes involve primary a 5-10-fold increase in differentiation-rate of motile filaments called hormogonia, and of heterocysts in vegetative filaments that evolves from hormogonia (Rodgers & Stewart, 1977).

Nostocales

Multicellular nitrogen-fixing cyanobacteria of the genus *Nostoc* are a common component of terrestrial microbial communities in a wide range of habitats, including subpolar and hot arid zones. Growth of *Nostoc* strains in both terrestrial and aquatic habitats often occur as filaments inside a gelatinous matrix (Dodds et al., 1995).

Nostoc strains are nitrogen-fixating cyanobacteria belonging to the *Nostocaceae* family in the order Nostocales. Members of the order Nostocales belong to section IV, characterized as filamentous cyanobacteria with the ability to divide on one plane (Castenholz & Waterbury, 1989). Differentiation in Nostocales may result in the production of different types of specialized cells; 1) heterocyst, 2) akinetes 3) hormogonia, specialized reproductive trichrome whose cells are morphologically different from vegetative cells, 4) tapered trichrome (Rippka et al., 1979; Waterbury, 2006). *Nostoc* is characterized by versatile physiology and displays one of the most complex life cycles among bacteria (Liaimer et al., 2016), as shown in Figure 1.

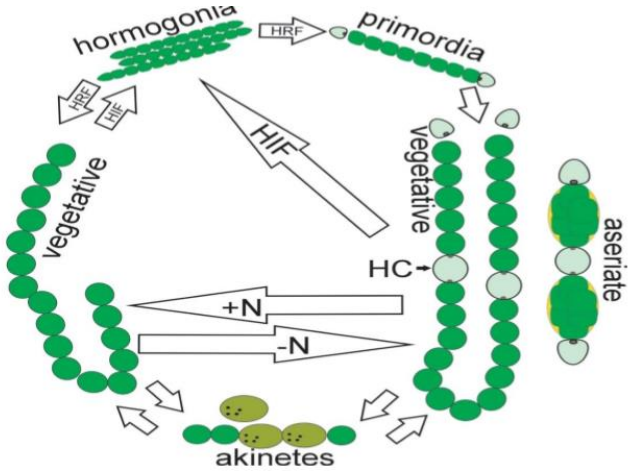

Figure 1: The lifecycle of Nostoc. Abbreviations: HC-Heterocyst, HIF-Hormogon Inducing Factors, HRF-Hormogon Repressing Factor. Illustration courtesy of Anton Liaimer.

Nitrogen fixation in these microorganisms is confined to specialized cells, heterocysts, which appear in semi-regular pattern between chains of vegetative cells, in response to a shortage of combined nitrogen in the environment. The photosynthesis in cyanobacteria takes place in the vegetative cells, where chlorophyll is stored in thylakoids in their cytoplasm (Heidrich et al., 2017). In addition, the life cycle of *Nostoc* includes the spore-like cells akinetes, which forms in response to nutrient deficiency other than Nitrogen, as well as motile multicellular filaments hormogonia, the dispersal units (Rippka et al., 1979; Sarma et al., 2004).

Nitrogen-fixating cyanobacteria, primarily members of the *Nostoc* genus are often engaged in several symbiotic relationships with plants and fungi (Duggan & Adams, 2008; Meeks et al., 2002). Recent research has shown that which plant partner the cyanobacteria has in these symbiotic relations affects the production of secondary metabolites, doing so by down-regulation the biosynthesis of metabolites present in free-living stages, and inducing the production of other unknown products (Liaimer et al., 2015). Therefore the genus *Nostoc*, with its complex lifecycle and their diverse association with other organisms, is a unique model for the discovery of novel metabolites and compounds (Liaimer et al., 2016). In this paper, the focus will be directed towards members of *Nostocales*, and their production of secondary metabolites.

Production of secondary metabolites

Cyanobacteria produce an impressive array of natural products, with a vast diversity of structures (Burja et al., 2001; Harrigan & Goetz, 2002). This includes over 1100 secondary metabolites with exotic chemical structures reported from 39 genera of cyanobacteria, isolated from different geographic origins (Dittmann et al., 2015). Some of these secondary metabolites are toxins that can cause severe health problems or even death for wild and domestic animals, or even for humans (de Figueiredo et al., 2006).

Cyanobacteria are without a doubt a rich source of natural products, represented as non-ribosomal peptides, polyketides, terpenes and alkaloids (Hoffmann et al., 2003; Pattanaik & Lindberg, 2015; Taylor et al., 2014), as well as their production of fatty acids and variations of pigments (Los & Mironov, 2015; O'Carra et al., 1980).

For long, the research on natural products from cyanobacteria had its focus on toxins, and especially on the widespread hepatoxin microcystin 1 because of its threat to drinking-water (Dittmann & Wiegand, 2006). But from the early ’80s, several other interesting and promising compounds have been isolated from cyanobacteria, with diverse bioactivities and traits, for

example as antiproteases (Bister et al., 2004), anti-cancer (Costa et al., 2012), allelopathic (Liaimer et al., 2016), anti-viral (Kanekiyo et al., 2005), anti-inflammatory (Villa et al., 2010) and anti-infective traits (Balunas et al., 2010), as well as the production of neurotoxins (Choi et al., 2010). These findings are increasing the interest in the usage of cyanobacteria as a source of secondary metabolites that could be used not only as pharmaceuticals but also for fuel production, food, and other biotechnological applications, even the pigments may be utilized (Abed et al., 2009; Ducat et al., 2011).

In fact, there are few other groups of organisms that have shown such large and diverse chemical profile as cyanobacteria have, other than Myxobacteria and Streptomycetes. Amazingly almost every new strain of cyanobacteria has its own unique set of secondary metabolites (Nunnery et al., 2010), which underlines that cyanobacteria are an excellent target for finding novel bioactive compounds.

Biosynthesis of secondary metabolites

A large part of the cyanobacterial secondary metabolites is peptides, or have peptide substances which are uniquely produced as a result of a naturally combined biosynthesis (Mandal & Rath, 2015; Nunnery et al., 2010; Ziegler et al., 1998). The productions of these peptides mainly happen by three different synthetic pathways; the non-ribosomal peptide synthases (NRPS), polyketide synthetases (PKS) and ribosomally where the peptides are post-translationally modified (RiPP) (Arnison et al., 2013; Koglin & Walsh, 2009).

Gene-clusters related to biosynthesis of these peptides have been assigned to an increasing number of natural products isolated from cyanobacteria (Jones et al., 2009; Welker & Von Döhren, 2006), where fascinating variations of enzymatic traits were observed, including many who rarely or never have been seen in other microorganisms (Kehr et al., 2011).

Most of the metabolites produced by cyanobacteria are assumed to be synthesized of non-ribosomal peptide synthase (NRPS), polyketide synthase (PKS)- or NRPS/PKS hybrid-pathways. This assumption is based on reported structures that are impossible to achieve by ordinary ribosomal synthesis (Welker & Von Döhren, 2006). Even though most of the metabolites from cyanobacteria are produced by these two pathways, several reports of biosynthetic pathways that start off with a ribosomally synthesized peptide that undergo posttranslational modification (RiPP) have been observed in cyanobacteria (Schmidt, 2010; Schmidt et al., 2005). In this paper, the focus is directed towards these three pathways, and in the next sections, these pathways will be discussed in some detail.

Non-ribosomal peptide synthases

The non-ribosomal peptide synthase (NRPS) is a gigantic multi-domain enzyme which consists of different modules where each is responsible for the incorporation of an single amino acid. The basic module is built up of domains for adenylation (A), peptidyl carrier domain (PCP) and a condensation domain (C) (Koglin & Walsh, 2009; Kohli et al., 2001), where the amino acids are activated by domain A as adenylates, and the amino acids and the growing peptide chain are bound as thioesters to the pantetheine unit in the PCP domain, and finally peptide bond formation is catalyzed by the C domain (Conti et al., 1997; Lautru & Challis, 2004).

The NRPs peptides are produced by enzyme complexes which are generated ribosomal by standard protein synthesis. The peptides produced by NRPS are often cyclic, have a high density of non-proteinogenic amino acids, and often contain amino acids connected by bonds other than peptide/disulfide bonds. The activation of amino acids in this multi-enzymatic process resembles the way amino acids are activated in ribosomal peptide synthesis, but the enzymes involved are neither structural or catalytical alike (Challis & Naismith, 2004).

There are also several alternative integrated modifying domains, among other the termination domain, where the release of the product with hydrolytic cleavage or intramolecular cyclization is catalyzed by thioesterase (TE) activity and can be integrated in the C-terminus of the last module (Kohli et al., 2001; Lautru & Challis, 2004). Other alternative modifying domains include the epimerization domain, which epimerize aminoacyl and peptidyl intermediates by thioester stage (Ansari et al., 2004). Other domains observed in NRPS with low frequencies include the oxidation domain, reduction domain and the formylation domain (Ansari et al., 2004). Integrated alternative associated enzymes are often a part of these modular complexes, such as dehydrogenases and halogenasaes (Wohlleben et al., 2009).

A distinct characteristic of the NRPS pathway is the ability to combine proteinogenic amino acids with non-proteinogenic amino acids, fatty acids, carbohydrates, and other building blocks to form complex molecules. The complex allows around 500 proteinogenic and non-proteinogenic amino acids (Walsh et al., 2013), in contrast to ribosomal peptide synthase which is limited to the 22 proteinogenic amino acids (Challis & Naismith, 2004).

The order of the NRPS modules corresponds with the order of amino acids in the final product, and the lack of specificity of the NRPS biosynthetic pathway contributes to the chemical diversity found in natural products from cyanobacteria (Fewer et al., 2007;

Stachelhaus et al., 1999). In fact, Nostocyclopeptide A1 is one of the few pure NRPS gene clusters that has been described in cyanobacteria (Becker et al., 2004).

Hybrid pathways (NRPS/PKS)

One main characteristic for the secondary metabolites found in cyanobacteria is the frequent mixture of NRPS and PKS modules in their biosynthetic pathways, and often within a single reading frame (Kehr et al., 2011; Welker & Von Döhren, 2006). Since there are many structural and catalytic similarities between these two pathways, it is only natural that one often finds hybrids of these. Both linear and cyclic peptides have been known to have hybrid pathways, and they have been found in both freshwater (Keishi Ishida et al., 2007; Tillett et al., 2000), marine (Chang et al., 2002; Zhang et al., 2017) and terrestrial cyanobacteria (Hoffmann et al., 2003; Magarvey et al., 2006).

The first NRPS/PKS hybrid pathway identified in cyanobacteria was the biosynthesis of the famous hepatoxin microcystin 1 from the freshwater cyanobacteria *Microcystis aeruginosa* (Nishizawa et al., 2000; Tillett et al., 2000). Other peptides with hybrid pathways include Cryptophycins which have been isolated from terrestrial strains of *Nostoc* either free-living or in symbioses with liches (Golakoti et al., 1995; Magarvey et al., 2006), and Barbamide and Jamaicamide, characterized from *Lynbya majuscula* (Chang et al., 2002; Edwards et al., 2004). In the following section, I am going to present some of the major peptide classes mainly from the genus *Nostoc*, produced by NRPS or hybrid NRPS/PKS pathways, where we have basic knowledge about the biosynthetic origin.

Anabaenopeptins

Anabaenopeptins are found across the phylum cyanobacteria and have among others been observed in the genera *Nostoc, Anabaena, Planktothrix* and *Microcystis* (Guljamow et al., 2017; Welker & Von Döhren, 2006). Anabaenopeptins are bioactive cyclic hexapeptides first isolated from the cyanobacteria *Anabaena flosaquae* (Harada et al., 1995), which are characterized by a lysine in position 5 in the formation of a ring from a N-6-peptide bond between Lys and the carboxyl group of amino acids in position 6 (Harada et al., 1995). Another trait of the Anabaenopeptins is that all the amino acids are in L-configuration, except the Lys in position 2 (Welker & Von Döhren, 2006). Anabaenopeptins vary in mass and have been observed with a mass range from 759 Da for Anabaenopeptin I (Murakami et al., 2000) to 956 Da for Oscillamide C (Sano et al., 2001).

Aeruginosins

Aeruginosins are a class of linear tetrapeptides commonly found in freshwater cyanobacteria and have an unusual hydroxy-phenyl lactic acid (Hpla) at the N-terminal and a 2-carboxy-6-hydroxyoctahydroindole (Choi) unit and an arginine derivate at the C terminus (Murakami et al., 1995). Most Aeruginosins are strong specific inhibitors of serine proteases (Ersmark et al., 2008; Keishi. Ishida et al., 1999). Aeruginosins has also been found in a wide range of *Nostoc* strains (Liaimer et al., 2016). Aeruginosin A is known to be produced by NRPS/PKS hybrid pathway (Keishi Ishida et al., 2007) presented in Figure 3, the two separate pathways NRPS and PKS and their typical domains are presented in Figure 2.

The loading module in the biosynthesis of Aeruginosin A has been predicted to activate phenylpyruvate which is reduced by an integrated KR domain to phenylacetate. The following adenylation domain activates the unusual Choi unit directly as a substrate (Keishi Ishida et al., 2007). However, the Aeruginosin enzyme complex doesn't consist of a reductase or a thioester domain, as shown in Figure 3, hence it is still unclear how the final product Aeruginosin A is released from the modular enzyme complex (Keishi Ishida et al., 2007).

Non-ribosomal peptide synthases (NRPS) **Polyketide synthases (PKS)**

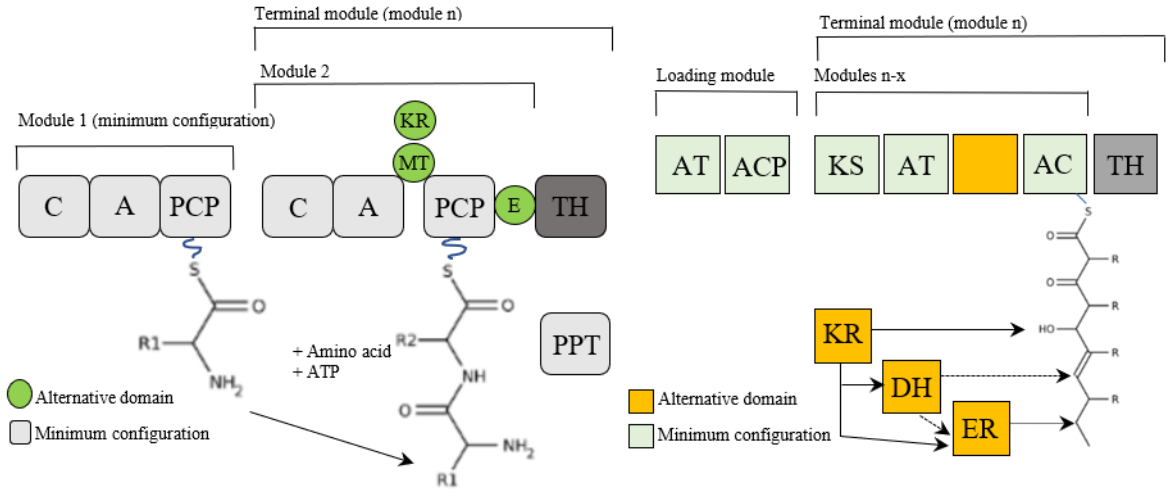

Figure 2: The NRPS and PKS pathway and their typical domains. Abbreviations: C: condensation domain, A: adenylation domain, PCP: peptidyl carrier protein, MT: Methyltransferase, E: epimerase, AT: Acyltransferase, ACP: Acyl carrier protein, KS: ketosynthase, KR: ketoreductase, DH: dehydrogenase, ER: enoyl reductase, TH: thioesterase. PPT: 4'PPtase (PCP-specific/4'-phosphopantetheinyl cofactor transferase). Illustration modified from Jenke-Kodama et al. (2005); Kehr et al. (2011); Koglin and Walsh (2009)

Aeruginosin A, a known NRPS/PKS hybrid

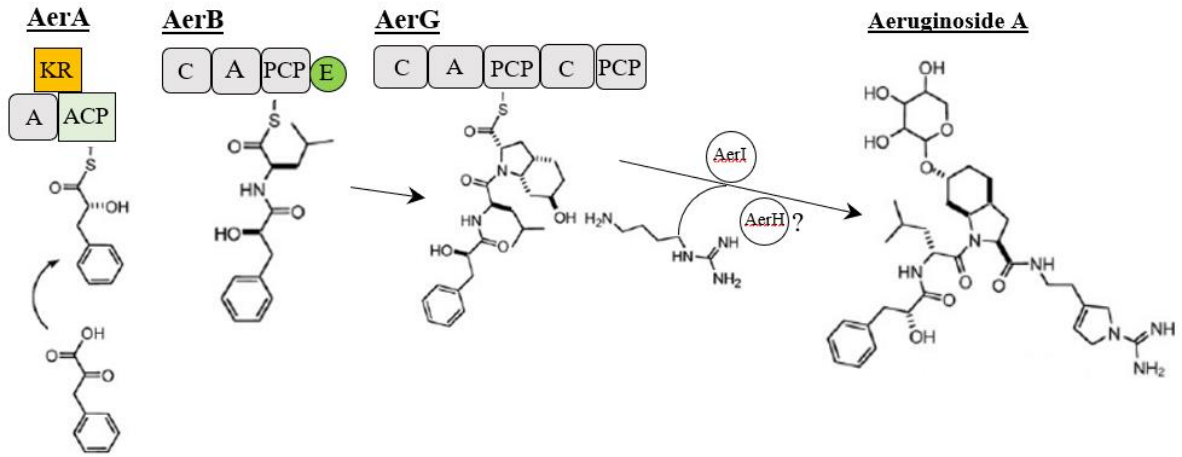

Figure 3: Model for the biosynthesis of Aeruginosin A and predicted domains of AerA-I and supposed AerH, where we clearly see the hybrid nature of Aeruginosin A. Each square with rounded edges/circle represents an NRPS domain or tailoring function, and each square represents a PKS domain. Abbreviations: A, adenylation domain; KR, ketoreductase domain; ACP, acyl carrier protein; C, condensation domain; PCP; peptidyl carrier protein; E, epimerization domain. Illustration modified from Keishi Ishida et al. (2007).

Nostopeptolides & Nostocyclopeptides

Nostopeptolides (Nos) are branched acylated octapeptides with a heptapeptide lactone structure (Figure 5) and are among others produced by the terrestrial cyanobacteria *Nostoc sp.* GSV224 (Golakoti et al., 2000). The Nostopeptolide NRPS/PKS gene cluster was the first described for a terrestrial strain (*Nostoc sp.* GSV224), and has 3 NRPS genes (nosA, C and D) and one PKS gene (nosB) for acetate insertion and to genes (nosE and F) involved in formation of 4-methyl proline (Hoffmann et al., 2003; Luesch et al., 2003), as well as one ABS transporter (nosG) (Hoffmann et al., 2003). Studies by Liaimer et al. (2015) have also shown that Nostopeptolides are involved in among regulation of hormogonia, and they serve a damper on hormogonia formation (Liaimer et al., 2016).

Nostocyclopeptides (Ncp) are cyclic heptapeptides (Figure 4), which possess a unique imino linkage in the macrocyclic ring (Golakoti et al., 2001). Nostocyclopeptides are structurally similar to Nostopeptolides, and the organization of gene clusters of Ncp and Nos shares similar traits, and there is a high degree of homology between the key genes in the operons (Becker et al., 2004). Studies have shown that multiple strains of *Nostoc* discovered both in soil and in symbiotic relations produce Nostocyclopeptide (Golakoti et al., 2001; Liaimer et al., 2016). Nostocyclopeptides may also be involved in regulation, similar to Nostopeptolides because of the high degree of homology (Liaimer et al., 2016).

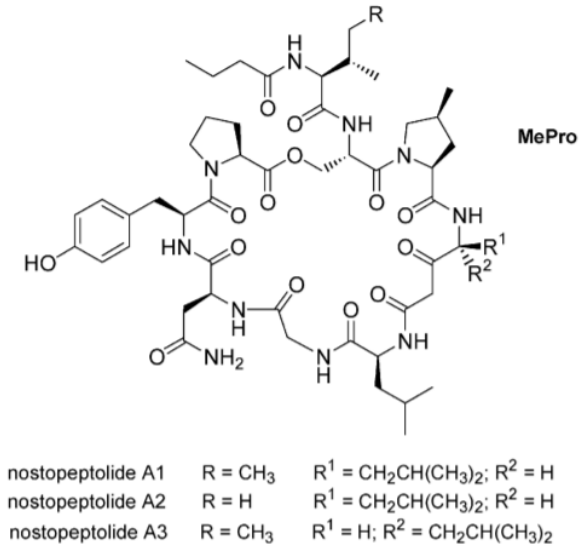

Figure 5: Chemical structure of Nostopeptolide A1-A3. Illustration courtesy of (Luesch et al., 2003).

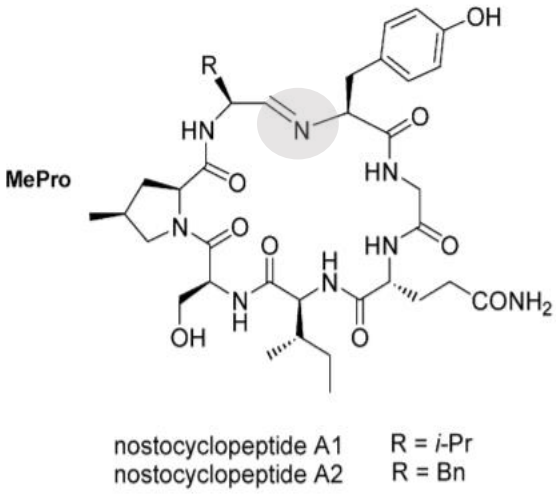

Figure 4: Chemical structure of Nostocyclopeptide A1 and A2. The imine linkage in Nostocyclopeptide are highlighted in grey. Illustration courtesy of (Luesch et al., 2003)

Polyketide Synthases

The bacterial polyketides are products of biosynthetic processes analogous to the fatty-acid biosynthesis. They are a remarkable class of natural products and in addition, to having an enormous range of functional and structural diversity, they have been proven to show antibiotic, anticancer, antifungal, antiparasitic and immunosuppressive properties (Singh et al., 2011; Staunton & Weissman, 2001). In contrast to the peptide-synthesizing enzymes, in PKS-systems different types of carboxylic acids are activated, assembled and then potentially modified (Kehr et al., 2011). All polyketide synthases use small acyl-coenzyme A (acyl CoA) units like propionyl, acetyl, malonyl or methyl malonyl CoA in sequential decarboxylative condensations reactions to form linear or cyclic carbon backbones (Staunton & Weissman, 2001).

The polyketide synthases have been classified by their structural resemblance with fatty acid synthases. Type I PKS are big modular proteins which carry all the active domains required for polyketide synthesis and are structurally like class I fungal and vertebrate fatty acids synthases. While in type II PKS the enzymes work repetitive and are typically involved in the biosynthetic of aromatic antibiotics in bacteria (Hopwood, 1997; Staunton & Weissman, 2001). The typical set of domains in an individual PKS consist of ketosynthase (KS), acyltransferase (A), and acyl carrier protein (ACP), in addition to the alternative domains ketoreductase (KR), dehydratase (DH), and enoyl reductase (ER) used to lead to another reduction state of keto-groups of polyketides (Hopwood, 1997; Staunton & Weissman, 2001), as seen in Figure 2. Curacin synthases are polyketides produced by strains of *Lyngbya majuscule*, and Curacin A has shown potent cancer cell toxicity (Gerwick et al., 1994).

Ribosomal peptide synthesis of complex peptides (RiPP)

Even though the major share of cyanobacterial peptides has been proven to be synthesized non-ribosomally, complex and modified peptides can be synthesized independently from NRPS and PKS enzymes (Schmidt et al., 2005). The ribosomal precursor peptides are typically built up of a leader peptide and a core peptide, which is transformed into the mature product (Figure 6) and associated post-translationally modifying enzymes (PTMs) catalyzes different types of macrocyclizations of the core peptide, and side-chain modification of amino acids (Oman & van der Donk, 2010).

In most RiPPs, the leader peptide or leader sequence is usually important for recognition by many of the post-translational modification enzymes and for export (Oman & van der Donk,

2010). Even though this biosynthesis of peptides is limited to the 22 proteinogenic amino acids (Challis & Naismith, 2004; Dittmann et al., 2015), many of these post-translational processing enzymes are highly tolerant to mutations in the core peptide which results in highly evolvable pathways (Arnison et al., 2013; Li et al., 2010; Oman & van der Donk, 2010). Hence, this group of peptides therefor still displays a high diversity and has a big bioactive potential, and cyanobacteria can be considered as one of the most prolific sources of ribosomal-produced natural products (Burja et al., 2001; Hetrick & van der Donk, 2017).

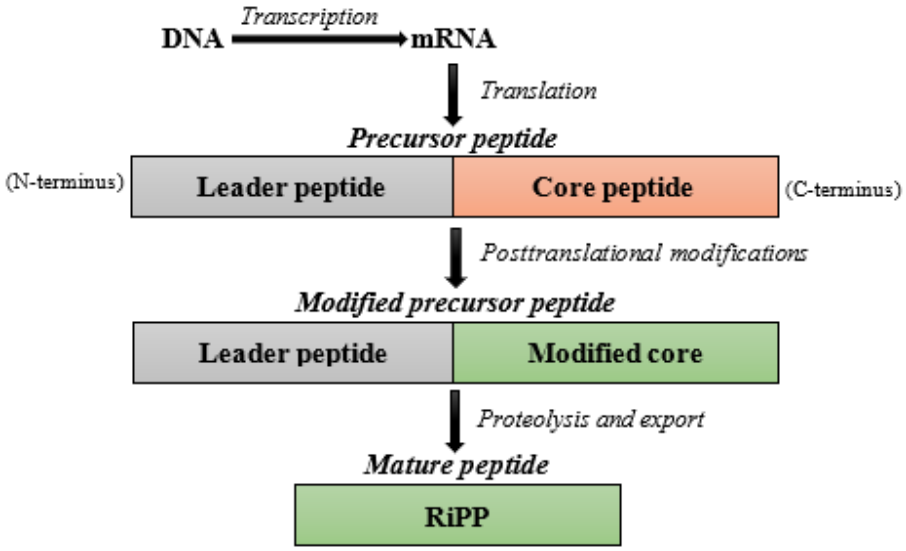

Figure 6: General biosynthetic pathway for RiPPs. Where the precursor peptide contains a core region that is transformed into the main product, with post-translational modifications guided by the leader peptide. Illustration modified from Arnison et al. (2013).

Common features of RiPP biosynthesis include post-translational modification involving Cys residues, where sulfur chemistry converts the thiols of cysteines to disulfides (e.g., lanthipeptides & cyanobactins), thioethers (e.g., sactipeptides), thiazol(in)es (e.g., bottromycins), and finally sulfoxides (e.g., lanthipeptide & amatoxins) (Arnison et al., 2013). Additionally, a common feature is the macrocyclization to increase metabolic stability and decrease conformational flexibility (Arnison et al., 2013), the typical macrocyclization of RiPPs is clearly shown in Figure 7-8.

The three biggest peptide families they produce are cyanobactins, lanthipeptides, and microviridins (Kehr et al., 2011). All known cyanobactins derive from cyanobacteria, and about 200 cyanobactins have been identified and evidence suggests that they might be present in 30% of cyanobacterial strains (Donia et al., 2008; Leikoski et al., 2010; Leikoski et al., 2009; Sivonen et al., 2010). The first ribosomal cyanobactin pathway which was discovered was the biosynthesis of Patellamides A and C, Figure 7, first isolated from *Prochloron*

didemni (Schmidt et al., 2005). Patellamides are pseudo-symmetrical cyclo-octapeptides which have proven to be moderately cytotoxic and have shown MDR reversing activity in cancer cells (Fu et al., 1998; Williams & Jacobs, 1993).

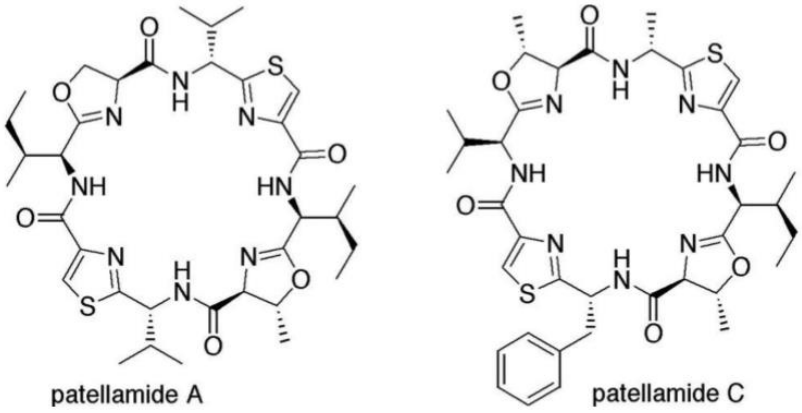

Figure 7: The chemical structure of Patellamide A and Patellamide C, illustration courtesy of Schmidt et al. (2005)

The lanthipeptides are a big class of peptides which is produced by a variety of bacteria and is characterized by the presence of intramolecular lanthionine and methyl-lanthionine bridges formed by dehydration of serine/threonine, respectively, followed by intramolecular addition of cysteine thiols to the resulting dehydroamino acid (Cubillos-Ruiz et al., 2017). Lanthipeptides have a variation of bioactivities, including antimicrobial ones commonly known as lantibiotics (Knerr & Donk, 2012).

The last big class of peptides is microviridins, which are the biggest known cyanobacterial oligopeptides. They are mainly found in the bloom of freshwater cyanobacteria (Fastner et al., 2001; Ziemert et al., 2008). The microviridins have an unusual cage-like structure and contain noncanonical lactone and lactam rings and several members of the family inhibit potent different serine-like proteases (Gatte-Picchi et al., 2014; Ishitsuka et al., 1990). This unusual cage-like structure is shown in Microviridin G isolated from *Nostoc Minutum* (Murakami et al., 1997), Figure 8.

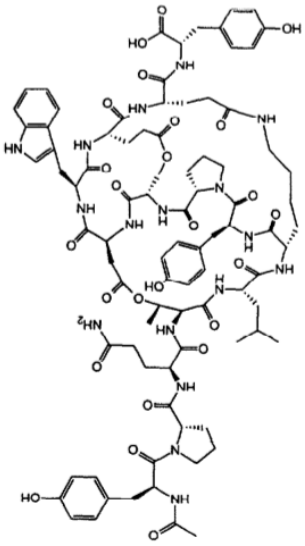

Figure 8: The chemical structure of Microviridin G, illustration courtesy of Murakami et al. (1997).

Bioinformatics as a tool for finding novel nature products

Bioinformatics has shown that the biosynthetic pathway of NRPS/PKS is an ancient part of (cyano)bacterial metabolism, thus cyanobacteria have been synthetizing secondary metabolites long before higher animals and plant existed. Hence the intoxication of humans and other higher animals is most certainly not the selective force for the evolution of such a diverse repertoire of toxic or otherwise biologically active secondary metabolites from cyanobacteria (Berry et al., 2008). However, the production of these structures together with natural selection made it more advantageous to produce these unique structures (Welker & Von Döhren, 2006).

The identification of biosynthetic genes responsible of the production of secondary metabolites is still a relatively unexplored area, and it remains many natural products for which a biosynthetic origin is unknown (Welker & Von Döhren, 2006). Hence knowledge about these pathways can reveal unique biochemical features, activities, and structures, as well as biotechnological applications (Dittmann et al., 2013; Hess, 2011).

Identifying putative biosynthetic gene clusters in the genome sequence protein *in silico* is generally a simple task with a BLAST search and further characterize and predict the biosynthetic products by the enzymes encoded in the gene clusters with specialized software tools (Ingolfsson & Yona, 2008; Punta & Ofran, 2008; Weber, 2014). The most common software for predicting secondary metabolites and their corresponding gene clusters is the NRPS predictor (Röttig et al., 2011), BAGEL (van Heel et al., 2013) and AntiSMASH (Blin et al., 2015; Medema et al., 2011) where the latter combines several databases and software's (BAGEL, NRPS predictor, NCBI BLAST+, Glimmer3, etc.) to identify and annotate secondary metabolite biosynthesis gene-clusters in both bacterial and fungal genomes (Blin et al., 2015; Medema et al., 2011).

Even though all genomic studies like this will be limited to already known homologs, bioinformatics is still a good tool for finding novel natural products from cyanobacteria and guide us towards new scientific findings (Dittmann et al., 2013).

Subject of study; *Nostoc* spp. KVJ20, KVJ10 & KVJ2

The subject for this study is three cyanobacteria belonging to the genus *Nostoc*, the strains are further known as KVJ2, KVJ10 & KVJ20. Members of the genus *Nostoc* are included in section IV, filamentous cyanobacteria with division in only one plane. These sub-strains live in symbioses with the liverwort *Blasia pusilla L* and are found inside cavities in symbiotic organs called auricles in the outer cellular layer in the wort, where each cavity is infected by one single clone, visualized in Figure 9. The sub-strains were first collected at the plant school at Kvaløya (62° N 18,81°E) in Tromsø, in Northern Norway (Liaimer et al., 2016).

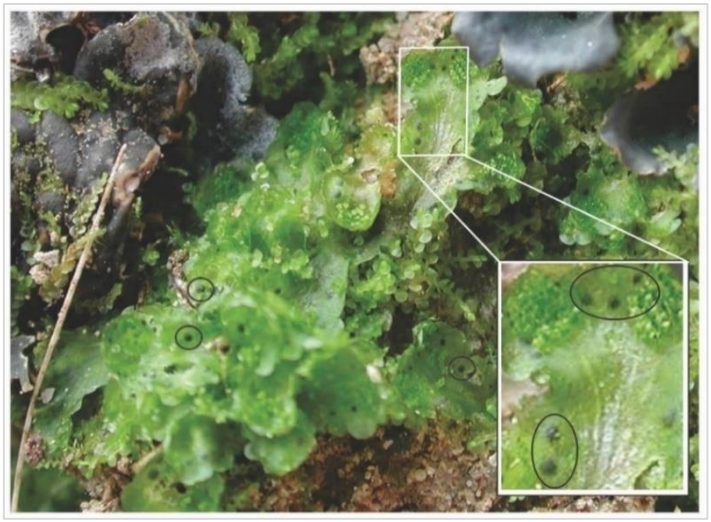

Figure 9: The Liverwort Blasia pusilla L. in its natural habitat. Strains of Nostoc are encircled in their auricles. Illustration courtesy of Liaimer et al. (2016).

In a former study by Liaimer et al. (2016), it has been shown that KVJ2, KVJ10, and KVJ20 produced a spectrum of substances. In the same study, Banyaside/Suomilide like compounds were found in extracts of KVJ20, with m/z H^+ on 899, 927, 997, 1045 and 1115, where the latter two where sulfated with a natural loss of 80 Da. Nostocyclopeptides with m/z H^+ 757 were also reported in KVJ20 and KVJ2.

In the supernatant of extracts from KVJ10, Nosperin m/z 564 Da was identified, which is an unusual product of NRPS biosynthesis involving trans-acyltransferase. Aeruginosin with m/z H^+ 889 was observed in KVJ2, and the fragmentation patterns of all these molecules shared a common feature of loss of either 176 or 162 Da, which is indicative of the presence of glucuronic acid or a hexose, respectively (Kapuścik et al., 2013; Reinhold et al., 1995).

In the same study by Liaimer et al. (2016), it was shown preliminary results indicating cytotoxic properties in KVJ2 & KVJ20 against several cell lines. In another recent study by

Guljamow et al. (2017) three Anabaenopeptins were isolated from the KVJ2, with 828, 842 & 812 $[M+H]^+$. Terrestrial cyanobacteria is as mentioned poorly explored as a source to novel natural products (Liaimer et al., 2016). Therefore, it is interesting to look further into the strains, as a potential source of novel secondary metabolites. Recently the draft genome of KVJ20, KVJ2 & KVJ10 has been released and deposited on NCBI with accession number: NZ_LSSA00000000.1, NNBU00000000.1, and NNBT00000000.1 respectively.

Aim

I. Identify potential secondary metabolite gene clusters in *Nostoc* by using bioinformatic tools.

II. To design and test primers sets suitable for qPCR for the identified gene clusters.

III. Study the gene-expression in the predicted genes with help of reverse transcription qPCR in response to different nutrient conditions, as well an in interaction with other *Nostoc* strains.

IV. Establish a UPLC-HR-MS profile for KVJ2, KVJ10, and KVJ20 in different modes of cultivation.

V. Identifying potential changes in gene expression patterns as a response to different modes of cultivation.

VI. Identify connections between gene expression patterns and the chemical profile in the different strains in response to different modes of cultivation.

VII. Identify known peptides produced by the strains and suggest potential products with dereplication and examination of fragmentation patterns from the UPLC-HR-MS profile.

VIII. Identify which growth conditions would give a higher yield of interesting secondary metabolites and determine which mode of cultivation is best suited for biotechnological applications.

Methods and Equipment

Workflow

In this study, we wanted to analyze gene expression and production of secondary metabolites, with the help of bioinformatic tools as AntiSMASH. The workflow started with predicting secondary metabolites in the strains, by depositing the genomes on AntiSMASH, before making primers for selected gene clusters. The exponentially growing cyanobacterial suspension was then subjected to nutrient deprivations, as well as subjected to competition to other Nostoc strain before extraction of secondary metabolites and gene expression analysis was conducted. In Figure 10 a shortened schematic representation of the workflow is shown; a more detailed description is described in the following chapter.

The biosynthesis of cyanobacterial secondary metabolites consumes a great deal of metabolic energy, hence clues to the function of these compounds may be revealed by exploring and altering the growth conditions under which they are produced (Briand et al., 2016). There is considerable evidence that some cryptic or poorly expressed secondary metabolites can be more activated under stress responses in bacteria (Yoon & Nodwell, 2014), which is the underlining basis for this project. By exposing the bacteria to different nutrient conditions, we hoped this would interfere with both the gene expression and the production of secondary metabolites.

To determine the gene expression of selected secondary metabolite genes chosen from bioinformatic analysis, we chose to use reverse transcriptase-quantitative PCR (RT-qPCR), which uses the same basic principles as the basic PCR technique. But instead of having amplicons after the PCR cycle as an endpoint in qPCR, the amount of DNA is measured after each cycle by using fluorescent markers that are incorporated into the PCR product (Heid et al., 1996; Martins & Vasconcelos, 2011). Thus, the increase in fluorescent signal is directly proportional to the number of amplicons generated (Heid et al., 1996). By using RT-qPCR the RNA transcript can be measured by converting the RNA template to its complementary DNA (cDNA) using reverse transcriptase, before being used as a template in the PCR (Bustin, 2002). Hence, we can measure the amount of RNA transcript in real time and quantify gene expression. So far, no published research on the relative expression of the complete set of NRPS, PKS and RiPP both with unknown and known products have been conducted on KVJ2, KVJ10, and KVJ20.

Ultra-high pressure liquid chromatography (UPLC) in combination with time-of-flight (TOF) mass spectrometry detectors have proven to be a very efficient tool for both the identification of new natural products and the dereplication of natural product extracts (Grata et al., 2008; Jean-Luc et al., 2010). By using this sophisticated analytic method, we could easily identify and assess compounds present in the different extracts, as well as compare the chemical profile of the different compounds.

The complete "pipeline" was executed for KVJ20 by me, as well as extraction of secondary metabolites from KVJ2 and mass spectrometry analysis. Gene expression data from KVJ2 and KVJ10 were obtained from earlier Bachelor students, with some additional qPCR runs for quality checking. Mass spectrometry data for KVJ10 was provided by my supervisor. All extracts and data have been treated with the same conditions and the same methods for extractions.

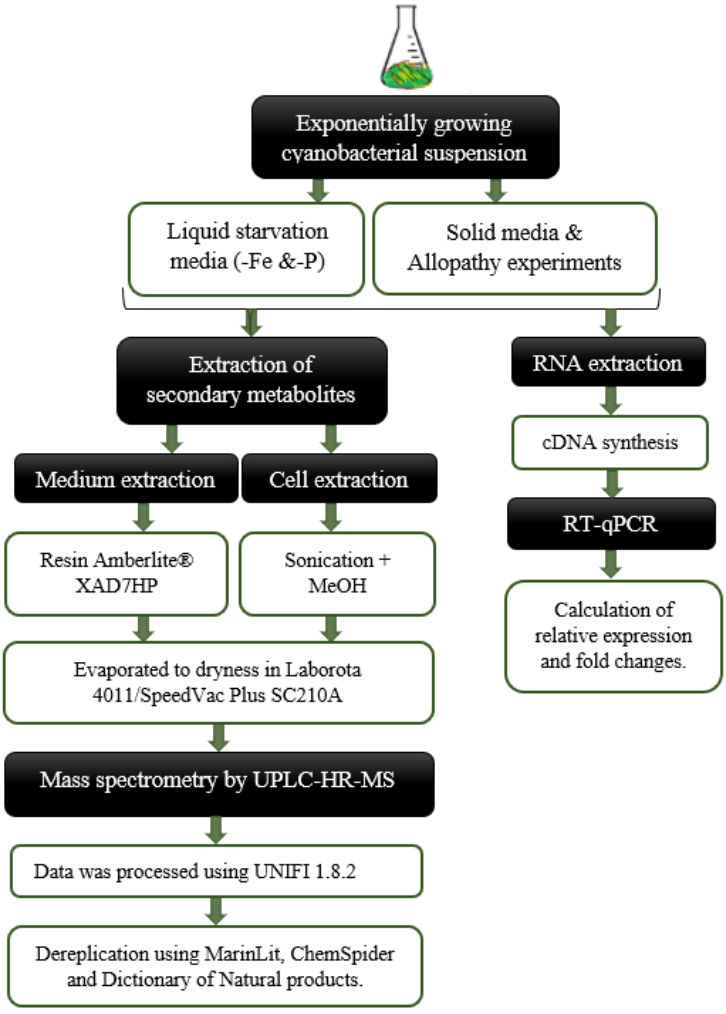

Figure 10: Workflow in general traits. MeOH: methanol RT-qPCR: Reverse transcriptase-quantitative Polymerase chain reaction. UPLC-HR-MS: Ultra-Performance Liquid Chromatography-High resolution-Mass spectrometry.

Cultivation conditions.

For cultivation of KVJ20, 2 L of $BG11_0$ and BG11 medium were made by recipe from stock solution, first described in Stanier et al. (1971). The $BG11_0$ medium is a well-used medium, which lacks sodium nitrate and is used for cultivation of cyanobacteria capable of dinitrogen fixation, while BG11 has sodium nitrate added. All the solutions being used for cultivation were autoclaved, to maintain a sterile environment for growth.

Liquid media was made by adding the stock solution in order from I-IV ($BG11_0$)/VII (BG11) in a 1000-fold dilution in 2 L of Milli-Q water in an Erlenmeyer flask. The stock solutions we used are listed in Appendix 1: BG11 recipe. Solid plates were made from the same stock recipe with 1% added agar and poured on plates.

For cultivation 50 mL $BG11_0$/BG11 liquid medium was added to six 100 mL sterile Erlenmeyer flask, with a scoop of bacteria from the sub-strain KVJ20-G re-isolated as pure culture from symbiosis with *Gunnera manicata*. This sub-strain still contains most of the same properties as the wildtype, in contrast to sub-strains maintained in liquid cultures. The flasks were incubated for 1-3 weeks at standard conditions at 23°C with constant light 30 µmol $m^{-2}s^{-1}$ (36W/77 Osram Fluora) and shaking.

Experimental setup

After cultivation the six exponentially growing (2 weeks old) cultures were aliquoted to 50 mL Falcon tubes, and the bacteria cells were collected by centrifugation (Eppendorf Centrifuge 5804 R) at 5000 rpm for 5 minutes, and then followed by two times wash in fresh $BG11_0$/BG11 medium. All pellets were combined, followed by an additional wash. The cell material was then homogenized in a small amount by a 0.4 mm syringe (BDMicrolance™).

Solid medium was prepared both with and without sodium nitrate from stock solution as previously described. Each agar plate was spotted with ten 20 µL drops of the cyanobacterial suspension, which later gave rise to colonies. Allelopathy experiments were set up by adding five drops of one *Nostoc* strain on one side of the agar plate, and five drops of another *Nostoc* strain on the other side, as shown in Figure 11. Each agar plate was covered in parafilm and cultivated at standard conditions until visible results.

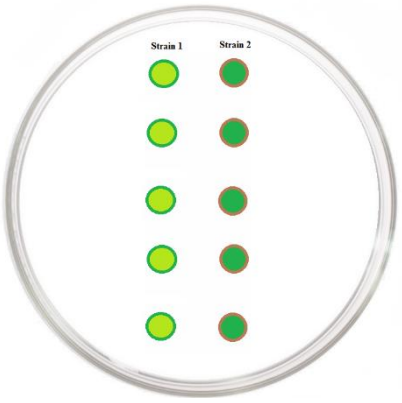

Figure 11: Illustration for how allelopathy experiments were conducted.

The remainder suspension was redistributed to the original cell density in 20 mL of the liquid media with and without nitrogen and in addition in phosphor-deficient and iron-deficient medium. Phosphor-deficient and iron-deficient media were simply made by not adding stock solution I and IV respectfully to the media. The starvation cultures were incubated under standard condition for 2 weeks. Agar plates and liquid media cultivations were made in triplicates, and all work was performed on a sterile bench to prevent contamination. The experimental set up is presented in Figure 12.

After one week of growth, samples from all cultures were taken for microscopy to study morphology and possible morphological differences in bacterial development and growth. Microscopy was done with Leica DFC420 fluorescence microscope and samples were looked at under brightfield with a 40x objective.

The cultures from liquid media, were transferred to 50 mL Falcon tubes and centrifuged for 5 minutes at 5000 rpm, and the supernatant was collected and stored at - 20°C for later extraction. Each pellet from the liquid media was divided into two parts, one for later secondary metabolite extraction and the other for RNA extraction, preserved in 300 µL of RNA*later*™ Stabilizer Solution (ThermoFisher), and stored at - 20°C. The colonies from agar plates were collected by inoculation loop and divided into two equal parts as described above, one part for RNA extraction and one for secondary metabolite extraction.

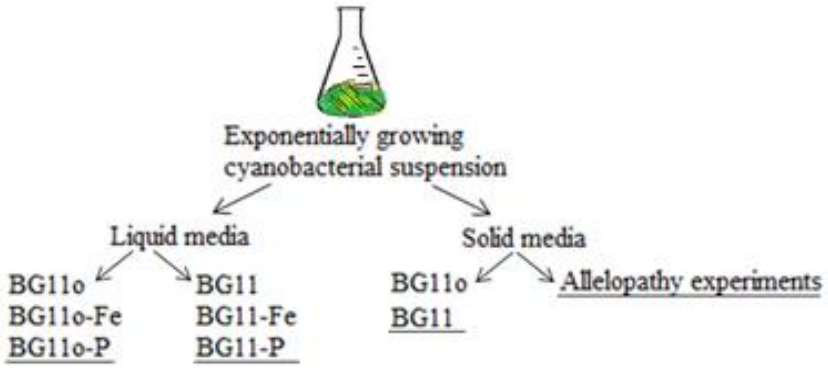

Figure 12: The experimental setup of the cultivation of the cyanobacteria.

Bioinformatics

The genome sequences for KVJ20, KVJ2 and KVJ10 were retrieved from NCBI, with accession number: NZ_LSSA00000000, NNBU00000000.1, and NNBT00000000.1 respectively, and submitted to the specialized database AntiSMASH, which perform antibiotics and secondary metabolite analysis, and allows the analysis of secondary metabolite biosynthesis gene clusters (Blin et al., 2015; Medema et al., 2011). In addition, a search in the Norine prediction tool (Pupin et al., 2015) was conducted for KVJ10. From the produced result from the database search, the different gene clusters were analyzed and one open reading frame from each cluster was chosen for primer design. Additionally, BLAST analyses were run with *Nostoc punctiforme* ATCC29133 as query in order to find genes for Nitrogenase (*NifH*), akinetes marker gene (*AvaK*), gas vesicle protein C (*GvpC*) and Ribonuclease P RNA gene (*RnpB*), motility protein (*PilT*). No *GvpC* gene was found in KVJ2, hence *PilT* was used instead.

Primer design

The genes that were chosen for primer design for the NRPS clusters was an NRPS gene, for PKS cluster a PKS gene, for RiPP clusters an ABC transporter and for the microviridins, a ribosomal modification protein (*RimK*) was chosen. The sequences of the target genes were exported to a target-specific primer designing software tool called Primer-BLAST (Ye et al., 2012). Primer design settings were set accordingly to suggestions by BioRad for Real-Time PCR, namely:

> Primer length: 20bp
> Amplicon size: 150-250bp
> GC content: ~50%
> Optimal Tm: 60°C
> Avoid repeats (e.g. ATATATAT) and long runs (e.g. CCCC) they may cause mispriming.
> Verify specificity using tools such as the Basic Local Alignment Search Tool

The primers designed for KVJ20, KVJ2, and KVJ10 are listed in Table 26-28 in Appendix along with gene clusters, possible product, locus and accession number from NCBI.

Primer test

All primers were tested before being used for real-time PCR using Whatman™ FTA® card technology, and were stored at -20°C. The primers were diluted to a concentration of 100 µM in sterile double-distilled water (MilliQ water). The suspension of *Nostoc* sp. KVJ20 was pipetted onto a CloneSaver™ FTA® Card (Whatman™) and treated according to the instructions.

Paper circles containing cyanobacteria were pushed out from the card and into small PCR Eppendorf tubes, before being cleaned with FTA cleaning solution, two times (à five minutes) and then with TE^{-1} two times (à five min). The Mastermix for PCR was made from recipe shown in Table 1, and the exact amounts of components were calculated up to a number of reactions that were run each time. All components in the Mastermix were stored at -20°C. Before running PCR 25 µL of Mastermix added to each Eppendorf tube containing paper circles with bacteria. The PCR program that was used in primer testing is listed in Table 2.

After completing the PCR, a 1% agarose gel was run with 90 Volts in order to test if products were made. For visualization under UV-light ethidium bromide (EtBr) was added to the gel, and 1x TAE buffer was used. To the PCR tubes, 5 µL of 6x Loading DNA dye (Fermentas) was added. The results were analyzed by ChemiDoc™MP Imaging System.

Table 1: Mastermix x1 for PCR (25 µL) reaction

Components	**Volume**
10 x PCR buffer, minus Mg	2,5 µL
10 mM dNTP mixture	0,2 µL
50 mM MgCl	0,75 µL
Primer Mix (10 µM each)	1 µL
Template DNA	> 1 µL
Platinum TaqDNA polymerase	0,1 µL
Autoclaved, distilled water (MQ water)	20,45 µL

Table 2: Polymerase chain reaction cycles.

Stage	**Temp**	**Time**	**Cycles**
First denaturation	94°C	1 minute	
Denaturation	94°C	30 seconds	30 cycles
Annealing	60°C	30 seconds	
Extension	72°C	30 seconds	
	72°C	6 minutes	
	8°C	∞	

RNA extraction

All samples were first centrifuged at 25000 rpm for 5 min to discard RNA*later*™ stabilizer solution. The RNA extraction took place under a fume hood. The samples were homogenized before 1 mL of TRI Reagent® (Sigma-Aldrich) was added to each Eppendorf tube, and incubated at 95°C for 5 minutes, followed by 5 minutes on ice, before 100 µL of bromochloropropane was added to each tube and mixed vigorously. The samples were incubated for 10 minutes in room temperature with bromochloropropane, before being centrifuged at 12000g at 4°C for 5 minutes. After this centrifugation, the samples had separated into three different layers. The upper layer was transferred to a new Eppendorf tube and an equal volume of isopropanol was added, and the samples were incubated at room temperature for 15 minutes and again centrifuged at 12000 g at 4°C for 10 minutes.

To wash the RNA the supernatant was discarded and 1 mL 75% Ethanol (EtOH) was added, followed by centrifugation at 8000g at 4°C for 5 minutes. The supernatant was removed, and the pellet was air-dried and dissolved in 50 µL of DEPC treated water supplemented by 2.5 units of SUPERrase • In™ RNase Inhibitor. The samples were treated with DNAse, by adding 5.3 µL 10x DNAse buffer (0.1 x sample volume) and 1 µL DNAse, followed by incubation for 25 minutes at 37°C. After incubation 6 µL of inactivation reagent was added (approximately 0.1x sample volume) and mixed, before incubation for 2 minutes at room temperature and centrifuged at 10000g for 2 minutes. After centrifugation, the supernatant was transferred to a new tube, and concentration and purity of RNA were measured using NanoDrop™ 2000 Spectrophotometer. A 1% agarose gel (as described earlier) was run with 5 µL RNA to verify that the RNA was intact and that there was no DNA contamination in the samples.

cDNA synthesis

The SuperScript™ II Reverse Transcriptase (RT) was used to reverse transcribe the RNA to cDNA. In the first step, four compounds were added to PCR tubes: 1 µL Hexamer primer, 4 µL dNTP, 1 µg RNA and the amount of DEPC H_2O was adjusted to fit the maximum volume of 12.5 µL after RNA was added. The samples were incubated for 5 minutes at 65°C on a heat block, followed by a quick cool down to 4°C on ice and spun down with a centrifuge to collect condensation, before 4 µL of 5x Second Strand Buffer (Invitrogen™) and 2 µL 0.1 M USB Dithiothreitol (DTT) (Thermo Scientific™) was added.

The samples were then gently mixed and centrifuged, before another incubation at 25°C for 2 min. Then 1 µL SuperScript II™ RT and 1 µL dH_2O was added and the tubes were incubated for 10 minutes at 25°C, then for 50 min at 42°C followed by an inactivation period for 15 minutes at 70°C. The samples were stored at -80°C until use.

Reverse transcription quantitative PCR

We chose to run two technical duplicates for each biological sample, and each growth condition was represented by two biological replicates (two best RNA samples for each condition). All primer pairs were tested on each sample, and the *RnpB* primers were used as an internal housekeeping reference. Reactions x2 were set up using the SsoFast™ EvaGreen® Supermix and Mastermix was made for each cDNA sample tested, Table 3. All the cDNA samples were diluted x100 in order to get appropriate cDNA concentration for the reaction. The primers were also diluted x40.

The reactions were set up in 96 well plates. The CFX96™ Real-Time PCR Detection System (Bio-Rad) was used to perform qPCR reactions. Data were analyzed with the CFX Manager™ Software program (Bio-Rad). The qPCR program is presented in Table 4.

The same threshold line was used on all runs, and relative expression was calculated by the formula: RE (relative expression) = $2^{-(cQgene - cQrnpB)}$, with standard deviation (STDV), and fold changes in expression by the formula: FC (fold changes) = $2^{-(\Delta cQexp - \Delta cQref)}$. For graphic presentation, the fold changes below one were converted to negative values by -1/FC.

Table 3: Mastermix for qPCR reactions.

Mastermix	**x 1 reaction**
SsoFast™ EvaGreen® Supermix	10 µL
2.5 µM reverse and forward primers	4 µL
cDNA	6 µL

Table 4: qPCR cycles.

Stage	**Temp**	**Time**	**Cycles**
First denaturation	95°C	30 sec	
Denaturation	95°C	5 sec	X40
Annealing/extension	60°C	5 sec	
Melt curve	65°C- 95°C	5 sec every 0,5°C	

Extraction of secondary metabolites

Medium extraction.

The nonionic resin Amberlite® XAD7HP (Sigma Aldrich) was used to extract the content from the supernatant after centrifugation to get rid of cell residue. 60 g of Amberlite® XAD7HP was conditioned by rinsing it with 2L dH_2O three times, just enough100% MeOH to cover the resin grains once and left for 30 minutes, and finally washed with 2 L dH_2O another three times. Once the Amberlite® XAD7HP was thoroughly cleaned it was air-dried covered with aluminum foil to avoid dust, after drying the Amberlite® XAD7HP was distributed to six 250 mL Erlenmeyer flasks.

The supernatant was centrifuged to remove any cell residue, and then added to the flasks containing 60g dry Amberlite® XAD7HP, the flask opening was covered with aluminum foil, the supernatant-resin mixture was stirred at low pace (150 rpm) overnight. Compounds present in the medium should have adhered to the Amberlite® XAD7HP grains.

The supernatant-resin mixture was filtered in small amounts through a porcelain filter with a Whatman® quality 1 filter paper on top (90 mm Ø x 100), and the Amberlite® XAD7HP was collected and added to a 250 mL Erlenmeyer flask containing 50 mL of 100% MeOH and stirred at slow pace overnight. MeOH replaced the compounds attached to the Amberlite® XAD7HP grains and washed out the organic compounds.

A rotary evaporation device (Laborota 4011, Heidolph™ rotavapor system) was used to dry the solution. The device was set on auto, with approximately < 37°C and 150 rpm. When working on the rotavapor system it is important to ensure that the solution doesn't boil. The distilled MeOH was disposed of in appropriate waste bottles and left under the fume hood for evaporation.

The dry matter was first dissolved in 3.3 mL of MilliQ, then 3.3 mL 50% MeOH followed by 3.3 mL 100% MeOH, and the fractions were combined. The combined solution was aliquoted into 10 mL glass tubes and evaporated to dryness in SpeedVac Plus SC210A (Savant™) coupled with Refrigerated Condensation Trap RT400 (Savant™).

When dry the solids were washed out with 250 µL MQ, 250 µL 50% MeOH and then 250 µL 100% MeOH, before being collected in HPLC Vials. The total dissolved matter is 750 µL in 1:1 MeOH:MQ.

Cell extraction

The cells were harvested from 2 weeks old growing cultures (BG11/-Fe/-P, $BG11_0$/-Fe/-P), and the pellet was transferred to 15 mL falcon tubes. 5 mL 100% MeOH was added to the pellet before the samples were sonicated in a Branson Sonifier SFX250® to homogenize the samples, to release any compounds retained inside of the cells. Parameters of the sonicator were set to; 3 min, duty cycle 30 and output control to 5. The cycles were repeated when necessary. After sonication, the samples were centrifuged at 1500 rpm for 5 minutes, and the supernatant was collected. Then 3 mL of 50% MeOH was added to the pellet and centrifuged again, and the supernatant was collected. Finally, 3 mL of MQ water was added and the sample was centrifuged, and the supernatant was collected. The fractions were combined.

Then the combined fractions were filtered with Acrodisc® Syringe Filters 0.45 µm, 25 mm before transferring the fractions to 10 mL glass tubes. The fractions were evaporated to dryness in SpeedVac Plus SC210A (Savant™) coupled with Refrigerated Condensation Trap RT400 (Savant™). The dry solids were washed as described for medium extraction. Extraction of colonies from solid media were performed as described above.

Mass Spectrometry

15 µL from the different fractions were placed in two UPLC tubes with 100 µL 50% MeOH to dilute the samples. UPLC-HR-MS analysis was performed on the samples using a Waters Acquity I-class UPLC system (Milford, MA, USA) interfaced with a PDA Detector and a VION IMS-qTOF, using electrospray ionization (ESI) in positive mode, wavelengths from 190-500 nanometers were detected. VION IMS- qTOF conditions for UPLC-HR-MS analysis includes capillary voltage (0.80kV), cone gas (50 L/h), desolvation temperature (350°C), desolvation gas (800 L/h), source temperature (120°C) and acquisition range (m/z 50–2000) The system was controlled and data was processed using UNIFI 1.8.2 (Waters). Chromatographic separation was performed with an BEH C18 1.7 µm (2.1 × 100 mm) column (Waters) maintained at 40°C. Selected peaks were dereplicated using MarinLit, ChemSpider, and Dictionary of Natural products, as well as extensive literature searches.

Results

Since my primary focus and work was dedicated to KVJ20, the results presented for KVJ2 and KVJ10 are often compared to the results from KVJ20. In the sections below results from the bioinformatic analysis, microscopy, allelopathic assay, qPCR and UPLC-HR-MS are described.

Bioinformatics

The draft genome of KVJ2, KVJ10, and KVJ20 were submitted to the AntiSMASH tool. A summarize of the predicted gene clusters are included for each strain in Table 5, as well as illustrations of some of the predicted gene clusters with known products in Figure 13-15. From KVJ20 a total of 19 gene clusters were predicted, 17 from KVJ2 and 18 gene clusters from KVJ10. Homologous gene clusters are shown in Table 6-7.

Table 5: A summary of the predicted gene clusters in KVJ20, KVJ2, and KVJ10 from AntiSMASH.

	NRPS/PKS		***PKS***		***RiPP***	
	TL	**Identified**	**TL**	**Identified**	**TL**	**Identified**
KVJ20	**6**	Anabaenopeptin Nostocyclopeptide Suomilide/Banyaside (Aeruginosin)	**2**	Heterocyst glycolipid	**11**	Microviridins (2) Lanthipeptides (2)
KVJ2	**7**	Aeruginosin Anabaenopeptin Nostocyclopeptide	**3**	Heterocyst glycolipid	**7**	Microviridins (1) Lanthipeptides (1)
KVJ10	**9**	Hapalosin, Nosperin, Nostoginin*	**3**	Heterocyst glycolipid	**6**	Lanthipeptides (2)

Homologous gene clusters

For some of the gene clusters, corresponding homologs were found in the other strains. See Table 6 for corresponding homologs for the NRPS and the PKS gene clusters, and Table 7 for corresponding homologs for the RiPP gene clusters.

KVJ20 and KVJ2 showed great homology between the NRPS/PKS gene clusters, while only 4 gene clusters also had homology with gene cluster in KVJ10. The remaining of the gene clusters are unique for each strain. For the RiPP genes, KVJ20 and KVJ2 shared homology in 7 RiPPs, while only 2 gene clusters also had homology with gene clusters in KVJ10.

Table 6: Summary of NRPS/PKS homologs between KVJ20, KVJ2, and KVJ10. Abbreviations; Sid: containing siderophores. Val*: containing Valine-Valine bounds. Hgl*: Similarity to heterocyst glycolipids, S/B: Suomilide/Banyaside, Aer: Aeruginosin, Ncp: Nostocyclopeptide, Apt: Anabaenopeptin, Hgl: Heterocyst glycolipids.*

Product	***S/B/Aer***	***Ncp***	***Apt***	***Unknown Sid****	***Unknown***	***Unknown Val****	***Hgl***	***Hgl****
KVJ20	20-N1	20-N4	20-N2	20-NP2	20-N3	20-NP1	20-P1	20-P2
KVJ2	2-N2	2-N5	2-N6	2-N3	2-N1	2-N4	2-P3	2-P2
KVJ10	-	-	-	10-NP1	10-N1	10-NP4	10-P1	-

*Table 7: Summary of RiPP homologs between KVJ20, KVJ2, and KVJ10. *predicted to lanthipeptides. Mvd: Microviridin.*

Product	*RiPP*	*RiPP*	*RiPP*	*RiPP*	*RiPP*	*RiPP*	*Mvd*
KVJ20	20-RiPP1	20-RiPP2	20-RiPP3	20-RiPP4	20-RiPP5	20-RiPP6	20-RiPP8
KVJ2	2-RiPP5	2-RiPP1	2-RiPP3*	2-RiPP4	2-RiPP6	2-RiPP7	2-RiPP2
KVJ10	-	10-RiPP5*	10-RiPP6*	-	-	-	-

Nostoc KVJ20

From the resulting gene cluster predictions for KVJ20 from AntiSMASH, four gene clusters were assigned to a product. The identified gene clusters and their predicted homology with MiBiG BGC-ID to other cyanobacterial gene clusters are shown in Figure 13. Geosmin a biosynthetic gene cluster from *Nostoc punctiforme* was also predicted as a homologous gene cluster but was not included for primer design. For the remaining gene clusters, there were no significant homology found to other cyanobacteria or a product suggestion.

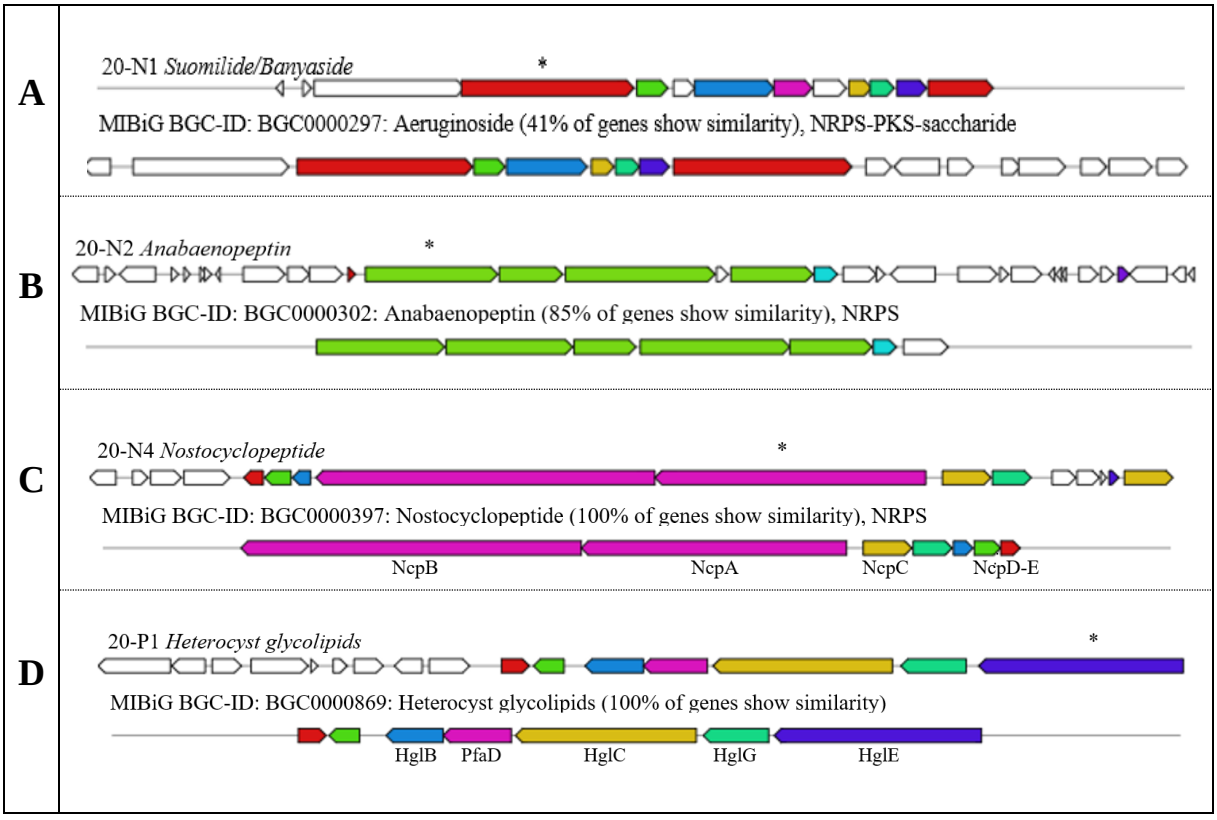

*Figure 13: Homologous known gene clusters from AntiSMASH with corresponding MIBiG BGC-ID. A: Cluster N1, Aeruginoside gene cluster from Planktothrix agardhii. B: Cluster N2, Anabaenopeptin gene cluster from Anabaena sp. 90. C: Cluster N4, Nostocyclopeptide gene cluster from Nostoc sp. ATCC. D: Cluster P1, Heterocyst glycolipid gene cluster from Nostoc sp. 'Peltigera membranacea cyanobiont'. The open reading frame marked with * was used for primer design. Abbreviations; Ncp: Nostocyclopeptide, Hgl: Heterocyst glycolipids, N1: NRPS1, N2: NRPS2, N4: NRPS4, P1: PKS1.*

Nostoc KVJ2

From the resulting gene cluster predictions for KVJ2 from AntiSMASH, four gene clusters were assigned to a product. The identified gene clusters and their predicted homology with MiBiG BGC-ID to other cyanobacterial gene clusters are shown in Figure 14. For the remaining gene clusters, there were no significant homology found to other cyanobacteria or a product suggestion.

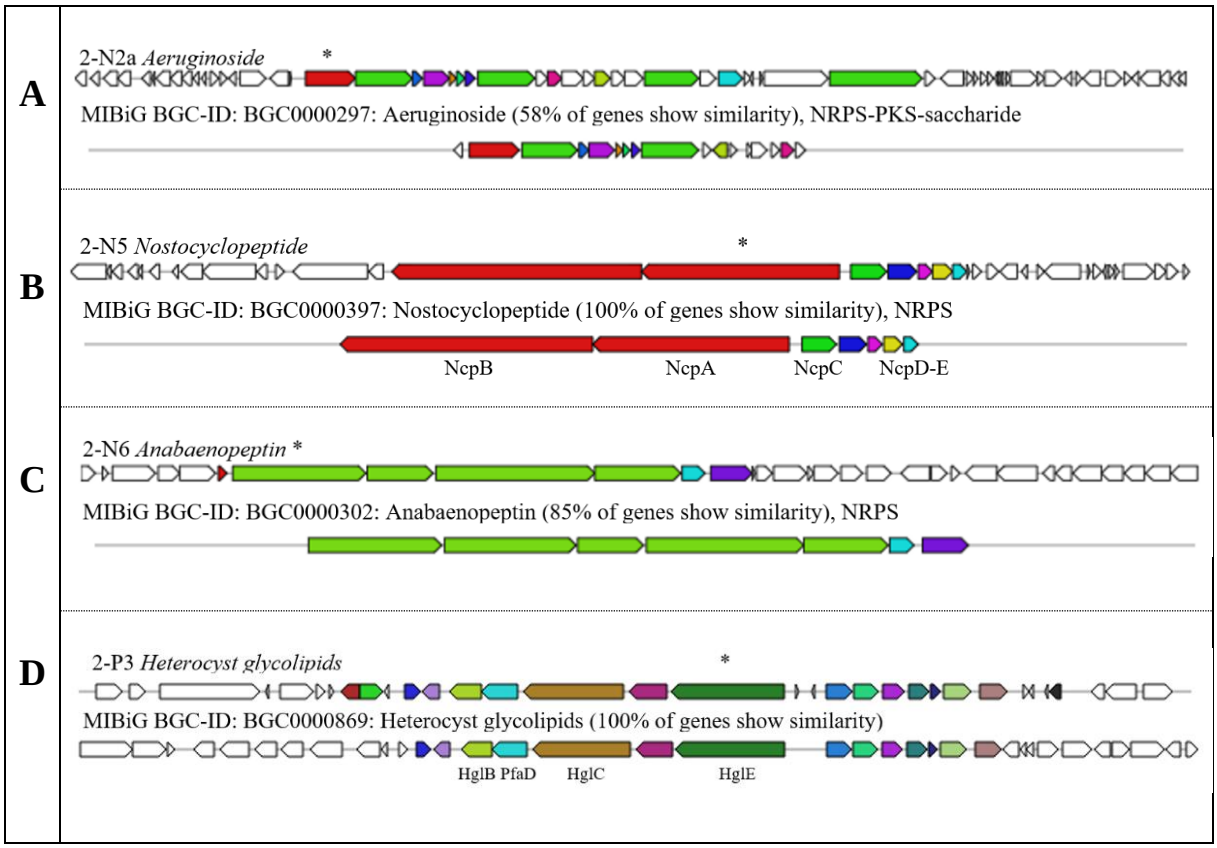

*Figure 14: Homologous known gene clusters from AntiSMASH with corresponding MIBiG BGC-ID. A: Cluster N2a, Aeruginoside gene cluster from Planktothrix agardhii. B: Cluster N5, Nostocyclopeptide gene cluster from Nostoc sp. ATCC. C: Cluster N6, Anabaenopeptin gene cluster from Anabaena sp. 90. D: Cluster P3, Heterocyst glycolipids gene cluster from Nostoc sp. 'Peltigera membranacea cyanobiont'. The open reading frame marked with * was used for primer design. Abbreviations; Ncp: Nostocyclopeptide, Hgl: Heterocyst glycolipids, N2a: NRPS2a, N5: NRPS5, N6: NRPS6, P3: PKS3.*

Nostoc KVJ10

From the resulting gene cluster predictions for KVJ10 from AntiSMASH, three gene clusters were assigned to a product. The identified gene clusters and their predicted homology with MiBiG BGC-ID to other cyanobacterial gene clusters are shown in Figure 15. From KVJ10 the NRPS2 was also predicted to be Nostoginin/Microginin from the Norine prediction tool. For the remaining gene clusters, there were no significant homology found to other cyanobacteria or a product suggestion.

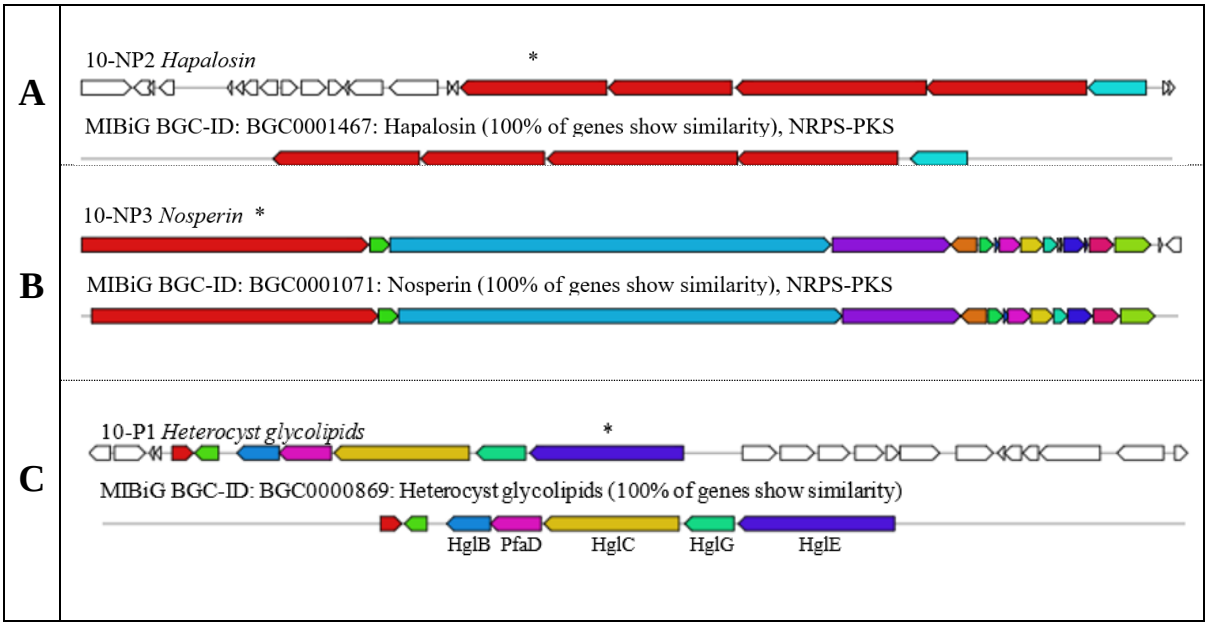

*Figure 15: Homologous known gene clusters from AntiSMASH with corresponding MIBiG BGC-ID. A: Cluster NP2, Hapalosin gene cluster from Fischerella sp. PCC 9431. B: Cluster NP3, Nosperin gene cluster from Nostoc sp. 'Peltigera membranacea cyanobiont'. C: Cluster P1, Heterocyst glycolipids gene cluster from Nostoc sp. 'Peltigera membranacea cyanobiont'. The open reading frame marked with * was used for primer design. Abbreviations: Hgl: Heterocyst glycolipids, NP2: NRPS/PKS2, NP3: NRPS/PKS3, P1: PKS1.*

Observed changes associated with different cultivation conditions.

The physiological appearance after one week is shown in Figure 16, clear differences in morphology were seen in all the different cultures. Growth both with and without nitrogen (N) appear as long filaments with vegetative cells, and without N regularly spaced heterocysts were observed. In starvation cultures, both with and without N a mayor morphological change could be observed, in the culture with N deprived of iron (+N-Fe) oversized heterocysts were observed, which is not usual for diazotrophic cyanobacteria cultures supplemented with N. And in culture without N deprived of iron (-N-Fe) an unusual morphological state, called aseriate growth was observed. In both starvation cultures without Phosphor (+/-N-P), the growth was poor, and the formation of survival cells, akinetes, were observed.

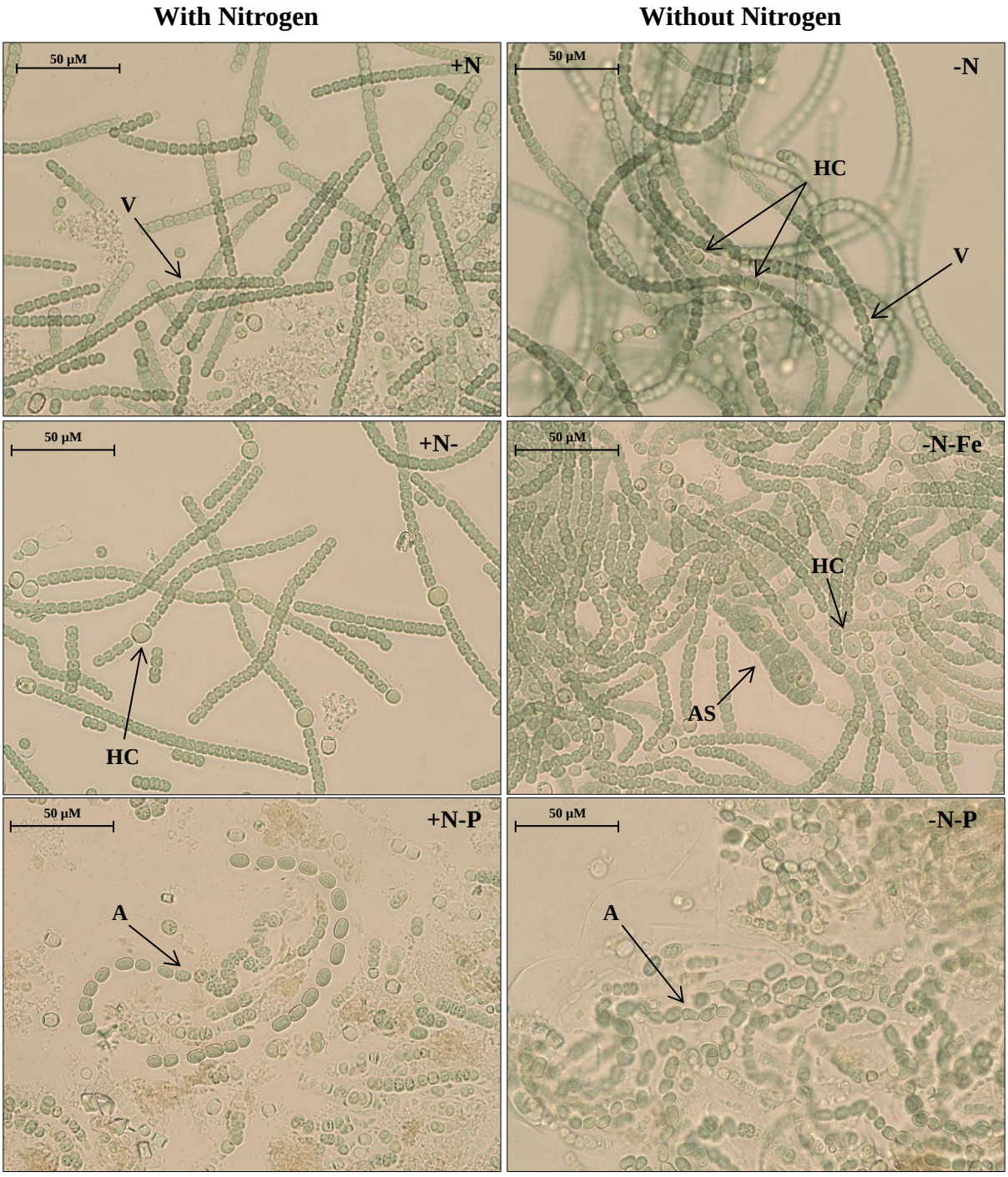

Figure 16: Microscopy pictures taken of KVJ20 cultivated under different cultivation parameters with Leica DFC420 fluorescence microscope under brightfield with a 40x objective. Abbreviations: N: nitrogen, Fe: Iron, P: Phosphate, V: Vegetative cells, HC: Heterocyst glycolipids, AS: aseriate growth, A: akinetes.

Allelopathic experiment

The three different strains were also cultivated on solid plates, as well as in interaction with each other to check for allelopathic abilities. In Figure 17 the results of these competition plates and the control on solid plates are shown.

All the competition plates were grown on plates without N, hence plates without N can be used as a control. In the competition plate with KVJ10 vs KVJ2, KVJ2 had weaker growth than the control and pigment change towards KVJ10, as well as vigorous spread away from KVJ10, which indicates that KVJ2 doesn't thrive in association with KVJ10, the same observation for spreading was made for KVJ20 in interaction with KVJ10. In the competition plate with KVJ2 vs KVJ20, KVJ2 has a slightly weaker growth, while KVJ20 seems to be unaffected, or even show better growth, both strains spread vigorously in no specific direction, which indicates that living in association with each other doesn't significantly affect growth.

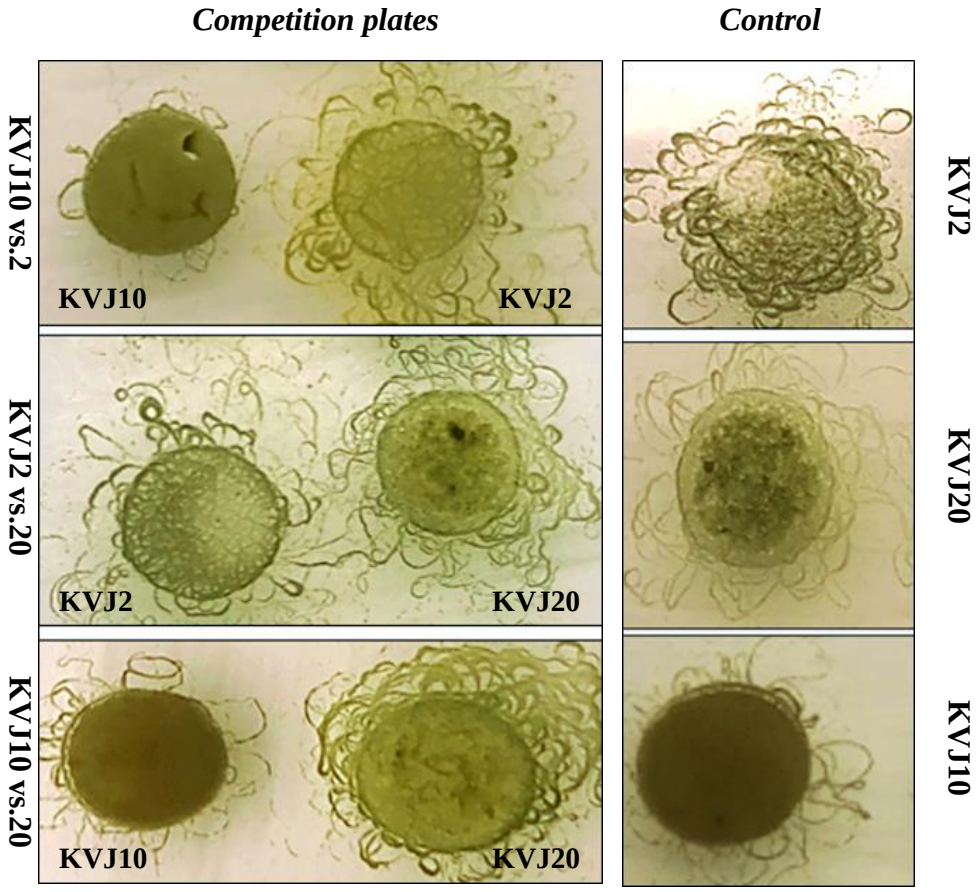

Figure 17: Results from allelopathic interactions between KVJ20, KVJ2 and KVJ10, and their respective controls.

Gene expression patterns

After primer design, all primers were tested and had a visible product in gel electrophorese and were considered liable for qPCR. The purity and concentration of RNA were measured using NanoDrop™ 2000 Spectrophotometer before cDNA synthesis and qPCR. The 260/280 ratio for most of the samples were close to 2.0, which indicated high purity of RNA, and no DNA contamination was observed in the samples.

For all the samples relative gene expression were calculated by the formula: $2^{-(cQgene - cQrnpB)}$, and fold changes from standard liquid media (-N) were calculated, as well as fold changes from respective controls. For clarification purposes, the samples and their respective controls are explained in Table 8. Several abbreviations are used in the sections below; FC: fold changes, -N: standard media = nitrogen deprived media ($BG11_0$), +N: nitrogen supplemented media (BG11), -P: phosphate deprived media, -Fe: iron deprived media, vs.2: interaction with KVJ2, vs.10: interaction with KVJ10 and vs.20: interaction with KVJ20. Other abbreviations are listed in the beginning. For gene expression upregulation was determined to be with values > 1.5, and downregulation with values < 0.6.

Table 8: Abbreviations and the explanation of samples and their respective controls.

Sample		***Explanation***
-N vs +N	**Liquid**	FC between -N and +N media in liquid culture.
	Solid	FC between -N and +N media in solid culture.
Solid vs. Liquid	**-N**	FC between -N solid culture and -N liquid culture.
	+N	FC between +N solid culture and +N liquid culture.
-P vs.+P	**-N**	FC between -N-P liquid and -N+P liquid culture.
	+N	FC between +N-P liquid and +N+P liquid culture.
-Fe vs.+Fe	**-N**	FC between -N-Fe liquid and -N+Fe liquid culture.
	+N	FC between +N-Fe liquid and +N+Fe liquid culture.
Competition vs. control	**vs. 2**	FC between interaction with KVJ2 and solid plate -N.
	vs. 10	FC between interaction with KVJ10 and solid plate -N.
	vs. 20	FC between interaction with KVJ20 and solid plate -N.

Analysis of gene expression patterns in KVJ20

Fold changes against respective controls for KVJ20

The fold changes in expression for KVJ20 between different growth conditions and their respective controls are shown in Table 9. Under diazotrophic growth (-N) in liquid culture compared with nitrogen supplemented media (-N vs. +N) the following gene clusters showed higher expression levels; *NifH*, *AvaK*, *N1 (S/B-like)*, *N3*, *RiPP2*, *RiPP6*, *RiPP9 (Mvd)* and *RiPP10 (Lan)*. The most notable change was recorded for *NifH* with 2.7 times increase. At the same time gene clusters *GvpC*, *PilT*, *P2*, *Ncp*, *NP1*, *RiPP3*, *RiPP5*, *RiPP7*, and *RiPP11* were expressed at lower levels than in +N. In solid culture -N compared with +N media *RiPP8* was recorded with 4x times increase in expression.

In solid culture compared with liquid (Solid vs. liquid) the following gene clusters showed higher expression levels in both -N and +N; *NifH*, *Hgl*, *S/B-like*, *Apt*, *NP2 (Sid)*, *RiPP2* and *RiPP9 (Mvd)*. The most notable change was recorded for *NP2 (Sid)* with a 20 and almost 12 times increase in -N and in +N, respectively. In addition, under diazotrophic growth, *Ncp* showed higher expression levels, while *N3* and *RiPP10 (Lan)* showed higher expression levels in cultures +N. At the same time gene clusters *AvaK*, *GvpC*, *PilT*, *NP1*, *RiPP4* and *RiPP8 (Mvd)* were expressed at lower levels than in liquid culture.

Under phosphate deprived media (-P) most of the genes were expressed at lower levels than in phosphate supplemented media in both -N and +N. However, the following gene clusters showed higher expression levels in +N media; *NifH*, *Apt*, *Ncp*, *NP2 (Sid)*, *RiPP7*, and *RiPP8 (Mvd)*. The most notable change was recorded for *Ncp* with 6 times increase in expression. In addition, *RiPP11 (Lan)* showed a ≈12 times increase in expression in phosphate deprived media, in both -N and +N.

Under iron deprived media, both in -N and +N the following genes showed higher expression levels than in iron supplemented media; *AvaK*, *Hgl*, *S/B-like*, and *Ncp*. The most notable change was recorded for *Ncp* with 19 and 3.5 times increase in -N and +N, respectively. In addition, *Apt* and *NP2 (Sid)* showed higher expression levels in -N-Fe, and *NifH*, *N3*, *NP1*, *RiPP1*, *RiPP2* and *RiPP10 (Lan)* showed higher expression levels in +N-Fe. At the same time gene clusters *P2*, *RiPP4*, *RiPP6*, *RiPP7* and *RiPP8 (Mvd)* were expressed at lower levels in iron deprived, both in -N and +N than in iron supplemented media. In interaction with KVJ2 and KVJ10 the following gene clusters showed higher expression levels than in control; *AvaK*, *GvpC*, *Ncp*, *NP1*, *RiPP5*, *RiPP8 (Mvd)* and *RiPP11 (Lan)*. The most notable change

was recorded for *Ncp* with a 6 and ≈8 times increase in interaction with KVJ2 and KVJ10 respectively. In addition, *PilT*, *Hgl*, *N3,* and *RiPP3* showed higher expression levels in interaction with KVJ2, with *PilT* being most prominent with 125 times increase in expression. At the same time gene clusters *NP2 (Sid)*, *RiPP2* and *RiPP6* were expressed at lower levels under competition than in control

Table 9: The fold changes in expression for KVJ20 in different cultivation and respective controls. Every value >1.5 and < 0.6 are in bold, and those with a significant increase is highlighted in dark grey. P=PKS, N=NRPS, NP=NRPS/PKS.

	-N vs.+N		***Solid vs. Liquid***		***-P vs.+P***		***-Fe vs.+Fe***		***Competition vs. control***	
Media	***Liquid***	***Solid***	***-N***	***+N***	***-N***	***+N***	***-N***	***+N***	***20 vs.2***	***20 vs.10***
20-NifH	**2,697**	1,122	**1,540**	**3,702**	0,611	**2,487**	1,488	**2,871**	**2,202**	1,466
20-AvaK	**2,345**	1,004	**0,050**	**0,118**	**0,373**	0,659	**1,745**	**4,852**	**2,045**	**2,466**
20-GvpC	**0,469**	1,022	**0,076**	**0,035**	**0,039**	**0,063**	1,059	**0,274**	**3,968**	**1,791**
20-PilT	**0,103**	1,068	**0,521**	**0,050**	**0,469**	**0,039**	1,360	**0,116**	**124,968**	0,869
20-P1 (Hgl)	1,368	1,254	**2,689**	**2,934**	**0,358**	**0,491**	**2,300**	**6,480**	**1,616**	1,356
20-P2	**0,593**	1,060	1,080	0,604	**0,166**	**0,124**	**0,157**	**0,090**	0,972	**0,440**
20-N1 (S/B like)	**2,330**	1,073	**2,211**	**4,803**	**0,090**	**0,275**	**1,536**	**1,988**	0,775	1,130
20-N2 (Apt)	1,084	1,110	**2,385**	**2,329**	**0,333**	**1,597**	**1,788**	0,844	1,137	1,142
20-N3	**2,093**	1,083	1,079	**2,087**	**0,357**	1,215	**0,508**	**4,356**	**2,367**	1,367
20-N4 (Ncp)	**0,192**	1,214	**4,167**	0,660	**0,199**	**6,040**	**19,190**	**3,547**	**6,242**	**7,787**
20-NP1 (Val-Val)	**0,495**	1,069	**0,566**	**0,262**	**0,399**	1,124	0,753	**1,846**	**1,818**	**1,572**
20-NP2 (Sid)	0,606	1,053	**19,977**	**11,498**	0,776	**1,749**	**2,408**	**0,561**	**0,107**	**0,321**
20- RiPP1	0,930	1,189	**1,584**	1,239	0,921	0,957	1,409	**2,684**	0,611	**0,428**
20-RIPP2	**2,276**	1,040	**1,549**	**3,392**	**0,443**	0,917	**0,142**	**1,774**	**0,506**	**0,386**
20-RIPP3	**0,204**	1,018	0,855	**0,171**	1,090	**0,249**	1,428	**0,254**	**1,945**	1,061
20-RIPP4	0,904	1,009	**0,494**	**0,443**	**0,179**	**0,178**	**0,165**	**0,126**	1,138	**0,551**
20-RIPP5	**0,287**	1,021	1,008	**0,283**	1,008	0,970	0,629	**0,340**	**3,318**	**2,622**
20-RIPP6	**1,788**	1,001	1,442	**2,577**	**0,173**	**0,374**	**0,068**	**0,424**	**0,456**	**0,484**
20-RIPP7	**0,488**	1,010	1,112	**0,538**	1,376	**2,938**	**0,497**	**0,591**	1,488	0,915
20-RIPP8 (Mvd)	1,128	**4,063**	**0,533**	**0,148**	**0,228**	**4,325**	**0,455**	**0,307**	**4,072**	**2,669**
20-RIPP9 (Mvd)	**1,649**	1,003	**2,398**	**3,943**	**0,123**	**0,489**	0,921	1,466	0,793	0,665
20-RIPP10 (Lan)	**2,469**	1,088	1,366	**3,100**	**0,082**	**0,181**	1,185	**2,575**	0,652	0,666
20-RIPP11 (Lan)	**0,331**	1,054	1,182	**0,371**	**12,964**	**12,607**	1,044	**0,367**	**4,811**	**1,856**

Fold changes against standard media (-N) for KVJ20

Fold changes for relative expression from standard liquid media (-N) for KVJ20 is shown in Table 10. In nitrogen supplemented media (+N) the following genes showed higher expression levels; *Gvp*C, *PilT*, *P2*, *Ncp*, *NP1*, *NP2 (Sid)*, *RiPP3*, *RiPP5*, *RiPP7*, and *RiPP11 (Lan)*. Where the most notable changes were recorded for *PilT* and *Ncp* with ≈10 times and 5 times increase. In solid media both with (+N solid) and without nitrogen (-N solid) the following genes showed higher expression levels; *Hgl*, *S/B-like*, *Apt*, *Ncp*, *NP2 (Sid)*, and *RiPP9 (Mvd)*. The most notable changes were recorded for *NP2 (Sid)* with 20 times and 19 times increase in -N and +N, respectively.

In phosphate deprived media with nitrogen (+N-P) the following genes showed higher expression levels; *Ncp*, *NP1*, *NP2 (Sid)*, *RiPP5*, *RiPP7*, *RiPP8 (Mvd)* and *RiPP11 (Lan)*. The most notable changes were recorded for *Ncp* and *RiPP11 (Lan)* with 31 and 38 times increase, respectively. In iron deprived media both with (+N-Fe) and without nitrogen (-N-Fe) the following genes showed higher expression levels; *AvaK*, *Hgl*, and *Ncp*. The most notable changes were recorded for *Ncp* with ≈19 times increase. In addition, the *S/B-like*, *Apt* and *NP2 (Sid)* showed higher expression levels in -N-Fe, while *N3*, *NP1*, and *RiPP1* showed higher expression levels in +N-Fe.

In interaction with KVJ2 and KVJ10 the following gene clusters showed higher expression levels; *NifH*, *Hgl*, *S/B-like*, *Apt*, *Ncp*, *NP2 (Sid)*, *RiPP5*, and *RiPP9 (Mvd)*. The most notable changes were recorded for *Ncp* with 26 times and 32 times increase in interaction with KVJ2 and KVJ10, respectively. In addition, the *PilT*, *N3*, *RiPP3*, *RiPP7*, *RiPP8 (Mvd)*, and *RiPP11 (Lan)* showed higher expression levels in interaction with KVJ2, most notably the *PilT* gene with 65 times increase.

Table 10: Fold changes for relative expression against standard liquid media (-N) for KVJ20. Every value >1.5 and <0.6 are in bold, and those with a significant increase is highlighted in dark grey. P=PKS, N=NRPS, NP=NRPS/PKS

	+N	***-N Solid***	***+N Solid***	***-N-P***	***+N-P***	***-N-Fe***	***+N-Fe***	***20 vs.2***	***20 vs.10***
20-NifH	**0,371**	**1,540**	1,373	0,611	0,922	1,488	1,065	**3,391**	**2,258**
20-AvaK	**0,426**	**0,050**	**0,050**	**0,373**	**0,281**	**1,745**	**2,069**	**0,103**	**0,124**
20-GvpC	**2,132**	**0,076**	**0,074**	**0,039**	**0,133**	1,059	**0,584**	**0,302**	**0,136**
20-PilT	**9,722**	**0,521**	**0,487**	**0,469**	**0,381**	1,360	1,129	**65,051**	**0,452**
20-P1 (Hgl)	0,731	**2,689**	**2,145**	**0,358**	**0,359**	**2,300**	**4,737**	**4,345**	**3,646**
20-P2	**1,688**	1,080	1,019	**0,166**	**0,209**	**0,157**	**0,152**	1,051	**0,475**
20-N1 (S/B like)	**0,429**	**2,211**	**2,061**	**0,090**	**0,118**	**1,536**	0,853	**1,715**	**2,498**
20-N2 (Apt)	0,923	**2,385**	**2,149**	**0,333**	1,474	**1,788**	0,779	**2,712**	**2,724**
20-N3	**0,478**	1,079	0,997	**0,357**	**0,580**	**0,508**	**2,081**	**2,554**	1,475
20-N4 (Ncp)	**5,197**	**4,167**	**3,432**	**0,199**	**31,392**	**19,190**	**18,436**	**26,009**	**32,444**
20-NP1 (Val-Val)	**2,020**	**0,566**	**0,530**	**0,399**	**2,270**	0,753	**3,730**	1,030	0,890
20-NP2 (Sid)	**1,650**	**19,977**	**18,976**	0,776	**2,886**	**2,408**	0,925	**2,134**	**6,411**
20- RiPP1	1,075	**1,584**	1,332	0,921	1,030	1,409	**2,886**	0,967	0,678
20-RIPP2	**0,439**	**1,549**	1,490	**0,443**	**0,403**	**0,142**	0,779	0,785	**0,598**
20-RIPP3	**4,895**	0,855	0,839	1,090	1,218	1,428	1,245	**1,663**	0,907
20-RIPP4	1,106	**0,494**	**0,490**	**0,179**	**0,196**	**0,165**	**0,139**	**0,562**	**0,272**
20-RIPP5	**3,486**	1,008	0,988	1,008	**3,381**	0,629	1,185	**3,346**	**2,644**
20-RIPP6	**0,559**	1,442	1,441	**0,173**	**0,209**	**0,068**	**0,237**	0,658	0,698
20-RIPP7	**2,048**	1,112	1,102	1,376	**6,018**	**0,497**	1,211	**1,655**	1,018
20-RIPP8 (Mvd)	0,886	**0,533**	**0,131**	**0,228**	**3,833**	**0,455**	**0,272**	**2,168**	1,422
20-RIPP9 (Mvd)	0,607	**2,398**	**2,391**	**0,123**	**0,296**	**0,921**	**0,889**	**1,902**	**1,595**
20-RIPP10 (Lan)	**0,405**	1,366	1,256	**0,082**	**0,073**	1,185	1,043	0,891	0,910
20-RIPP11 (Lan)	**3,017**	1,182	1,121	**12,964**	**38,041**	1,044	1,106	**5,684**	**2,193**

Analysis of gene expression patterns in KVJ2

Fold changes against respective controls for KVJ2

The fold changes in expression for KVJ2 between different growth conditions and their respective controls are shown in Table 11. Under diazotrophic growth (-N) in liquid and solid culture compared with nitrogen supplemented media (-N vs. +N) the following gene clusters showed higher expression levels; *NifH*, *PilT*, *P2*, *N1*, *N4*, *RiPP1*, *RiPP2 (Mvd)*, and *RiPP4*. The most notable change was recorded for *NifH* and *RiPP4* with 140 and 43 times increase in liquid -N, respectively. In addition, the following genes showed higher expression levels in -N liquid; *AvaK*, *P1*, *Hgl*, *Aer*, *Ncp*, *Apt*, and *RiPP7*, with *AvaK* showing 22 times increase in expression. At the same time, the gene cluster *RiPP5* were expressed at lower levels than in +N.

In solid culture -N compared with liquid (Solid vs. liquid) most of the genes were expressed at lower levels than in liquid culture. However, the following gene clusters showed higher expression levels in +N solid culture; *NifH*, *AvaK*, *Hgl*, *Aer*, *N3*, *Ncp*, and *Apt.* Where *N3* also was seen with higher expression levels in -N. The most notable changes were recorded for *NifH* and *AvaK* with a 31 and almost 15 times increase, respectively. At the same time gene clusters *N4*, *RiPP1*, *RiPP3 (Lan)*, *RiPP5* and *RiPP6* were expressed at lower levels than in liquid culture. Under phosphate deprived media (-P vs.+P) most of the genes were expressed at lower levels than in phosphate supplemented media in both -N and +N. However, *AvaK* and *P1* were found with higher expression levels in -N, and *N1* and *RiPP4* with higher expression levels in +N. The most notable change was recorded for *RiPP4* in +N with 10 times increase in expression.

Under iron deprived media (-Fe vs.+Fe) the following genes showed higher expression levels in -N-Fe than in iron supplemented media; *Aer*, *N3*, *RiPP3 (Lan)*, *RiPP5*, and *RiPP6.* The most notable change was recorded for *RiPP5* with ≈5 times increase. At the same time the gene clusters *AvaK*, *P1*, and *P2* were expressed at lower levels than in iron supplemented media. In +N-Fe the following genes showed higher expression levels than in iron supplemented media; *PilT*, *RiPP1*, and *RiPP4*, where *RiPP4* were recorded with 13 times increase in expression. At the same time, the *RiPP6* gene was expressed at lower levels than in iron supplemented media.

In interaction with KVJ10 and KVJ20 the following gene clusters showed higher expression levels than in control; *N1*, *RiPP3 (Lan)* and *RiPP6*. The most notable changes were recorded

for *N1* with 3 times increase with KVJ10, and *RiPP3 (Lan)* with 5 times increase with KVJ20. In addition, *N2b* and *RiPP6* showed higher expression levels with KVJ10, and *P1*, *N3*, *RiPP5* and *RiPP7* showed higher expression levels with KVJ20. At the same time, several gene clusters were expressed at lower levels under competition, especially with KVJ10.

Table 11: The fold changes in expression for KVJ2 in different cultivation and respective controls. Every value >1.5 and < 0.6 are in bold, and those with a significant increase is highlighted in dark grey. P=PKS, N=NRPS, NP=NRPS/PKS.

	-N vs. N		***Solid vs. Liquid***		***-P vs.+P***		***-Fe vs.+Fe***		***Competition vs. control***	
Media	***Liquid***	***Solid***	***-N***	***+N***	***-N***	***+N***	***-N***	***+N***	***2 vs.10***	***2 vs.20***
2-NifH	**140,800**	**2,144**	**0,471**	**30,964**	**0,585**	0,977	0,901	0,944	**0,014**	1,066
2-AvaK	**22,549**	**0,372**	**0,241**	**14,647**	**3,979**	0,773	**0,590**	0,811	**0,022**	**0,516**
2-PilT	**3,482**	**3,074**	1,233	1,397	0,176	0,691	1,059	**1,633**	**0,044**	**0,503**
2-P1	**5,098**	1,123	**0,174**	0,791	**1,583**	**0,571**	**0,599**	0,919	0,746	**2,211**
2-P2	**23,466**	**8,126**	**0,237**	0,685	**0,030**	1,092	**0,438**	1,050	**0,113**	0,908
2-P3 (Hgl)	**2,923**	1,063	0,630	**1,732**	**0,488**	1,466	1,259	1,451	0,671	1,301
2-N1	**3,122**	**1,553**	**0,539**	1,083	1,206	**1,558**	1,268	1,426	**3,312**	**1,540**
2-N2a (Aer)	**7,235**	1,063	1,019	**6,940**	0,630	0,796	**1,784**	0,928	**0,066**	1,035
2-N2b	0,818	1,412	0,914	**0,529**	**0,236**	**0,480**	1,149	1,264	**1,726**	1,343
2-N3	0,904	1,167	**1,962**	**1,521**	**0,497**	0,833	**2,301**	0,846	**0,424**	**1,815**
2-N4	**3,972**	**4,257**	**0,404**	**0,377**	0,791	0,602	0,848	0,789	0,892	1,167
2-N5 (Ncp)	**3,706**	0,841	0,755	**3,329**	0,667	0,803	1,106	1,016	**0,072**	1,115
2-N6 (Apt)	**5,426**	1,474	0,719	**2,648**	**0,523**	**0,484**	0,751	1,118	**0,144**	1,075
2-RiPP1	**4,112**	**9,334**	**0,395**	**0,174**	**0,112**	1,251	0,968	**2,019**	**0,093**	1,297
2-RiPP2 (Mvd)	**3,058**	**1,513**	**0,558**	1,127	**0,173**	**0,631**	1,472	0,886	**0,300**	0,871
2-RiPP3 (Lan)	0,726	**0,396**	**0,302**	**0,553**	**0,155**	**0,531**	**1,806**	0,895	**2,132**	**5,389**
2-RiPP4	**43,638**	**3,358**	**0,074**	0,964	**0,100**	**10,068**	0,860	**13,501**	**0,208**	1,402
2-RiPP5	**0,401**	**0,581**	**0,503**	**0,346**	**0,306**	0,642	**4,659**	0,851	1,072	**3,965**
2-RiPP6	**0,564**	**1,532**	**0,196**	**0,072**	**0,287**	0,656	**3,204**	**0,477**	**1,886**	**4,007**
2-RiPP7	**8,056**	0,677	**0,055**	0,651	**0,023**	0,682	0,606	0,799	1,270	**3,005**

Fold changes against standard media for KVJ2

Fold changes for relative expression from standard liquid media (-N) for KVJ2 is shown in Table 12. In nitrogen supplemented media (+N) the *RiPP5* and *RiPP6* gene showed higher expression levels, where *RiPP5* showed 2.5 times increase in expression. In solid media both with (+N solid) and without nitrogen (-N solid) the *N3* gene showed higher expression levels.

In phosphate deprived media without nitrogen (-N-P) the *AvaK* and *P1* gene showed higher expression levels, and in +N-P the *RiPP5* gene showed higher expression levels. The most notable changes were recorded for *AvaK* in -N-P with 4 times increase in expression. In iron deprived media without nitrogen (-N-Fe) the *Aer*, *N3*, *RiPP3 (Lan)* and *RiPP5* genes showed higher expression levels, while in +N-Fe the *N2b* and *RiPP5* genes showed higher expression levels. The most notable change was recorded from *RiPP5* in -N-Fe with 4.7 times increase in expression compared with standard cultivation.

In interaction with KVJ10, the *N1* and *N2b* gene clusters showed higher expression levels and with KVJ20 the following genes showed higher expression levels; *N3*, *RiPP3 (Lan)* and *RiPP5*. The most notable changes were recorded for *N3* with 3.5 times in interaction with KVJ20.

Table 12: Fold changes for relative expression against standard liquid media (-N) for KVJ2. Every value >1.5 and <0.6 are in bold, and those with a significant increase is highlighted in dark grey. P=PKS, N=NRPS, NP=NRPS/PKS.

	+N	***-N Solid***	***+N solid***	***-N-P***	***+N-P***	***-N-Fe***	***+N-Fe***	***2 vs.10***	***2 vs.20***
2-NifH	**0,007**	**0,471**	**0,220**	**0,585**	**0,007**	0,901	**0,007**	**0,007**	**0,503**
2-AvaK	**0,044**	**0,241**	0,650	**3,979**	**0,034**	**0,590**	**0,036**	**0,005**	**0,125**
2-PilT	**0,287**	1,233	**0,401**	**0,176**	**0,199**	1,059	**0,469**	**0,055**	**0,620**
2-P1	**0,196**	**0,174**	**0,155**	**1,583**	**0,112**	**0,599**	**0,180**	**0,130**	**0,386**
2-P2	**0,043**	**0,237**	**0,029**	**0,030**	**0,047**	**0,438**	**0,045**	**0,027**	**0,215**
2-P3 (Hgl)	**0,342**	0,630	**0,593**	**0,488**	**0,501**	1,259	**0,496**	**0,423**	0,819
2-N1	**0,320**	**0,539**	**0,347**	1,206	**0,499**	1,268	**0,457**	**1,784**	0,829
2-N2a (Aer)	**0,138**	1,019	0,959	0,630	**0,110**	**1,784**	**0,128**	**0,067**	1,055
2-N2b	1,223	0,914	0,647	**0,236**	**0,587**	1,149	**1,545**	**1,577**	1,227
2-N3	1,106	**1,962**	**1,682**	**0,497**	0,921	**2,301**	0,935	0,832	**3,562**
2-N4	**0,252**	**0,404**	**0,095**	0,791	**0,152**	0,848	**0,199**	**0,360**	**0,471**
2-N5 (Ncp)	**0,270**	0,755	0,898	0,667	**0,217**	1,106	**0,274**	**0,054**	0,842
2-N6 (Apt)	**0,184**	0,719	**0,488**	**0,523**	**0,089**	0,751	**0,206**	**0,103**	0,774
2-RiPP1	**0,243**	**0,395**	**0,042**	**0,112**	**0,304**	0,968	**0,491**	**0,037**	**0,512**
2-RiPP2 (Mvd)	**0,327**	**0,558**	**0,369**	**0,173**	**0,206**	1,472	**0,290**	**0,168**	**0,485**
2-RiPP3 (Lan)	1,378	**0,302**	0,762	**0,155**	0,732	**1,806**	1,233	0,644	**1,627**
2-RiPP4	**0,023**	**0,074**	**0,022**	**0,100**	**0,231**	0,860	**0,309**	**0,015**	**0,104**
2-RiPP5	**2,497**	**0,503**	0,865	**0,306**	**1,604**	**4,659**	**2,124**	**0,539**	**1,993**
2-RiPP6	**1,775**	**0,196**	**0,128**	**0,287**	1,165	3,204	0,846	**0,369**	0,785
2-RiPP7	**0,124**	**0,055**	**0,081**	**0,023**	**0,085**	0,606	**0,099**	**0,069**	**0,164**

Analysis of gene expression patterns in KVJ10

Fold changes against respective controls in KVJ10

The fold changes in expression for KVJ10 between different growth conditions and their respective controls are shown in Table 13. Under diazotrophic growth (-N) in liquid and solid culture compared with nitrogen supplemented media (-N vs. +N) the following gene clusters showed higher expression levels; *NifH*, *GvpC*, *Hgl*, *NP4*, and *NP5*. The most notable changes were recorded for *Hgl* and *NifH* with 25 and 15 times increase in liquid -N, respectively. In addition, the following genes showed higher expression levels in -N liquid; *N3*, *Hap*, *RiPP3*, and *RiPP4*, while *AvaK* showed higher expression levels in -N solid. At the same time several genes clusters were expressed at lower levels in -N solid; *P2*, *P3*, *N1*, *Ngn*, *RiPP1*, *RiPP3* and *RiPP5 (Lan)*.

In solid culture compared with liquid (Solid vs. liquid) both in -N and in +N the following gene clusters showed higher expression levels; *N3*, *NP1*, *Hap*, *NP4*, *NP5*, and *RiPP6 (Lan)*.

The most notable changes were recorded for *NP1* and *NP4* with 11 and 6 times increase in +N solid culture. In addition, the following gene clusters showed higher expression levels in -N solid culture; *AvaK*, *P3*, *N4*, and *RiPP2*, with *AvaK* showing a 10-fold increase in expression. While in +N solid culture the following gene clusters showed higher expression levels; *Hgl*, *P2*, *Ngn*, *RiPP1*, *RiPP3*, *RiPP4*, and *RiPP5 (Lan)*. Where *RiPP1* showed 5.4 times increase in expression. At the same time, the *GvpC* and *Ngn* genes were expressed at lower levels in -N solid than in -N liquid culture.

Under phosphate deprived growth (-P vs.+P) the following genes showed higher expression levels in -N-P than in phosphate supplemented media; *NifH*, *AvaK*, *P2*, and *N4*. With *P2* having the most notable change with 3 times increase. In +N-P the *P2* and *NP4* genes showed higher expression levels than in phosphate supplemented media. At the same time gene clusters *GvpC*, *N3*, *NP1*, and *RiPP3* were expressed at lower levels in both -N and +N. In addition, the gene clusters *NP4*, *NP5*, *RiPP1*, and *RiPP4* were expressed at lower levels in -N-P, while *NifH*, *P3*, and *Hap* were expressed at lower levels in +N-P.

Under iron deprived media (-Fe vs.+Fe) without nitrogen (-N-Fe) the following genes showed higher expression levels in than in iron supplemented media; *NifH*, *AvaK*, *Hgl*, *P2*, *N4*, *RiPP1*, *RiPP3*, and *RiPP5 (Lan)*. In +N-Fe the following genes showed higher expression levels than in iron supplemented media; *Hgl*, *NP1*, and *RiPP5 (Lan)*. The most notable changes were recorded for *AvaK* and *RiPP1* with ≈27 and 6.6 times increase in expression in -N-Fe, respectively. At the same time, the gene clusters *GvpC* and *RiPP6 (Lan)* were expressed at lower levels in -N-Fe, while *P3* was expressed at lower levels in +N-Fe.

In interaction with KVJ2 and KVJ20 the following gene clusters showed higher expression levels than in control; *Hgl*, *N1*, *N3*, *N4*, *Nsp*, *RiPP1*, *RiPP2*, *RiPP3* and *RiPP6 (Lan)*. In addition, *P2* and *NP5* showed higher expression levels with KVJ2, with *P2* showing a 73-fold increase in expression. In interaction with KVJ20 the following gene clusters showed higher expression levels than in control; *NifH*, *GvpC*, *Ngn*, *Hap*, and *RiPP4*, with *RiPP4* showing a 4- fold increase in expression. The most notable change was recorded for *RiPP1* with 86 times increase with KVJ2. At the same time the gene clusters *AvaK*, *NP1* and *RiPP5 (Lan)* were expressed at lower levels in both -N and +N.

Table 13: The fold changes in expression for KVJ10 in different cultivation and respective controls. Every value >1.5 and < 0.6 are in bold, and those with a significant increase is highlighted in dark grey. P=PKS, N=NRPS, NP=NRPS/PKS.

	-N vs.+N		***Solid vs. Liquid***		***-P vs.+P***		***-Fe vs.+Fe***		***Competition vs. control***	
Media	***Liquid***	***Solid***	***-N***	***+N***	***-N***	***+N***	***-N***	***+N***	***10 vs.2***	***10 vs.20***
10-NifH	**14,963**	**14,025**	0,886	0,945	**1,998**	**0,264**	**2,834**	1,040	**0,109**	**3,115**
10-AvaK	**0,338**	**3,179**	**10,086**	1,074	**1,962**	1,416	**26,842**	1,266	**0,062**	**0,136**
10-GvpC	**4,621**	**1,667**	**0,448**	1,242	**0,167**	**0,188**	**0,586**	1,000	**0,373**	**3,428**
10-P1 (Hgl)	**24,770**	**5,346**	0,827	**3,831**	1,035	0,697	**2,160**	**1,516**	**1,787**	**2,407**
10-P2	0,941	**0,206**	1,009	**4,605**	**2,937**	**1,504**	**2,581**	1,453	**73,460**	1,357
10-P3	**0,332**	**0,595**	**1,738**	0,970	1,252	**0,333**	1,085	**0,295**	0,860	0,742
10-N1	**0,302**	**0,217**	0,746	1,040	1,291	0,846	1,565	0,867	**2,270**	**2,444**
10-N2 (Ngn)	0,867	**0,289**	**0,572**	**1,712**	1,137	1,252	1,469	1,109	0,690	**2,188**
10-N3	**2,212**	1,373	**1,530**	**2,465**	**0,161**	**0,241**	1,066	0,610	**7,716**	**2,198**
10-N4	**0,398**	0,683	**2,046**	1,192	**2,700**	1,107	**3,334**	1,055	**4,158**	**1,728**
10-NP1	**2,898**	0,935	**3,612**	**11,196**	**0,223**	**0,451**	1,157	**2,406**	**0,305**	**0,503**
10-NP2 (Hap)	**2,328**	1,266	**1,912**	**3,516**	0,635	**0,501**	1,043	1,394	**0,017**	**2,046**
10-NP3 (Nsp)	0,942	1,137	0,990	0,820	1,101	0,904	1,220	0,915	**1,830**	**1,624**
10-NP4	**5,662**	**2,074**	**2,236**	**6,104**	**0,488**	**2,552**	1,058	1,132	1,141	**0,258**
10-NP5	**1,678**	**1,639**	**2,189**	**2,241**	**0,237**	0,601	1,233	1,442	**2,558**	0,898
10-RiPP1	1,076	**0,286**	1,437	**5,412**	**0,461**	0,726	**6,621**	0,752	**86,572**	**2,171**
10-RiPP2	**0,542**	1,368	**1,922**	0,762	1,097	0,794	0,674	0,628	**11,150**	**1,690**
10-RiPP3	**2,463**	**0,486**	0,705	**3,574**	**0,257**	**0,412**	**5,397**	0,866	**48,897**	**1,946**
10-RiPP4	**1,514**	0,779	1,446	**2,812**	**0,483**	1,236	1,467	1,115	**0,241**	**3,985**
10-RIPP5 (Lan)	0,624	**0,290**	1,062	**2,286**	0,683	1,284	**1,674**	**1,635**	**0,182**	**0,511**
10-Ripp6 (Lan)	0,782	0,666	**1,790**	**2,099**	1,230	0,719	**0,559**	0,793	**14,150**	**1,978**

Fold changes against standard media (-N) for KVJ10

Fold changes for relative expression from standard liquid media (-N) for KVJ10 is shown in Table 14. In nitrogen supplemented media (+N) the following gene clusters showed higher expression levels; *AvaK*, *P3*, *N1*, *N4*, *RiPP2*, and *RiPP5 (Lan).* The most notable change was recorded for *N1* with 3.3 times increase.

In solid media both with (+N solid) and without nitrogen (-N solid) the following gene clusters showed higher expression levels; *AvaK*, *P3*, *N4*, *NP1*, *Hap*, and *RiPP6 (Lan)*. In addition, *N3*, *NP4*, *NP5*, and *RiPP2* were expressed at higher levels. At the same time the gene clusters *P2*, *N1*, *Ngn*, *RiPP1*, *RiPP4*, and *RiPP5 (Lan)* were expressed at higher levels in +N solid. Where the most notable changes were recorded for *AvaK* in -N solid and *RiPP1* in +N solid, with 10 and 5 times increase, respectively.

In phosphate deprived media both with (+N-P) and without nitrogen (-N-P) the following gene clusters showed higher expression levels; *AvaK*, *P2*, and *N4*. In addition, the *NifH* gene cluster was greater expressed in -N-P, while in +N-P the *N1* and *RiPP5 (Lan)* gene clusters showed higher expression levels. The most notable change was recorded for *AvaK* in +N-P with 4 times increase in expression. In iron deprived media both with (+N-Fe) and without

nitrogen (-N-Fe) the following gene clusters showed higher expression levels; *AvaK*, *P2*, *N1*, *N4*, and *RiPP5 (Lan)*. In addition, in -N-Fe the following gene clusters showed higher expression levels; *NifH*, *Hgl*, *RiPP1*, and *RiPP3*. The most notable changes were recorded for *AvaK* and *RiPP1* in -N-Fe with 27 and 6.6 times increase in expression.

In interaction with KVJ2 and KVJ20 the following gene clusters showed higher expression levels; *N1*, *N3*, *N4*, *Nsp*, *NP5*, *RiPP1*, *RiPP2*, and *RiPP6 (Lan)*. In addition, the *P2*, *NP4*, and the *RiPP3* gene showed higher expression levels. While the following gene clusters showed higher expression levels with KVJ20; *NifH*, *GvpC*, *Hgl*, *NP1*, *Hap*, and *RiPP4*. The most notable changes were recorded for *P2* and *RiPP1* with KVJ2, with 74 and 124 times increase in expression, respectively.

Table 14: Fold changes for relative expression against standard liquid media (-N) for KVJ10. Every value >1.5 and <0.6 are in bold, and those with a significant increase is highlighted in dark grey. P=PKS, N=NRPS, NP=NRPS/PKS.

	+N	***-N Solid***	***+N Solid***	***-N-P***	***+N-P***	***-N-Fe***	***+N-Fe***	***10 vs.2***	***10 vs.20***
10-NifH	**0,067**	0,886	**0,063**	**1,998**	**0,018**	**2,834**	**0,070**	**0,097**	**2,759**
10-AvaK	**2,954**	**10,086**	**3,173**	**1,962**	**4,184**	**26,842**	**3,741**	0,624	1,374
10-GvpC	**0,216**	**0,448**	**0,269**	**0,167**	**0,041**	**0,586**	**0,216**	**0,167**	**1,536**
10-P1 (Hgl)	**0,040**	0,827	**0,155**	1,035	**0,028**	**2,160**	**0,061**	1,477	**1,990**
10-P2	1,062	1,009	**4,892**	**2,937**	**1,598**	**2,581**	**1,544**	**74,133**	1,369
10-P3	**3,013**	**1,738**	**2,923**	1,252	1,004	1,085	0,888	1,494	1,289
10-N1	**3,310**	0,746	**3,444**	1,291	**2,799**	**1,565**	**2,870**	**1,694**	**1,824**
10-N2 (Ngn)	1,154	**0,572**	**1,976**	1,137	1,445	1,469	1,279	**0,394**	1,251
10-N3	**0,452**	**1,530**	1,114	**0,161**	**0,109**	1,066	**0,276**	**11,805**	**3,363**
10-N4	**2,513**	**2,046**	**2,997**	**2,700**	**2,782**	**3,334**	**2,652**	**8,508**	**3,536**
10-NP1	**0,345**	**3,612**	**3,863**	**0,223**	**0,156**	1,157	0,830	1,102	**1,816**
10-NP2 (Hap)	**0,429**	**1,912**	**1,510**	0,635	**0,215**	1,043	**0,599**	**0,033**	**3,912**
10-NP3 (Nsp)	1,061	0,990	0,870	1,101	0,960	1,220	0,971	**1,811**	**1,607**
10-NP4	**0,177**	**2,236**	1,078	**0,488**	**0,451**	1,058	**0,200**	**2,551**	**0,577**
10-NP5	**0,596**	**2,189**	1,336	**0,237**	**0,358**	1,233	0,860	**5,600**	**1,966**
10-RiPP1	0,930	1,437	**5,031**	**0,461**	0,675	**6,621**	0,699	**124,384**	**3,119**
10-RiPP2	**1,844**	**1,922**	1,406	1,097	1,465	0,674	1,157	**21,431**	**3,248**
10-RiPP3	**0,406**	0,705	1,451	**0,257**	**0,167**	**5,397**	**0,352**	**34,469**	1,372
10-RiPP4	0,660	1,446	**1,857**	**0,483**	0,816	1,467	0,737	**0,349**	**5,762**
10-RIPP5 (Lan)	**1,602**	1,062	**3,662**	0,683	**2,057**	**1,674**	**2,619**	**0,193**	**0,543**
10-Ripp6 (Lan)	1,279	**1,790**	**2,685**	1,230	0,920	**0,559**	1,014	**25,323**	**3,541**

Comparison of the gene expression patterns between homologous gene clusters

Several of the studied genes in KVJ20 shared homology with NRPS/PKS/RiPP genes from KVJ2 and KVJ10, a summary of the homologous genes are shown in Table 6-7. In the sections below the graphic representations, Figure 18-23 of gene expression patterns for some of the homologous genes are shown.

Gene expression patterns between homologous NRPS & PKS gene clusters

In Figure 18, a comparison of the FC in expression to respective controls for *Aer* & *S/B-like* gene cluster, corresponding to the 20-*N1* gene cluster in KVJ20 and 2-*N2* gene cluster in KVJ2 is shown. The exp pattern of the Aer & *S/B-like* gene clusters share similarities between KVJ20 and KVJ2, with the most notable similarities in gene expression observed in -N vs +N and in solid culture + N.

In Figure 19, a comparison of the FC in expression to respective controls for *Ap*t gene cluster, corresponding to the 20-*N2* gene cluster in KVJ20 and 2-*N6* gene cluster in KVJ2, where the most notable similarities are observed in -N vs +N and in solid culture +N. In Figure 20, a comparison of the FC in expression to respective controls for the possible Siderophore gene cluster, corresponding to the 20-*NP2* in KVJ20, 2-*N3* in KVJ2 and 10-*NP1* in KVJ10. The *Sid* gene clusters from KVJ20 and KVJ2 is almost entirely similar, as well as having some similarities with KVJ10, especially in solid vs liquid and -N-P, and in -N-Fe.

In Figure 21, a comparison of the FC in expression to respective controls for the unknown NRPS gene cluster, corresponding to 20-*N3* in KVJ20, 2-*N1* in KVJ2 and 10-*N1* in KVJ10. The gene exp from KVJ20 and KVJ2 share a great similarity in stress cultures supplemented with N, while the gene exp from KVJ2 shared similarity with KVJ10 in stress cultures without N.

When comparing the *Hgl* gene cluster, corresponding to 20-*P1* in KVJ20, 2-*P3* in KVJ2 and 10-*P1* in KVJ10, similarities between all three strains were observed. Especially in -N vs +N and in -Fe vs +Fe. For the remaining homologous gene clusters, no obvious similar gene expression patterns were found.

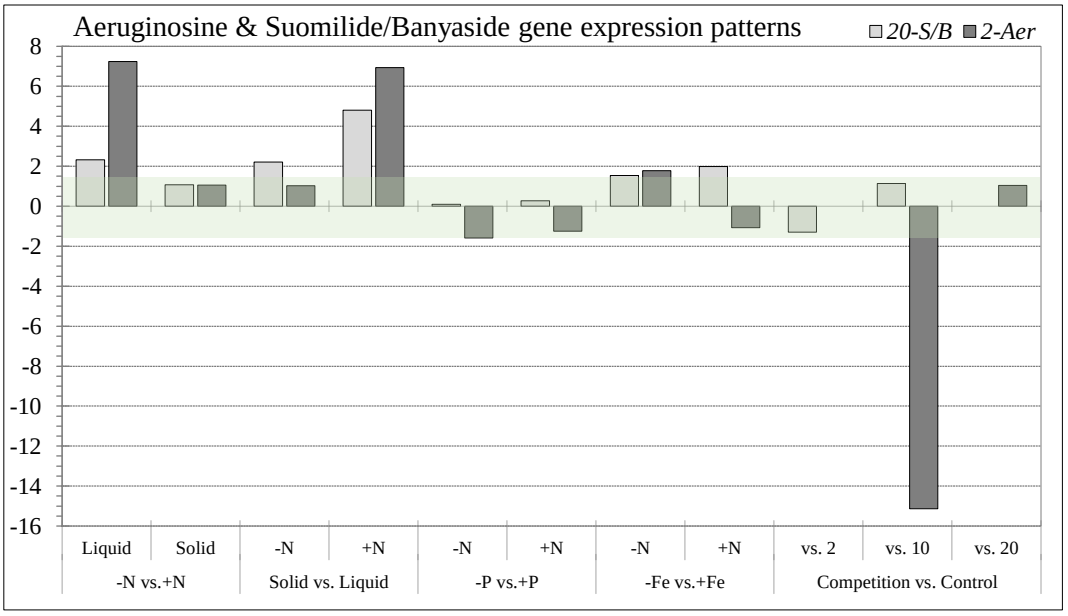

Figure 18: Comparison of FC in expression to respective controls for the Aeruginosin gene cluster from KVJ2 (2-Aer) and Suomilide/Banyaside-like gene cluster from KVJ20 (20-S/B). Highlighted field marks ±1.5.

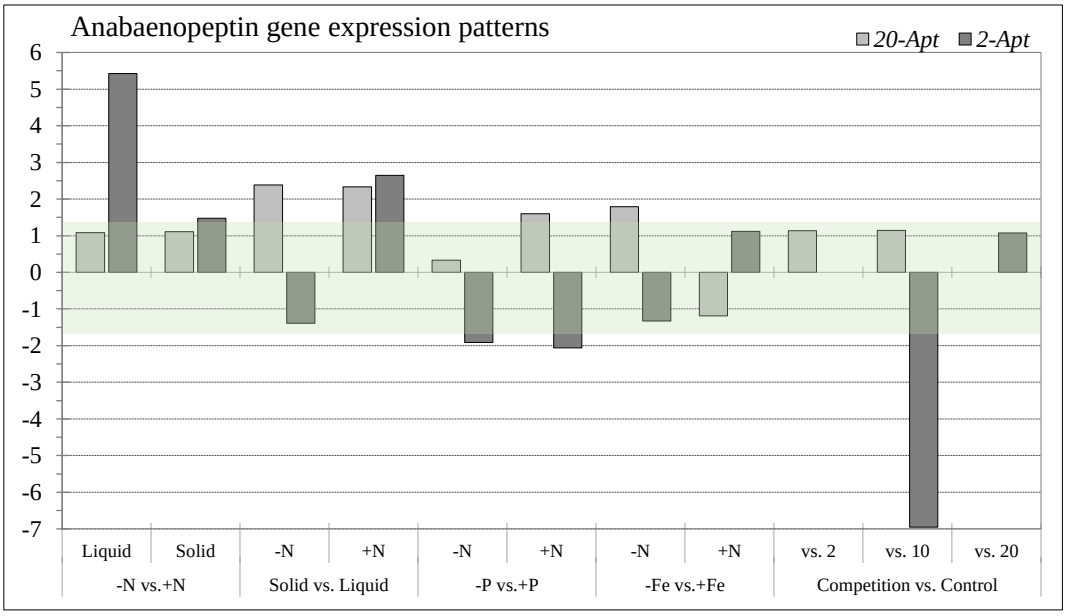

Figure 19: Comparison of FC in expression to respective controls for the Anabaenopeptin gene cluster from KVJ20 (20-Apt) and KVJ2 (2-Apt). Highlighted field marks ±1.5.

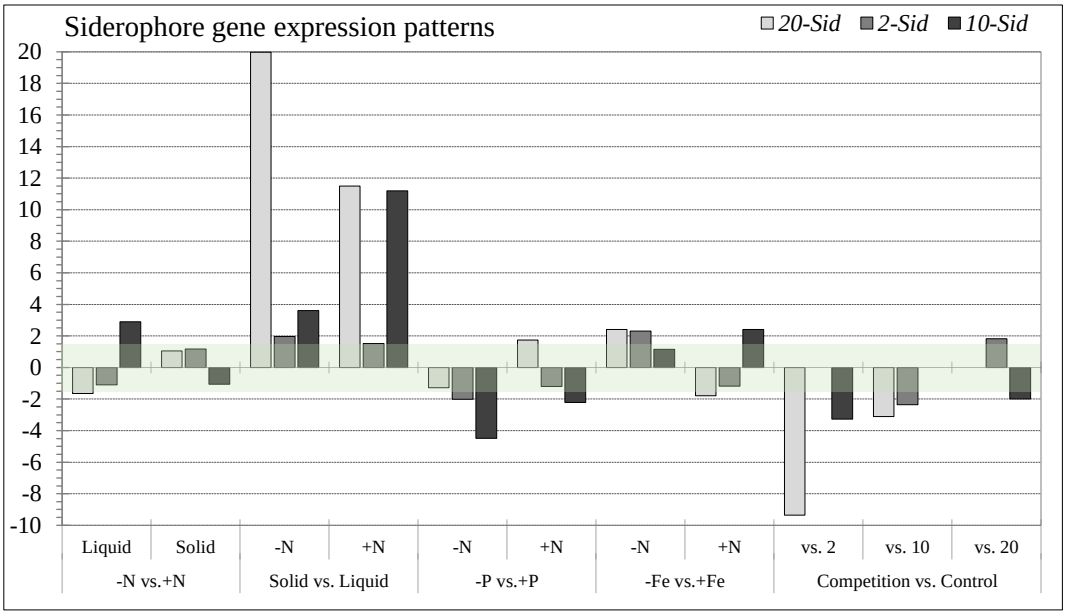

Figure 20: Comparison of FC in expression to respective controls for the possible Siderophore gene cluster from KVJ20 (20-Sid), KVJ2 (2-Sid) and KVJ10 (10-Sid). Highlighted field marks ±1.5.

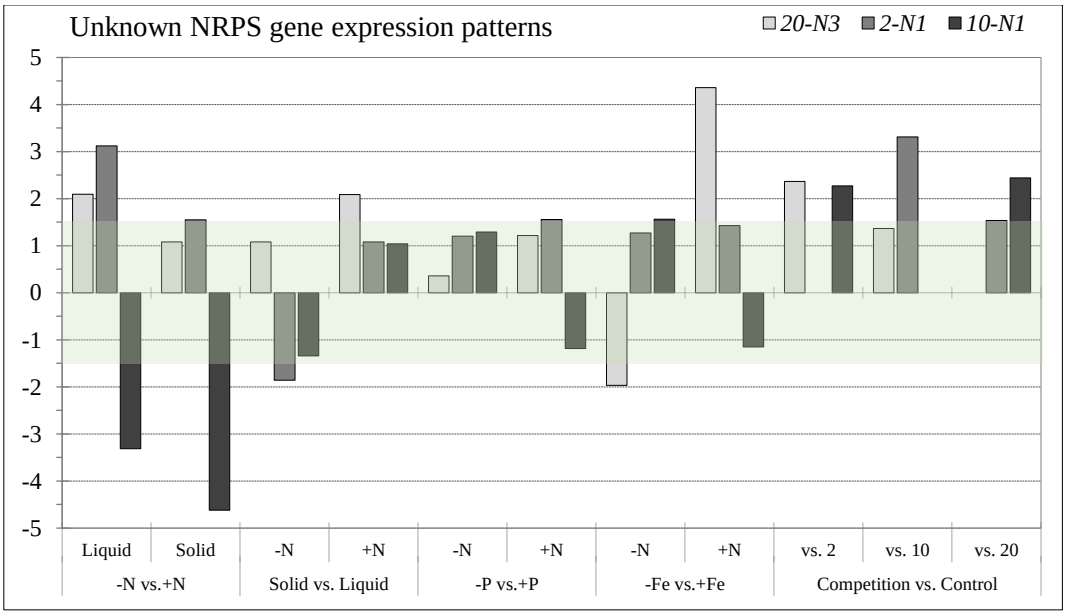

Figure 21: Comparison of FC in expression to respective controls for the unknown NRPS gene cluster from KVJ20 (20-N3), KVJ2 (2-N1) and KVJ10 (10-N1). Highlighted field marks ±1.5.

Gene expression patterns between homologous RiPP gene clusters

The comparison of the FC to respective controls for the *Mvd* gene clusters from KVJ20 (20-*RiPP8*) and KVJ2 (2-*RiPP2*) are shown in Figure 22, where both *Mvd* gene clusters showed an upregulation in -N, as well as a downregulation in -N-P. A comparison of the FC to respective controls for the *RiPP2* in KVJ20, *RiPP1* in KVJ2 and *RiPP5* in KVJ10 are shown in Figure 23. The RiPP genes show similar expression in KVJ20 and KVJ2, especially highly downregulated in -N-P and in interaction with KVJ10.

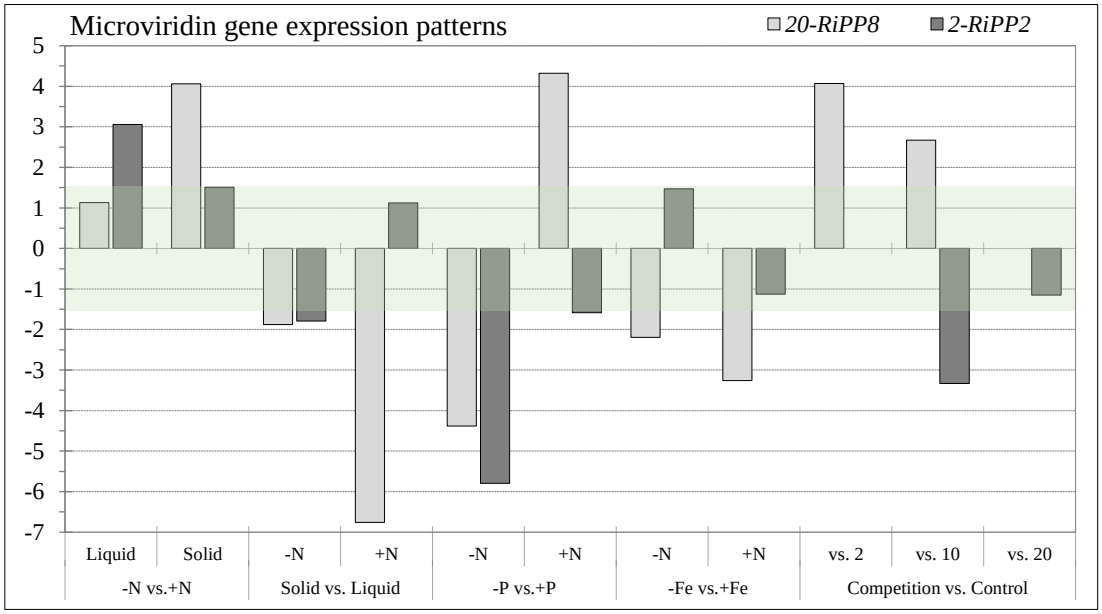

Figure 22: Comparison of FC in expression to respective controls for the Microviridin gene cluster from KVJ20 (20-RiPP8) and KVJ2 (2-RiPP2). Highlighted field marks ±1.5.

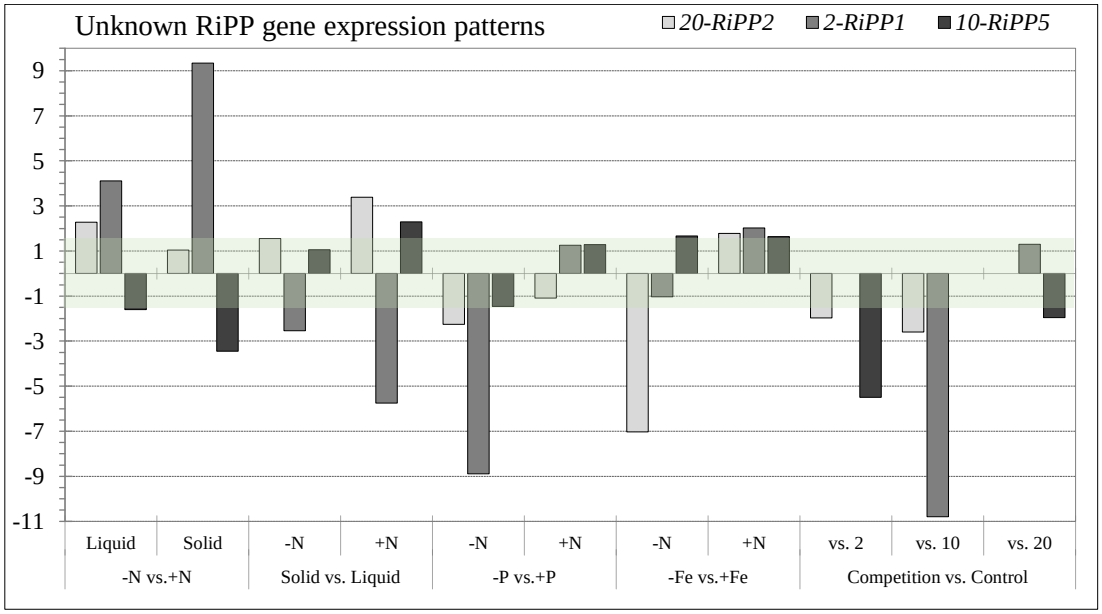

Figure 23: Comparison of FC in expression to respective controls for the unknown RiPP gene cluster from KVJ20 (20-RiPP2), KVJ2 (2-RiPP1) and KVJ10 (10-RiPP5). Highlighted field marks ±1.5.

UPLC-HR-MS profiling and Metabolite identification

Sonicated cell pellets and filtered supernatants from KVJ20, KVJ2, and KVJ10 were subjected to UPLC-HR-MS analyses. Total ion current (TIC) chromatograms for cell and medium extracts are shown in 24-29, peaks that stood out, and with molecular weight > 350 Da were investigated further. The most prominent peaks are labeled with molecular weight in Da. The TIC chromatograms show a summed intensity of all ions in each sample scan versus retention time in minutes. The TIC chromatograms are stacked upon each other with a 90° angle, with scaling = 10, hence the difference between each baseline is not directly corresponding to relative peak size.

A summary of the ions observed with UPLC-HR-MS screening of the cell, media and interaction extracts from KVJ20, KVJ2, and KVJ10 with peak intensities over 5% relative to the highest observed are represented in Table 15-16 All peaks were dereplicating against several databases, in addition the fragmentation pattern of the most prominent peaks were analyzed for the identification of known peptides, and several metabolites were identified by analyzing the fragmentation pattern. Examples of fragmentation profiles are shown in Appendix 4: Fragmentation pattern examples. Summary of the compounds found in KVJ20, KVJ2, and KVJ10 assigned to known secondary metabolites produced by cyanobacteria are represented in Table 17. The peak intensity, i.e. ratios between the identified compounds is shown Table 18-23.

Chromatograms

TIC chromatogram KVJ20

Figure 24 shows the UPLC-HR-MS profile of the cell extracts from KVJ20, from the profile it’s clear that most of the highest peaks are present in -N. One of the most prominent peaks is eluted after 4.09 minutes and is an S/B-like compound with m/z 997 and 1077 (sulfated).

Figure 25 shows the UPLC-HR-MS profile of the media extracts from KVJ20. The most prominent peak is eluted after 6.74 min and is an unknown compound with m/z 379. As well as the S/B-like compound (RT 4.08) with m/z 997 and 1077 (sulfated) is clearly higher in nitrogen and phosphate deprived medium (-N-P).

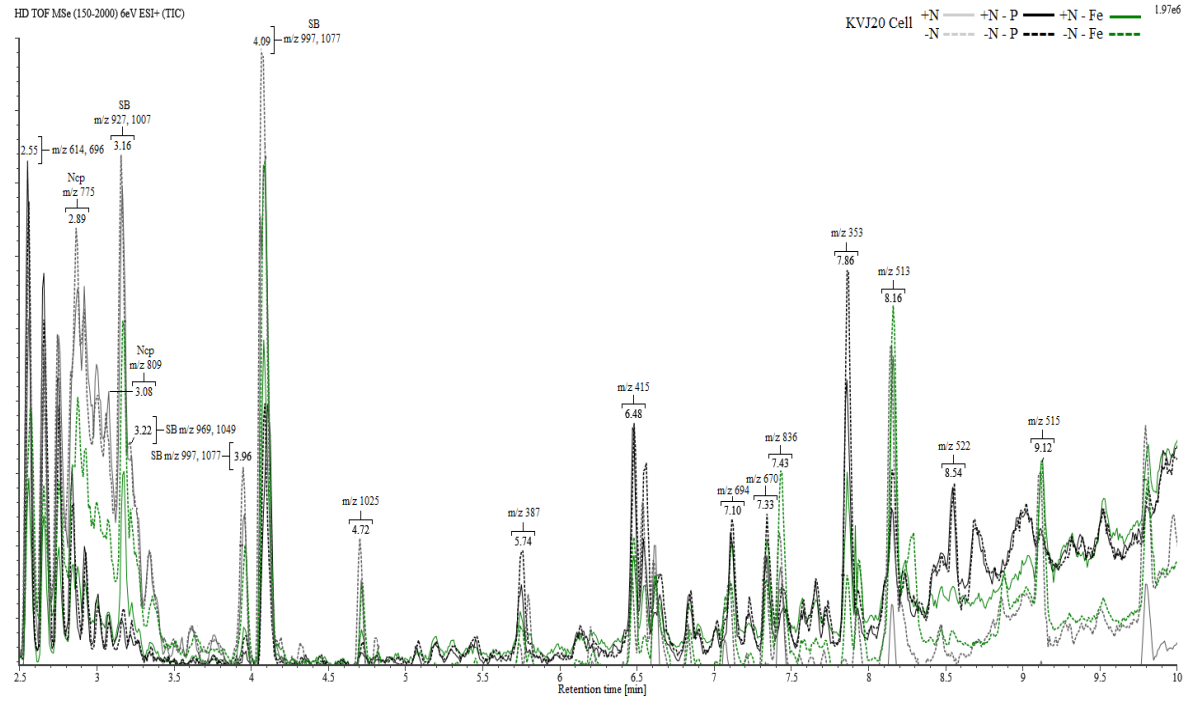

Figure 24: Total ion current (TIC) chromatograms from UPLC-HR-MS analysis of cell extracts from KVJ20. Each line represents UPLC-HR-MS spectra for one sample; -N, +N, -N-P, +N-P, -N-Fe, +N-Fe. Investigated peaks are marked with m/z in Dalton and Retention time (min).

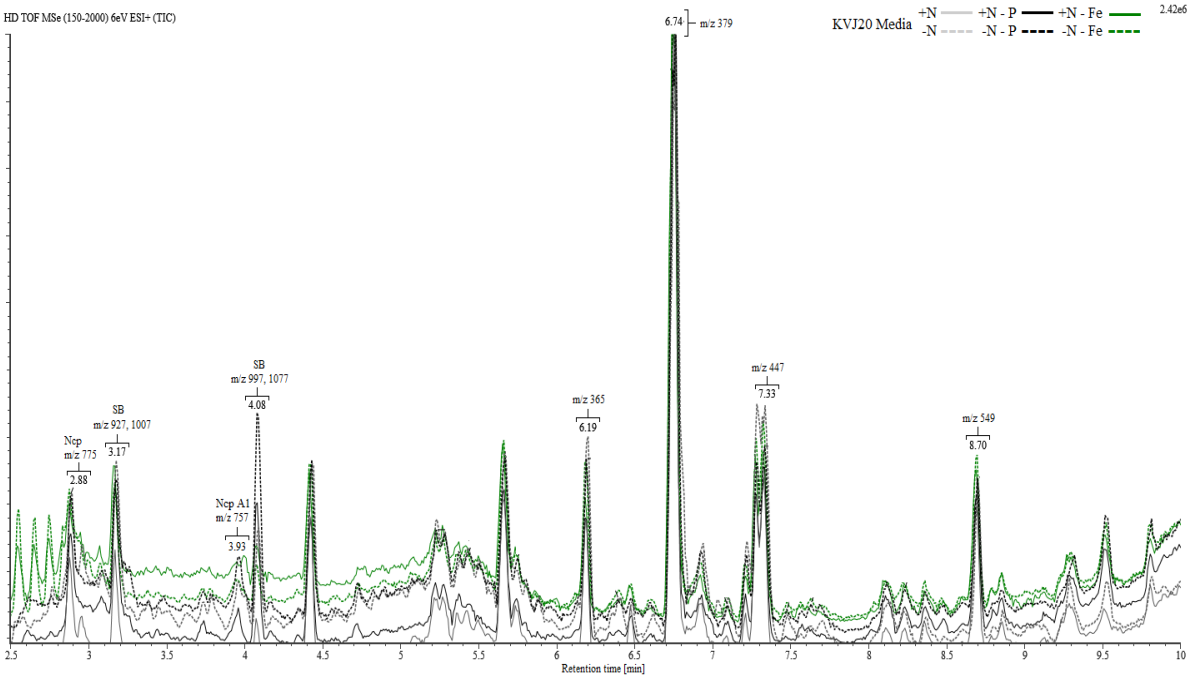

Figure 25: Total ion current (TIC) chromatograms from UPLC-HR-MS analysis of media extracts from KVJ20. Each line represents UPLC-HR-MS spectra for one sample; -N, +N, -N-P, +N-P, -N-Fe, +N-Fe. Investigated peaks are marked with m/z in Dalton and Retention time (min).

TIC chromatogram KVJ2

Figure 26 shows the UPLC-HR-MS profile of the cell extracts from KVJ2. Three of the most prominent peaks in the sample set include Ncp with an m/z 775 (RT 2.88) and m/z 809 (RT 3.07), and Aer with m/z 889 (RT 3.01). One unknown compound in +N stands out from the other samples and eluted after 6.54 min with m/z 415.

Figure 27 shows the UPLC-HR-MS profile of the media extracts from KVJ2. The most prominent peak is eluted after 6.75 min and is an unknown compound with m/z 379. The peak intensity of Ncp A3 with m/z 805 (RT 4.03) is clearly higher in iron deprived media with Nitrogen (+N-Fe).

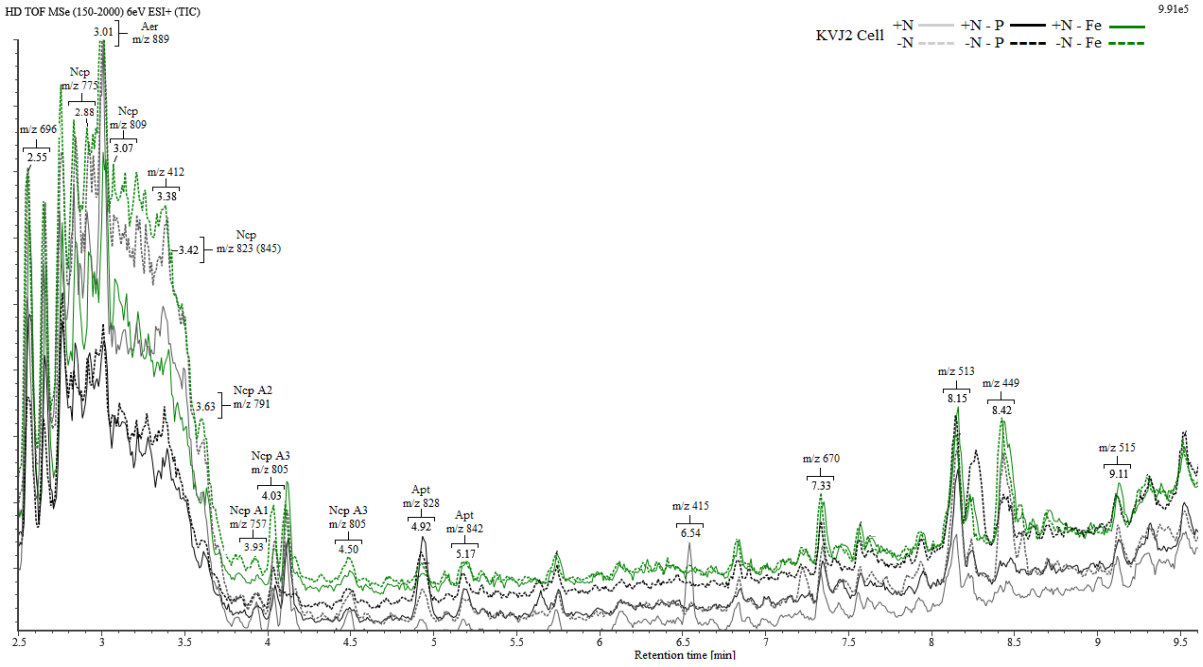

Figure 26: Total ion current (TIC) chromatograms from UPLC-HR-MS analysis of cell extracts from KVJ2. Each line represents UPLC-HR-MS spectra for one sample; -N, +N, -N-P, +N-P, -N-Fe, +N-Fe. Investigated peaks are marked with m/z in Dalton and Retention time (min).

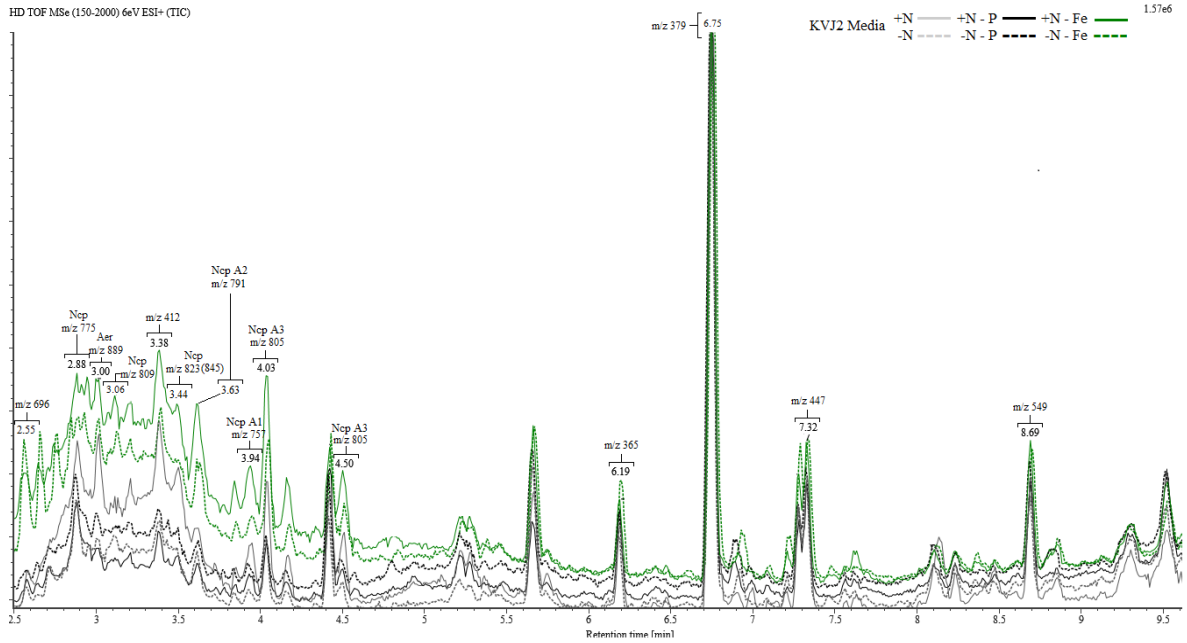

Figure 27: Total ion current (TIC) chromatograms from UPLC-HR-MS analysis of media extracts from KVJ2. Each line represents UPLC-HR-MS spectra for one sample; -N, +N, -N-P, +N-P, -N-Fe, +N-Fe. Investigated peaks are marked with m/z in Dalton and Retention time (min).

TIC chromatogram KVJ10

Figure 28 shows the UPLC-HR-MS profile of the cell extracts from KVJ10. One of the most prominent peaks eluted after 9.63 min and were identified as Hap with m/z 490, with sodium adduct as m/z 512. In nitrogen and iron deprived medium (-N-Fe) one peak stood out from the other with an unknown compound with an m/z 520 (RT 8.66) with a sodium adduct as m/z 542.

Figure 29 shows the UPLC-HR-MS profile of the media extracts from KVJ10. One of the most prominent peaks eluted after 6.83 min with m/z 379. In +N-Fe one peak stood out from the other with an unknown compound with an m/z 534 (RT 7.11) with a sodium adduct as m/z 556. In -N-P one peak stood out from the other with an unknown compound with an m/z 504 (RT 10.06) with a sodium adduct as m/z 526.

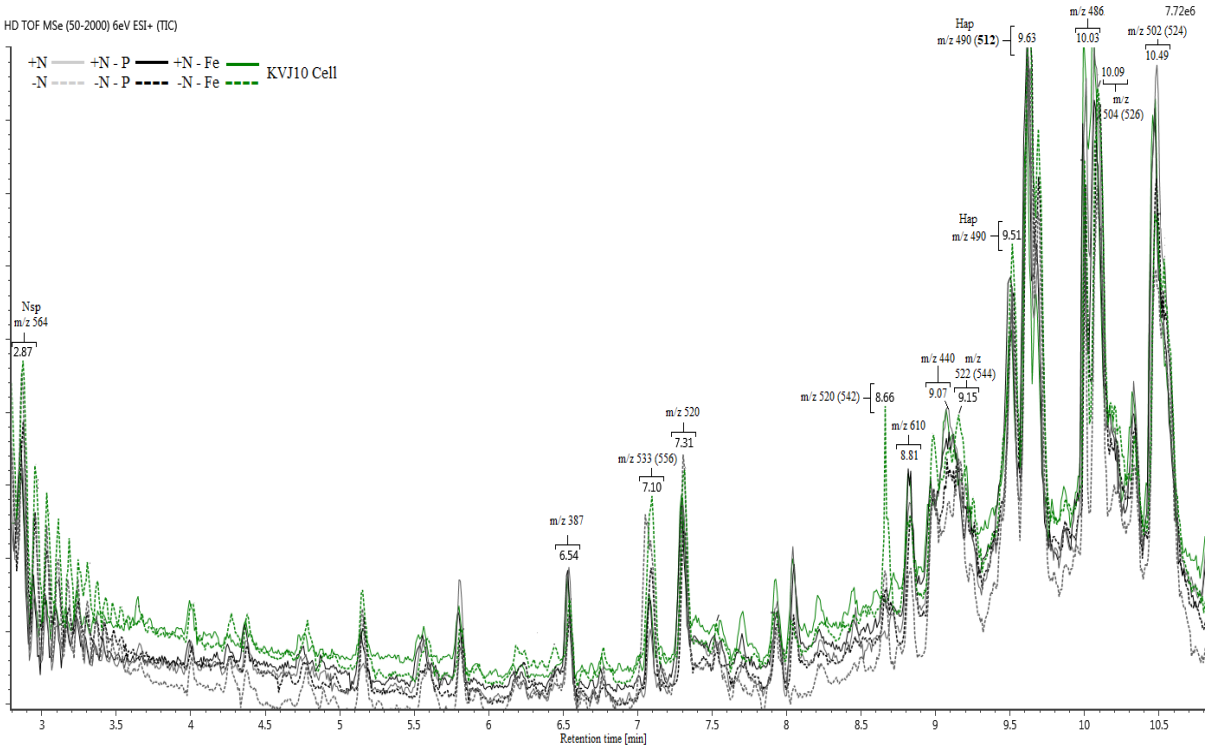

Figure 28: Total ion current (TIC) chromatograms from UPLC-HR-MS analysis of cell extracts from KVJ10. Each line represents UPLC-HR-MS spectra for one sample; -N, +N, -N-P, +N-P, -N-Fe, +N-Fe. Investigated peaks are marked with m/z in Dalton and Retention time (min).

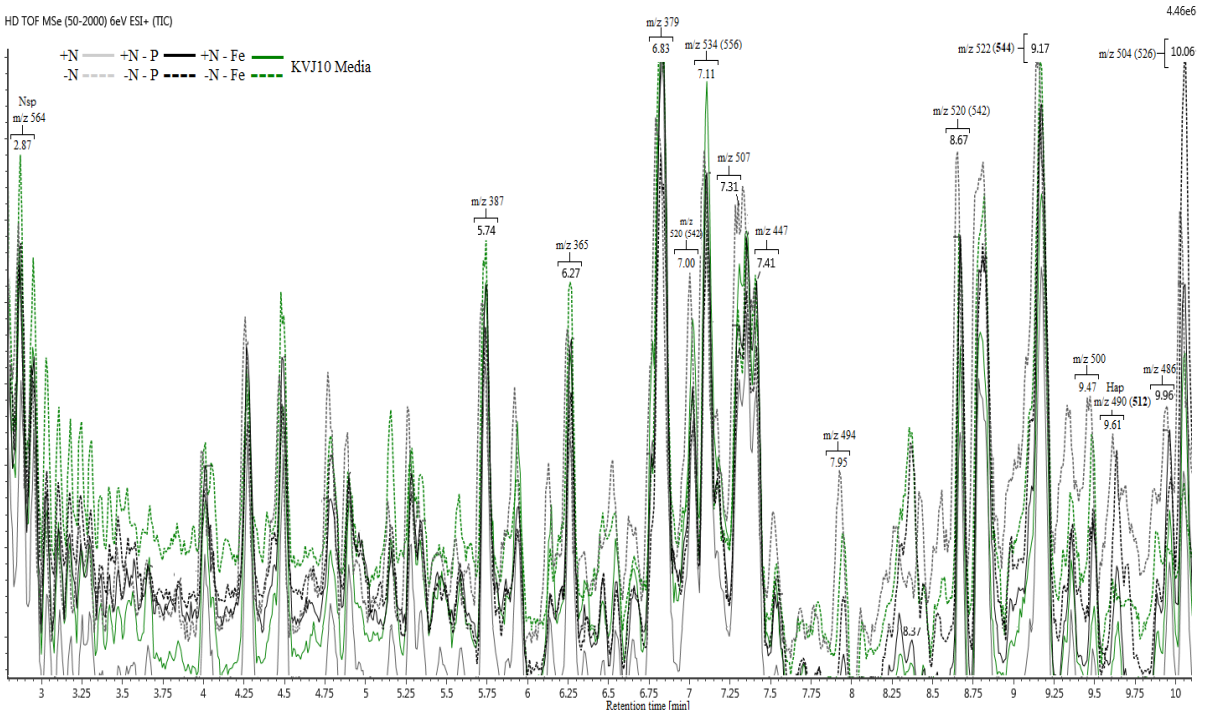

Figure 29: Total ion current (TIC) chromatograms from UPLC-HR-MS analysis of media extracts from KVJ10. Each line represents UPLC-HR-MS spectra for one sample; -N, +N, -N-P, +N-P, -N-Fe, +N-Fe. Investigated peaks are marked with m/z in Dalton and Retention time (min).

Summary of chemical profiles and the identified secondary metabolites

Cell extracts, media extracts, and colony extracts were subjected to UPLC-HR-MS. Peaks with intensities over 5% relative to the highest observed in each sample were considered. A total of 83 compounds were found, representing 76 individual compounds in the range from 350 – 1100 Da. A summary of the ions observed by UPLC-HR-MS screening of the cell and media extracts of KVJ20, KVJ2, and KVJ10 are shown in Table 15.

From KVJ20 the most prominent peaks observed from the cell-extracts include the unknown compounds with m/z of; 415, 513, 614 and 696. As well as Ncp with m/z 775 and m/z 809, and S/B-like peptides both not sulfated and sulfated with m/z 927 (sulfated m/z 1007) and m/z 997 (sulfated m/z 1077). Several of the compounds seen in cell extracts were also seen in media extracts, and the most prominent peaks in the media extracts include unknown compounds with m/z of; 379, 447 and 471, as well as S/B-like peptides with m/z 997 (sulfated m/z 1077).

The most prominent peaks observed in KVJ2 include Ncp with m/z 809 and m/z 823 and Aer with m/z 889, as well as the unknown compounds with m/z 564, m/z 608 and m/z 652. While in the media extracts from KVJ2 the most prominent peaks include several Ncp, as well as two unknown compounds with m/z 379 and m/z 447. Several of the compounds found in cell extracts of KVJ2 is also found in KVJ20, including m/z of; 415, 513, 515, and 696, as well as Ncp with m/z of 757, 775 and 809. From the media extracts the following m/z were found in media extracts from both KVJ20 and KVJ2; 365, 379, 447, 471, 549, 696, as well as Ncp.

From KVJ10 the most prominent peak in cell extracts include the unknown compounds with m/z 486, m/z 502 observed mostly as sodium adduct (m/z 524), m/z 504 observed mostly as sodium adduct (m/z 526) and Hap with m/z 490 mostly observed as sodium adduct (m/z 512). In contrast to KVJ2, KVJ10 doesn't share many compounds with KVJ20, only one compound was found to be similar to KVJ20, with an m/z 387 from the cell extract. The compounds with m/z of; 365, 379 and 447 were found in media extracts of all three strains. In general, for all the strains there were little differences in observed peaks in growth with and without nitrogen, besides from difference in intensity of the compounds.

*Table 15: Summary of the ions m/z (Na adduct) observed by UPLC-HR-MS screening of the cell and growth media both with and without Nitrogen of KVJ20, KVJ2, and KVJ10. Prominent peaks are in bold, and peaks found in both cell and medium extracts are underscored. *peaks identified by similar partial similar fragmentation patterns.*

Strain	*Cell-bound*		*Growth medium*	
	+N	*-N*	*+N*	*-N*
KVJ20	353, 387, **415** **513**, 515, 522 614, 670, 694, **696** Ncp757, **Ncp775, Ncp809** **SB927**, SB969*, **SB997** **SB1007**, 1025, SB1049* **SB1077**	353, 387, **415** **513**, 515, 522 **614**, 670, 694, **696** **Ncp775, Ncp809**, 836 **SB927**, SB969*, **SB997** **SB1007**, 1025, SB1049* **SB1077**	365**, 379**, 387, **447**, 471 549 696 Ncp757, Ncp775, Ncp809 SB927, SB997 SB1007 SB1077	365, **379**, 387, **447**, **471** 549 696 Ncp757, Ncp775, Ncp809 SB927, **SB997** SB1007 **SB1077**
KVJ2	402, 412, 415, 449 513, 515, **564** **608**, **652**, 670, 696 Ncp757, Ncp775, Ncp791 Ncp805*, **Ncp809** Apt812 **Ncp823**(845), Apt828 Apt842, **Aer889**	402, 412, 449 513, 515, **564** **608**, **652**, 670, 696 Ncp757, Ncp775, Ncp791 Ncp805*, **Ncp809**, Apt812 **Ncp823**(845), Apt828 Apt842, **Aer889**	365, **379,** 412, **447**, 471 549, 564 608, 652 Ncp757, **Ncp775**, **Ncp791** **Ncp805***, **Ncp809** **Ncp823**(845) **Aer889**	365, **379,** 412, **447**, 471 549, **564** **608**, 652, 696, **Ncp757**, Ncp775, Ncp791 Ncp805*, Ncp809 **Ncp823** Aer889
KVJ10	387 440, 476, **486**, Hap490(**512**) 502(**524**), 504(**526**) 520(542) 534(556), Nsp564 597, 599, 610 701, 734	387 **486,** Hap490(**512**) 502(**524**), 504(**526**) 520(542), 522(544) 534(556), Nsp564 597, 599, 610 701, 734, 745	365, **379**, **387** **447**, Hap490(512) 500, 504(**526**), 507, 520(542) **522**(544), **534(556)**, 538, Nsp564 701, 745	365, **379**, **387** **447**, 486, Hap490(512), 494 500, **504(526)**, 507, 520(**542**), 522(**544**) **534(556)**, 538, Nsp564 599 701, 745

A summary of the ions observed by UPLC-HR-MS screening from solid growth media and interaction plates of KVJ20, KVJ2, and KVJ10 are shown in Table 16. From the solid plates, considerably fewer compounds were found compared to cell and media extracts. All the compounds found in colony extracts were also found in either cell extracts or media extracts as well. In general, for all the strains there were little differences in observed peaks in growth with and without nitrogen on solid, and in interaction, besides from difference in intensity of the compounds.

Table 16: Summary of the ions m/z (Na adduct) observed by UPLC-HR-MS screening of interaction strains and control of KVJ20, KVJ2, and KVJ10. Prominent peaks are in bold.

Strain	*Control*	*Interaction*	
	-N	***KVJ10***	***KVJ2***
KVJ20	353, 387 **415,** 513, 515 **614, 696** **Ncp775, Ncp809** **SB927, SB997** **SB1007, SB1077**	353 415, **513, 515** **614, 696** **Ncp775, Ncp809** **SB927, SB997** **SB1007, SB1077**	353, 387 **415,** 513, 515 614, **696** Ncp775, Ncp809 SB927, **SB997** SB1007, **SB1077**
		KVJ10	***KVJ20***
KVJ2	402, 412 513, 515, **564** **608,** 696 **Ncp775** **Ncp809, Ncp823**, Aer889	402, 412 513, 515, **564** **608,** 652, 696 Ncp775 **Ncp809, Ncp823**, Aer889	402, 412 513, 515, **564** **608,** 652, 696 **Ncp775** **Ncp809, Ncp823**, Aer889
		KVJ2	***KVJ20***
KVJ10	387 **440**, **486**, Hap490(**512**) 502(**524**), 504(**526**), 520, 597, **599** 610, 701, 734, 745	486, Hap490(512) 502(524), **504**(526)	486, Hap490(512) 502(524), **504**(526), 599

A summary of the compounds found in KVJ20, KVJ2, and KVJ10 assigned to known secondary metabolites produced by cyanobacteria are shown in Table 17. An Aer with m/z of 889 was found in KVJ2, and had similar fragmentation pattern to Aer865 (Appendix 4), and had a natural loss of 162 Da (Kapuścik et al., 2013). Three variants of Apt were also found in KVJ2, with m/z of 812, 828 Da and 842 Da, with almost identical fragmentation patterns from previous records of Apt (Guljamow et al., 2017) (Appendix 4).

KVJ20 produced an array of substances ranging from m/z 927 Da to m/z 1077 Da sharing similar fragmentation patterns (Appendix 4), where several of the fragment ions were similar to Suomilide from *Nodularia spumigena* (Fujii et al., 2000). All the fragmentation spectra also had a prominent fragment ion of m/z 610 Da, and have previously been recorded in natural and synthetic Banyaside (Schindler et al., 2010). All the variants of this S/B-like compounds showed a neutral loss of 80 Da, corresponding to a sulfate group, another indicative for Suomilides and Banyasides (Fujii et al., 2000; Liaimer et al., 2016; Schindler et al., 2010)

Both cell, medium and solid plate extract of KVJ20 and KVJ2 produced an array of Ncp ranging from m/z 757 Da to m/z 823 Da, where the latter also was observed as sodium adduct as m/z 845 Da. Six variants of Ncp were found in KVJ2 with m/z of; 757, 775, 791, 805, 809 and 823 Da. While only three variants were found in KVJ20 with m/z of; 757, 775 and 809 Da. All the variants were identified by similar fragmentation pattern matches (Appendix 4) from Golakoti et al. (2001); Liaimer et al. (2016); Nowruzi et al. (2012). In KVJ10 two compounds could be identified, Nsp m/z 564 Da was identified by similar fragmentation patterns (Appendix 4) (Kampa et al., 2013), and Hap m/z 490 Da mostly observed as a sodium adduct with m/z 512 adducts, was identified by several databases.

Table 17: Summary of the compounds found in KVJ20, KVJ2, and KVJ10 assigned to known secondary metabolites produced by cyanobacteria.

m/z H^+	Strain	Diagnostic feature	Reference
Aeruginosin (Aer)			
889	KVJ2	Neutral loss of 162 Da Fragmentation pattern similar to Aeruginosin 865	Kapuscik et al. (2013); Liaimer et al. (2016).
Anabaenopeptin (Apt)			
812 828 842	KVJ2	Fragmentation pattern match	Guljamow et al. (2017).
Banyaside/Suomilide-like (S/B)			
927, 969, 997 1007, 1049, 1077 (sulfated)	KVJ20	Fragmentation pattern similar to Suomilide and Banyaside Prominent ion of 610 da Natural loss of 80 da (sulfated)	Fujii et al. (2000); Liaimer et al. (2016); Schindler et al. (2010).
Nosperin (Nsp)			
564	KVJ10	Fragmentation pattern match	Kampa et al. (2013); Liaimer et al. (2016).
Hapalosin (Hap)			
490 (512)	KVJ10	m/z match in databases	Stratmann et al. (1994).
Nostocyclopeptide (Ncp)			
757, 775	KVJ2, KVJ20		
791	KVJ2		Golakoti et al. (2001); Liaimer et al. (2016); Nowruzi et al. (2012).
805*	KVJ2	Fragmentation pattern match	
809	KVJ2, KVJ20		
823	KVJ2		

Relative peak intensity of identified secondary metabolites

From all the observed compounds relative peak intensity relative to the highest one in the sample was calculated. For the complete list of relative peak intensity, see Appendix 3: Relative peak intensity in percentage. In the sections below how the relative peak intensity, i.e. ratio between the identified compounds changes in different growth cultivations is described.

Relative peak intensity in KVJ20

In Table 18, the relative peak intensity in percentage for the identified secondary metabolites in KVJ20 is shown. Ncp775 was found particularly with high intensity in cell extracts with N (+N), and with decreasing intensity in iron (-Fe) and phosphate deprived (-P) cultivation. While Ncp809 was found with high intensity in cell extracts in nitrogen deprived media (-N), and with decreasing intensity in -Fe and -P cultivation. From solid culture -N and in interaction with KVJ10 (vs.10), Ncp775 and Ncp809 were found with high intensity.

All the sulfated S/B-like peptides showed the same peak intensity pattern as the corresponding not sulfated ones, with high intensity in all the cell extract samples but with decreasing intensity in the phosphate deprived mediums. All the S/B-like peptides showed high peak

intensity in cell extracts, with m/z 997 (m/z 1077) having the highest intensity. In solid culture, all the S/B-like peptides showed high intensity in nitrogen deprived media and in association with KVJ10. When comparing the ratio between Ncp:S/B, seen in Table 19, It's clear that the S/B-like peptide is found in greater yield than Nostocyclopeptide in all samples.

Table 18:Relative peak intensity in different cultivations in percentage for identified secondary metabolites from KVJ20. Ncp: Nostocyclopeptide, S/B: Suomilide/Banyaside-like peptide. Relative peak intensity > 20% is highlighted in bold.

m/z H^+	***ID***	***Sample***	***-N***	***-N-Fe***	***-N-P***	***+N***	***+N-Fe***	***+N-P***	***-NS***	***+NS***	***vs.2***	***vs.10***
757	**Ncp**	Cell	0	3	0	8	0	0	4	0	0	3
		Media	5	2	3	5	3	4	-	-	-	-
775	**Ncp**	Cell	**50**	**48**	0	**94**	**33**	0	44	4	**22**	**63**
		Media	17	5	2	7	6	6	-	-	-	-
809	**Ncp**	Cell	**63**	**37**	5	**91**	**30**	0	**60**	9	**22**	**80**
		Media	10	5	7	4	5	8	-	-	-	-
927	**S/B**	Cell	**46**	**42**	4	**45**	**47**	0	**61**	16	**20**	**62**
		Media	15	7	11	9	10	15	-	-	-	-
969	**S/B**	Cell	18	15	4	19	13	0	4	6	0	4
		Media	0	0	5	0	0	1	-	-	-	-
997	**S/B**	Cell	**100**	**100**	40	**100**	**100**	14	**100**	57	44	**100**
		Media	7	1	26	3	1	15	-	-	-	-
1007	**S/B**	Cell	**43**	**39**	4	**42**	**43**	0	**54**	15	19	15
		Media	13	8	11	8	10	13	-	-	-	-
1049	**S/B**	Cell	16	15	4	18	12	0	0	5	0	4
		Media	0	0	4	0	0	1	-	-	-	-
1077	**S/B**	Cell	**80**	**74**	40	**65**	**90**	15	**81**	**52**	**47**	**83**
		Media	8	2	22	3	2	13	-	-	-	-

Table 19: Ratio Ncp:S/B-like peptide of total relative peak intensity in different cultivations from KVJ20.

KVJ20	***-N***	***-N-Fe***	***-N-P***	***+N***	***+N-Fe***	***+N-P***
Cell	1:2,7	1:3,2	1:19	1:1,5	1:4,8	0:29
Medie	1:1,3	1:1,5	1:6,6	1:1,4	1:1,6	1:3,2

Relative peak intensity in KVJ2

In Table 20, the relative peak intensity for the identified secondary metabolites in KVJ2 is shown. In KVJ2 six Ncp were found with m/z of; 757, 775, 791, 805, 809 and 823. Ncp775 was found with high intensity in all cell extracts, especially in -N, +N and -P media both with and without N. While from the media extract Ncp775 was only found with high intensity in +N and in +N-Fe cultivation. Ncp791 and Ncp805 were found with higher intensity in media extracts than in the cell extracts, especially in +N-Fe cultivation. Ncp809 was found with high intensity in cell extracts, especially in N-Fe and -N-P. While Ncp823 was found with high intensity in all cell extracts, with the exception in +N-Fe, however, Ncp823 was found with

high intensity in media extract in +N-Fe and +N. From solid culture with nitrogen, Ncp775 was found with high intensity.

Three of the same Ncp were found in both KVJ20 and KVJ2 with m/z 757, m/z 775 and m/z 809. Ncp757 had relative similar peak intensity in both KVJ20 and KVJ2 both from cell extracts and from solid culture. Ncp775 from KVJ2 was found with greater intensity in all cell extracts compared to Ncp775 found in KVJ20, especially in phosphate deprived media. The Ncp809 from KVJ20 was found with greater intensity than in KVJ2, in -N, +N and -N-Fe, while Ncp809 from KVJ2 was found with greater intensity than in KVJ20 in +N-Fe and in phosphate deprived media. From solid culture, Ncp809 in KVJ20 was found with greater intensity than KVJ2 in all samples, especially in interaction with KVJ10.

One Aer with m/z 889 was found in KVJ2, with the highest intensity in the cell extract in +N-Fe. Three Apt with m/z 812, m/z 828 and m/z 842 were found, and they all shared a similar pattern with increasing peak intensity in phosphate deprived media (-P), with Apt828 showing the highest intensity of those three in the cell extract. In solid culture, only Aer889 could be detected with significant intensity. When comparing the ratio between Ncp:Apt:Aer, seen in Table 21, Ncp is clearly produced in a higher ratio in all the samples, followed by Aer and Apt.

Table 20: Relative peak intensity in different cultivations in percentage for identified secondary metabolites from KVJ2. Ncp: Nostocyclopeptide, Apt: Anabaenopeptin, Aer: Aeruginosin. Relative peak intensity > 20% is highlighted in bold.

m/z H⁺	***ID***	***Sample***	***-N***	***-N-Fe***	***-N-P***	***+N***	***+N-Fe***	***+N-P***	***-NS***	***+NS***	***vs.20***	***vs.10***
757	**Ncp**	Cell	4	4	5	5	4	5	1	2	1	1
		Media	6	10	7	**20**	**22**	10	-	-	-	-
775	**Ncp**	Cell	**86**	**79**	**100**	**100**	**62**	**100**	**37**	**77**	**37**	19
		Media	17	**21**	17	**72**	**54**	16	-	-	-	-
791	**Ncp**	Cell	5	6	4	1	8	5	1	0	0	1
		Media	9	16	6	6	**26**	6	-	-	-	-
805	**Ncp**	Cell	6	6	6	4	7	6	3	1	3	3
		Media	15	**23**	10	**27**	**36**	11	-	-	-	-
809	**Ncp**	Cell	13	18	**57**	**22**	**90**	**25**	13	0	9	16
		Media	**25**	**26**	6	12	**43**	2	-	-	-	-
823	**Ncp**	Cell	**100**	**100**	**88**	**85**	**23**	**80**	**52**	**38**	**37**	**39**
		Media	**40**	**36**	16	**75**	**51**	18	-	-	-	-
812	**Apt**	Cell	1	0	4	0	0	7	0	0	0	0
		Media	0	0	0	0	0	0	-	-	-	-
828	**Apt**	Cell	5	3	16	2	4	**28**	1	0	0	1
		Media	0	1	0	1	1	4	-	-	-	-
842	**Apt**	Cell	2	1	4	1	2	7	0	0	0	0
		Media	0	0	0	0	0	0	-	-	-	-
889	**Aer**	Cell	**41**	**47**	**29**	**45**	**56**	**29**	**21**	14	**23**	16
		Media	10	16	12	**37**	**26**	10	-	-	-	-

Table 21: Ratio Ncp:Apt:Aer of total relative peak intensity in different cultivations from KVJ2

KVJ2	***-N***	***-N-Fe***	***-N-P***	***+N***	***+N-Fe***	***+N-P***
Cell	27:1:5	53:1:12	11:1:1.2	72:1:15	32:1:9	8:1.5:1
Media	11:0:1	132:1:16	6:0:1.2	212:1:37	232:1:26	16:1:2.5

Relative peak intensity in KVJ10

In Table 22, the relative peak intensity for the identified secondary metabolites in KVJ10 is shown. Hap with m/z 490, mostly observed as its sodium adduct with m/z 512 had great intensity in all cell extracts, and especially in -N and phosphate deprived medium, as well as having high intensity in solid culture, both with and without N. While Nsp with m/z 564 had greater intensity in media extract, -N and in -N-P. When comparing the ratio between Hap:Nsp, seen in Table 23, Hap is clearly produced in higher yield in all cell extracts, while the ratio between Hap and Nsp goes down in medium extracts.

Table 22: Relative peak intensity in different cultivations in percentage for identified secondary metabolites from KVJ10. Hap: Hapalosin, Nsp: Nosperin. Relative peak intensity > 20% is highlighted in bold.

m/z H^+	***ID***	***Sample***	***-N***	***-N-Fe***	***-N-P***	***+N***	***+N-Fe***	***+N-P***	***-NS***	***+NS***	***vs.2***	***vs.20***
490	**Hap**	Cell	**21**	**34**	**24**	**31**	**27**	**27**	**46**	**29**	8	8
		Media	7	1	15	3	4	6	-	-	-	-
512*	**Hap**	Cell	**100**	**80**	**100**	**67**	**50**	**100**	**62**	**60**	4	5
		Media	6	1	14	**3**	**3**	6	-	-	-	-
564	**Nsp**	Cell	5	6	3	11	10	8	4	4	0	0
		Media	**21**	4	19	6	13	8	-	-	-	-

Table 23: Ratio Hap:Nsp of total relative peak intensity in different cultivations from KVJ2.

Kvj10	***-N***	***-N-Fe***	***-N-P***	***+N***	***+N-Fe***	***+N-P***
Cell	25:1	19:1	41:1	9:1	7,7:1	16:1
Medie	1:1,6	1:2	1,5:1	1:1	1:1,8	1,5:1

Discussion

The aim of the study was to identify potential secondary metabolite gene clusters in Nostoc spp. KVJ20, KVJ2, and KVJ10 by using bioinformatic tools, as well as studying the gene expression of the predicted genes in response to different growth conditions. And finally, establish a UPLC-HR-MS profile for the three strains in different modes of cultivations. Where the overall goal was to identify if altering growth conditions would give a higher yield of interesting secondary metabolites, hence determine which mode of cultivation is best suited for further isolation and biotechnological applications.

Observed morphological changes and allelopathic interactions

Cyanobacteria belonging to the genus *Nostoc* displays great diversity in morphology with the differentiation of several specialized cells (Rippka et al., 1979; Waterbury, 2006). After cultivation in nutrient stress cultures in two weeks, the changes in morphology were observed by microscopy for KVJ20. As expected in a nitrogen fixating cyanobacteria the development of heterocysts were present in -N cultures (Rippka et al., 1979), as well as long peal like chains of vegetative cells, and shorter chains of vegetative cells and no heterocysts were observed in +N cultures, as expected. The development of resting spore-like cells akinetes were seen upon deprivation of phosphate, which is expected as well since phosphate is essential for the growth of all living organisms, and such reaction has previously been observed in other phosphate deprived cyanobacteria (Perez et al., 2016).

In addition, in cultures deprived of iron and nitrogen, an unusual growth stage was observed, the aseriate growth stage where the vegetative cells clump together where it became hard, or even impossible to differentiate one cell from another. Previous studies have shown an upregulation of colony forming in cyanobacteria with iron limitation, and it's suggested that tighter “packaging” gives an advantage under such nutrient limitation, where recycling and enhancement of nutrient concentration within the colony are likely (Tzubari et al., 2018).

In cultures supplemented with N but deprived of iron, the formation of heterocysts was observed, which is unexpected since the bacteria should have no need to fix nitrogen in a nitrogen supplemented media. Iron is an important part of every photosynthetic organism, and especially in nitrogen fixating bacteria (Raven, 1988; Schoffman et al., 2016), and iron is also found as a structural component of nitrate assimilation enzymes an in the nitrogen-fixing enzyme nitrogenase (Kustka et al., 2002). Studies have also shown that the availability of iron plays an important role in the signaling of nitrogen in cyanobacteria (López-Gomollón et al.,

2007). Iron limitation also induces a decrease in the photosynthetic activity (Raven, 1988), hence also decrease the energy available for nitrate assimilation (Morel et al., 1991; Raven, 1988). Therefore when Fe is scarce, the uptake of nitrate (our source to nitrogen in media) is not as effective because of the role iron has in the photosynthetic electron transport chain (Raven, 1988; Schoffman et al., 2016), hence the bacteria might have perceived the iron starvation as also nitrogen starvation with result formation of heterocyst as a response. However, the nitrogen fixation taking place in heterocysts also requires a large amount of photosynthetically derived energy (Raven, 1988). Whether those heterocysts observed in media with nitrogen deprived of iron are active or efficient requires additional studies.

Cyanobacteria are known for having a variation of allelopathic traits, and previous activity has previously been described in all of the strains (Liaimer et al., 2016). From the allelopathic assay seen in Figure 17, both KVJ20 and KVJ2 were greatly affected in competition with KVJ10, while KVJ10 seems unaffected in the interaction. This inhibitory trait has also previously been observed for KVJ10 (Liaimer et al., 2016), and the strain is often referred to as a "killer strain" in the scientific community. We have also noted that the outcomes for KVJ2 and KVJ10 exposed to KVJ10 are different, where KVJ2 shows signs of bleaching, while KVJ20 is repelled, pursuing an escape strategy.

Bioinformatics

Bioinformatics has yet again proven to be a good tool to aid in the search for secondary metabolites, and several of the genes that were predicted by AntiSMASH matched compounds also found in the MS spectra, which confirms the reliability of the prediction. Nostoginin was however not predicted through direct gene cluster homology, but rather by comparison of AntiSMASH predicted chemical structures to Norine database via a link from the AntiSMASH prediction page. However, most of the predicted genes were also not assigned to a product and shows the lack of information on secondary metabolites in terrestrial cyanobacteria, and again reveals the bias against marine cyanobacteria previously suggested (Liaimer et al., 2016). From the bioinformatics a great homology between the genes in KVJ20 and KVJ2 were revealed, however KVJ20 stands out with the prediction of two microviridins, and otherwise is richer in RiPP biosynthetic clusters.

Growth conditions affecting gene expression

Previous studies have shown that by altering the cultivation condition several cryptic gene clusters can be awoken, as well as give insight into the functions of the genes (Yoon & Nodwell, 2014), as well as reveal novel secondary metabolites. Hence, we found it worthwhile to analyze how the gene expression patterns changes in response to different nutrients, and how it changes from standard growth media for cyanobacteria.

General traits of housekeeping genes

The *NifH* gene is a marker for the nitrogen fixation process and was highly upregulated in all three strains when deprived of N, as well as in solid culture. This is as expected since in nitrogen-depleted media diazotrophic cyanobacteria are known to fix nitrogen (Buikema & Haselkorn, 1991; Man-Aharonovich et al., 2007; Wang et al., 2015). Due to this, the upregulation of this gene can also be used as a sign of good quality of the gene expression data. It should be noted however that in solid culture no specific reactions to nitrogen deprived media were seen, this might be explained by those colonies growing on agar will have a gradient of nutrients and might be scarce of several nutrients.

Formation of akinetes, spore-like cells which form in response to nutrient limitation other than Nitrogen (Rippka et al., 1979; Sarma et al., 2004), have previously been linked with the expression of *AvaK*, and it's been used as a specific akinete marker gene (Zhou & Wolk, 2002). Hence the *AvaK* gene was expected to be upregulated in phosphate deprived media and have previously been observed in higher expression in deprivation of phosphate (Argueta et al., 2004). However, this does not support our findings in KVJ20, where the observation of akinetes were seen in phosphate depleted media, we did not see the corresponding upregulation of the *AvaK* gene. In addition, an upregulation of the *AvaK* gene was seen in iron deprived media, both in KVJ20 and KVJ10. From the morphology observations, we also saw the development of heterocyst in KVJ20 in iron-depleted media, and the envelopes of heterocyst and akinetes have known similarities in the chemical composition (Wolk et al., 1994). In both KVJ2 and KVJ10 the *AvaK* gene was greatly upregulated in phosphate deprived media, as well as in solid culture which is expected, however our results also suggest that the *Avak* gene might not be such a universal akinete marker as previously believed.

Motility in cyanobacteria have been observed in many different occasions (Wilde & Mullineaux, 2015), and the *PilT* gene has been shown to be essential for motility and natural competence (Okamoto & Ohmori, 2002; Yoshihara et al., 2001). For KVJ20 the *PilT* was

greatly upregulated in interaction with KVJ2 as well in +N, while the *PilT* was upregulated in -N culture in KVJ2. The high upregulation of *PilT* in KVJ20 in interaction with KVJ2 is particularly interesting, because one may suggest that these two strains have similar regulation of the transition into the motile stage.

The production of gas vesicles is well documented in diazotrophic cyanobacteria (Cohen-Bazire et al., 1969; Yang et al., 2017), and the *GvpC* gene is a gas vesicles marker gene. Transcription of the *GvpC* gene has only been observed under hormogonia (the motile stage) formation, hence the *GvpC* gene is a good indicator for upregulated motility (Damerval et al., 1987). In similarity with *PilT*, another indicator of motility the *GvpC* gene was also upregulated in KVJ20 in interaction with KVJ2. While in KVJ10 the *GvpC* gene was upregulated in nitrogen-depleted media as well as in interaction with KVJ20. The KVJ2 strains lack *Gvp* gene cluster, suggesting that gas vesicles are not essential for hormogonia differentiation.

Heterocyst glycolipids are lipids specific to heterocyst formation (Wolk et al., 1994; Wolk & Simon, 1969). The heterocyst protects the nitrogen fixation associated proteins from oxygen (Rippka et al., 1979), hence the regulation of *Hgl* is expected to be similar to those of nitrogen fixation (*NifH*). The upregulation of the *Hgl* was observed in the same patterns as *NifH* in all three strains, as expected.

Gene expression patterns in NRPS, PKS & RiPP gene clusters

Several of the NRPS/PKS/RiPP gene clusters from the three strains were upregulated in interaction conditions, as well as in nutrient-deprived media in all three strains. In the sections below a discussion about gene expression patterns, and similarities in gene expression observed in KVJ20 and KVJ2 is done collectively due to the high degree of homology between the strains, and the similarities between the different homologous gene clusters in the three strains are also discussed in the section below.

The *Ncp* gene cluster found in KVJ20 was highly upregulated in nutrient depleted media and in interaction conditions, hence its likely upregulated in a response to stress. When comparing the gene expression in KVJ20 against standard media, the *Ncp* gene had 31x higher expression in nitrogen supplemented media deprived of phosphate. While when comparing the *Ncp* gene clusters from KVJ20 and KVJ2 almost completely opposite gene expression patterns were observed.

The *Aer* gene cluster was found in both KVJ20 (*S/B-like*) and in KVJ2 (*Aer*), where both were higher expressed in standard media (-N) and in solid media with N. When comparing the Aer gene cluster from KVJ20 with KVJ2, the two gene clusters share similarity in expression and is likely to be regulated by the same mechanism. The *Apt* gene clusters were found in both KVJ20 and KVJ2 and shared great homology however, they do not share similar expression patterns, where the *Apt* gene cluster from KVJ2 is upregulated in standard media, while in KVJ20 it's upregulated in phosphate and iron deprived media. This might also explain why no *Apt* was found in KVJ20 with UPLC-HR-MS since the same characteristics seen in Anabaenopeptins from KVJ2 were used in the search in KVJ20.

For the unknown NRPS gene clusters (20-*N3* and 2-*N1*) we observed a similar exp pattern between KVJ20 and KVJ2, especially in media supplemented with N. Hence, this gene clusters might have similar functions in the two strains. Another interesting feature of these gene clusters is that is always upregulated in interaction strains, which makes it interesting for further research on allelopathic compounds in these three strains.

In KVJ2 the *PKS2* gene was highly upregulated in nitrogen deprived media, this gene was also predicted to be a heterocyst glycolipid like peptide by AntiSMASH, and the expression of it in nitrogen deprived media supports the prediction. And the corresponding homologous gene in KVJ20 (20-*P2*) did not show similarities in gene expression with *PKS2* from KVJ2. However, this *Hgl*-like gene cluster did have completely similar gene expression pattern as the heterocyst gene cluster in KVJ2, hence this *Hgl*-like gene cluster might be induced by the same response as the heterocyst glycolipid gene cluster and have a role in the production of heterocysts.

In contrast with KVJ20, several of the NRPS & PKS gene clusters in KVJ2 were shown to be higher expressed in standard media (-N). However, the *NRPS3* from KVJ2 showed an upregulation in nitrogen and iron-depleted media compared with standard media. From KVJ20 the predicted lanthipeptide (*RiPP11*) gene cluster was greatly upregulated in phosphate deprived media and in interaction with KVJ2, as well had a 38x higher expression in nitrogen supplemented media without phosphate compared with standard media. The microviridin gene cluster from KVJ20 (*RiPP8*) showed almost a 4x increase in phosphate deprived media supplemented with nitrogen compared to standard media. This upregulation of microviridin is interesting since some variants have shown inhibitory activities against elastase a serine-type protease (Ziemert et al., 2010), which also is a target enzyme when battling lung emphysema (Shapiro, 2002). In addition, the *Mvd* gene cluster from KVJ20 was

homologous with the *Mvd* gene cluster (2-*RiPP2*) from KVJ2 and shared similar gene expression patterns, hence might have similar functions in the two strains. However, when in interaction with KVJ10 they displayed a completely different expression, wherein KVJ20 its upregulated, and in KVJ2 its downregulated. Which may be related to the differences in outcome seen in the allelopathic analysis in these strains exposed to KVJ10, and it remains to be elucidated.

In KVJ2 the *RiPP4* gene cluster stood out and was highly upregulated in standard media (-N) and in nitrogen supplemented media deprived of phosphate and iron. In contrast with KVJ20, only a few RiPP gene clusters from KVJ2 showed an upregulation in interaction and nutrient deprived media compared with standard media, this includes; lanthipeptide (*RiPP3*), *RiPP5*, and *RiPP6*. From the homologous RiPP gene clusters in KVJ20 and KVJ2, only a few showed similar gene expression patterns, including the *Mvd* gene cluster. The homologous gene clusters 20-*RiPP2* from KVJ20 and 2-*RiPP1* from KVJ2 showed similar gene expression patterns, where they both showed a great downregulation in interaction with KVJ10, hence is likely, not involved in mechanisms involved in coping with KVJ10. Lastly, similarities between the homologous gene clusters 20-*RiPP6* from KVJ20 and 2-*RiPP7* from KVJ2 were found and were clearly downregulated in nutrient-deprived media, hence these genes are not induced by nutrient stress however, might play have similar functions in the two strains.

The only homologous gene clusters that also showed similar gene expression patterns in all three strains, was the possible siderophore gene clusters corresponding to 20-*NP2* in KVJ20, 2-*N3* in KVJ2 and 10-*NP1* in KVJ10. The possible siderophore gene clusters were greatly downregulated in all interaction cultures, hence is not important in the different allelopathic traits observed. Production of siderophores which are involved in iron acquisition have been observed in cyanobacteria as a response to iron limitations (Jeanjean et al., 2008), this upregulation of siderophore gene clusters in iron-depleted media was observed in all three strains. In addition, the siderophore gene clusters were greatly upregulated in solid culture, which also can be explained by a response to iron limitations. Colonies growing on agar plates forms a gradient of nutrients in the colony, hence also leading to iron limitations.

On the other hand, several genes in KVJ10 showed a high upregulation in interaction with KVJ2, including the *PKS2* give with a 73x, *RiPP1* with an 86x and *RiPP3* with almost a 50x increase in expression, all of these were also upregulated in nutrient-deprived media as well, however not in such great amount, hence we suggest that these genes might be responsible for

the allelopathic activity. This same high upregulation of RiPPs were also seen in interaction with KVJ2 when comparing the expression to standard media (-N). Hence for KVJ10, it's clear that altering nutrient conditions, results in great upregulation of RiPP which are relatively low expressed in ordinary standard conditions (-N). No obvious similarities in gene expression of homologous RiPP gene clusters between KVJ10, KVJ20, and KVJ2 were observed.

Several of the RiPP gene clusters were greatly upregulated in interaction strains, especially for KVJ10 and KVJ20, including some of the RiPPs predicted as lanthipeptides which is particularly interesting for further research since several lanthipeptides have previously displayed antibiotic properties (Knerr & Donk, 2012). The fact that many of the genes showed a much higher expression in other media than standard media, shows that by altering growth conditions, you can also awake cryptic genes, especially RiPPs. By comparing gene expression in for example nutrient deprived media with standard (-N) media, we also got an insight in which media is best suited for the enrichment of the compounds. The fact, that some of the RiPP gene cluster is induced both during starvation stress and under competition, may suggest that in natural conditions cyanobacteria produce antimicrobial compounds when starved in order to release nutrients from dead targeted microorganisms.

Growth conditions altering the chemical diversity

In this study, we aimed to describe the chemical diversity in three *Nostoc* strains subjected to different growth conditions, with an overall goal to investigate the biotechnological potential of these peptides and decide which cultivation is best suited for the extraction of secondary metabolites. Hence in the sections below both the general traits of the chemical diversity and the relative peak intensity and biotechnological potential is discussed.

The chemical diversity in general traits.

Cyanobacteria have proven to be a unique source of secondary metabolites, and by altering growth conditions we hoped to get a notable effect in chemical diversity, which in fact we got, where a great shift, especially in relative intensity was seen. Most of the compounds weren't identified by common databases, but by fragmentation patterns instead, this shows the clear biased in research on marine cyanobacteria previously described (Liaimer et al., 2016).

From the UPLC-HR-MS analysis of KVJ20 the previously identified S/B-like peptide (Liaimer et al., 2016) with m/z 927 and m/z 997 and their sulfated peptides were found as well as a new S/B-like peptide with m/z 969, all with a ion of m/z 610 in their fragmentation

pattern, which also have been observed both in natural and synthetic Banyaside, which is structurally similar to Suomilide but produced in *Nostoc* (Schindler et al., 2010). In previously studies Ncp with an m/z 757 have been found in KVJ20 (Liaimer et al., 2016), which supports our findings. In addition to the previously found Ncp, several other Ncp variants were found in KVJ20 with m/z 775 and m/z 809.

From the UPLC-HR-MS analysis of KVJ2 we found Aeruginosin, Nostocyclopeptide (m/z 757) and several Anabaenopeptins which all have been observed in previous studies (Guljamow et al., 2017; Liaimer et al., 2016), which supports our finding. In addition, KVJ2 also produced several other variants of Ncp, which have not been observed in previous studies, which proves that by altering the growth conditions, several other and new interesting secondary metabolites can be found. Several of the same compounds found in KVJ2 were also found in KVJ20, which emphasize the high homology shared between the two strains.

In contrast to KVJ2 and KVJ20, the UPLC-HR-MS profile of KVJ10 is quite different, and have a completely different chemical profile, but only one peak in common with KVJ20 from the cell extracts. This data is consistent with the bioinformatics gene cluster predictions. KVJ10 have previously been observed to be a source of Nosperin (Liaimer et al., 2016), which supports our findings of Nosperin with m/z 564. In addition, Hapalosin mostly observed as a sodium adduct with m/z 512 was found and have not been described in the strain prior to this.

In the media extracts of all the strains, prominent peaks with m/z 379 and m/z 447 were found and are suggested to be common compounds belonging to the *Nostoc* genus. Many of the compounds found in the media extracts, were also found in cell extracts. For all the strains little difference between the chemical diversity between the different growth cultivation was found however, the peak intensity, i.e. ratios between the compounds, varied a lot in the different cultivation types.

From the allelopathic assays, no unique compounds other than those found in cell and media extracts were found, even though allelopathic traits are observed. This might be a result from the fact that such allelopathic compounds are often excreted in the media (Liaimer et al., 2016), but we extracted from the colonies rather than from the agar with hopes of also seeing some of the excreted compounds still present in the cells. It should also be mentioned that the extraction for the co-cultivation was done after only one week, and normally they are grown in co-cultivation in three weeks, but we needed to do the extraction relatively early do avoid

cell-death. Hence, this might be the reason why we don't see any specific peaks in this trial, since the concentration of allelopathic compounds may be under the detection limits for the mass spectrometry, or to close to the baseline in the chromatography. Another explanation might be that in solid grown colonies, only cells at the edges are exposed to the competitor factors, while the inner parts of the colony are screened. So, the overall yield of elicited competition induced compounds becomes low. We need to work out an experimental set up with liquid cultures, where competitors are either separated by membranes, or one uses extracts of one strain to induce reactions in another.

Several of the compounds that were predicted from the bioinformatic analysis, and proven to be present by the gene expression analysis were not detected by UPLC-HR-MS. These peptides include Nostoginin in KVJ10 and Anabaenopeptin in KVJ20. While analyzing the UPLC-HR-MS data in retrospect, a peptide with m/z 856 was observed in KVJ20 which could be a possible candidate for Apt. This peptide had similar retention time, as well as the mass of already known Apt. However, it is not included the results, since it was only found in very low amounts in a few of the extracts.

Relative peak intensity and biotechnological potential.

When considering which cultivation is best suited for highest success rate with extraction and isolation of compound of interest several things need to be considered, here we suggest that relative yield to highest peak in sample, ratio with the other identified secondary metabolites as well as if the compound is cell bound or secreted in the media needs to be considered. By looking at the relative yield, we get a suggestion of how much the compound is present in comparison with other compounds in the sample, the same is true for ratio with other identified secondary metabolites, where the optimal situation is to have a high relative yield. If the compound is cell-bound additional steps in extraction is needed to release the compound, whereas if the compound is secreted in the media simple extraction process may be conducted. Another plus side with compounds secreted in media is that allelopathic compounds often are secreted in the media (Liaimer et al., 2016).

Many of the observed compound and their relative peak size does not overlap with the observed gene expression patterns, with the exception of Aeruginosin and Nostocyclopeptides in KVJ2, and the Suomilide/Banyaside-like peptide in KVJ20. This indicates that even though the gene expression is high this does not directly correspond to the amount of peptide being produced. One suggestion has been that some peptides are produced at a constant rate, trapped

and only dispersed at certain times (Liaimer et al., 2015). Need also to emphasize that even though several of the compounds were found with high relative yield in interaction strains indicating that they might play a role in the allelopathic properties, the same compounds were also found with high relative yield with nutrient deprivation, in interaction cyanobacteria grew in colonies which are characterized by gradients of both nutritional conditions and other exposures to external factors, hence the upregulation can be due to both nutrient deprivation and interaction, and no clear conclusion can be drawn.

Both KVJ20 and KVJ2 have proven to be good producers of Nostocyclopeptide and have a high relative yield of the compounds in standard media (-N). Where for KVJ2 the Ncp:Apt:Aer ratio was generally high for Nostocyclopeptide, especially in nitrogen supplemented media extracts with and without iron, where the ratio of Ncp:Apt:Aer was 212:1:37 in nitrogen supplemented media. Nostocyclopeptide in KVJ2 is also found secreted in the media in greater amounts, hence when choosing between KVJ20 and KVJ2, KVJ2 medium extracts supplemented with nitrogen would be more suitable for the isolation of such Nostocyclopeptides. In addition, Nostocyclopeptides have been proven to have antitoxic properties against microcystins in other *Nostoc* strains (Jokela et al., 2010), and might explain why we see an upregulation of the Ncp gene as well as the high relative yield of the compound in KVJ20 when in interaction with KVJ10.

For KVJ20 in interaction with KVJ10, the S/B-like peptides and Ncp m/z 809 were found with great peak intensity and is an indication that these compounds play a role in coping with KVJ10. In interaction with KVJ10, and we also saw vigorous spreading away from KVJ10 in allelopathic assays, hence the S/B-like peptides and Ncp might play a part in regulating this vigorous spread. The S/B-like peptides were mainly found in cell extracts, hence it's likely that the peptide is cell-bound. The S/B-like peptides were only found in media extracts when deprived of phosphate, which can possibly be due to cell death, hence releasing the compounds. S/B was also found in high yield in almost all samples, hence isolation can be conducted from ordinary media. However, when considering the Ncp:S/B ratio in yield, a medium supplemented with nitrogen and without iron is desired.

Aeruginosin in KVJ2 was found in high relative yield in both cell extracts and medium extracts in nitrogen supplemented media both with and without iron. Due to the high yield found in medium extracts, isolation of Aeruginosin can easily be conducted from media extracts of KVJ2 cultivated in nitrogen supplemented medium.

From analyzing the relative peak intensity, we saw that Anabaenopeptin is clearly cell-bound, and was only found in small amounts in KVJ2, but with considerably higher yield in phosphate deprived conditions. Which supports previous findings showing that Anabaenopeptin is produced in higher yield in phosphate limitations (Repka et al., 2004). Hence a phosphate deprived media could possibly be used for the isolation of Anabaenopeptins.

Nosperin, a unique member of the pederin family of natural products (Kampa et al., 2013) was only found in smaller amounts in the cell extracts of KVJ10. Nosperin has previously been suggested to play a role in symbiotic associations (Kampa et al., 2013), hence explain the observed low yield. However, in the medium extracts without nitrogen Nosperin was found with a higher yield than in cell extract, therefore for isolation and further investigation of Nosperin can likely be conducted from medium extracts from KVJ10 cultivation in standard media.

The new finding of Hapalosin in KVJ10 open for new biotechnological potential for usage of the strain and the sodium adduct with m/z 512 was found with high yield in standard media, making it relatively easy to isolate. Hapalosin was found in 25x times higher yield than Nosperin in cell extracts in standard media (-N), and in 41x in nitrogen and phosphate deprived media, and both these cultivations are suitable for isolation of Hapalosin. In addition, we saw that Hapalosin might be cell-bound due to the low yield found in medium extracts, where high yield is only observed in phosphate deprived media, which might be explained by cell-death causing the peptide to be released in the media. In Table 24, a summary of the suggested cultivation for KVJ20, KVJ2 and KVJ10 most suitable for enrichment of respective identified compounds are shown.

Table 24: Suggested cultivation and extraction type most suitable for enrichment of respective identified compounds. N.d: not detected.

Identified compound	***KVJ20***	***KVJ2***	***KVJ10***
Aeruginosin	n.d	Media extract: +N	n.d
Anabaenopeptin	n.d	Cell extract: +N-P	n.d
Hapalosin	n.d	n.d	Cell extract: -N
Nosperin	n.d	n.d	Media extract: -N
Nostocyclopeptide	Cell extract: +N	Media extract: +N	n.d
Suomilide/Banyaside-like	Cell extract: -N	n.d	n.d

From this study, KVJ10 stands out as a potential source of new antibiotics due to both its "super killer" traits and the great upregulation of RiPP gene clusters in interaction with KVJ2 and KVJ20 in addition, be a potential source of new analogs of Hapalosin. Hapalosin has previously shown multidrug-resistance (MDR) reversing activity in tumor cells which after chemotherapeutic treatment have developed resistance to other unrelated drugs (Stratmann et al., 1994). This is one of the most difficult problems associated with cancer therapy. In previous studies, it has however been stated that a more potent version of the already known Hapalosin and its analogs isolated from *Hapalosiphon welwitschii* W. & G. S. West, is needed to be a clinically useful compound (Kashihara et al., 2000; O'Connell et al., 1999). Still, the discovery of Hapalosin in KVJ10 and further isolation and characterization may still give new insight to the chemistry behind the MDR reversing activity.

Outlooks

After this research, we stand left with many unanswered questions, as well as many interesting further prospects. From the allelopathic assay, we couldn't detect any compound which clearly stood out in the extracts, which might be since most allelopathic compounds are extracted in the media, hence still trapped in the agar. We also saw that many of the genes that were highly upregulated in interaction strains, were also upregulated in nutrient-deprived media, hence no clear conclusion which genes are responsible for the allelopathic activity can be drawn. This can be solved by altering the allelopathic assay; we suggest having liquid cultures, where competitors are either separated by membranes, or one uses extracts of one strain to induce reactions in another. In liquid culture nutrients are evenly dispersed, hence you eliminate the factor of nutrient deprivation, and clear conclusions about which genes might be responsible for allelopathic activity can be drawn.

This study has shown that by altering the cultivation conditions changes in both gene expression and in the chemical diversity is seen. For further studies, other cultivation parameters can be altered, and the possibilities are almost endless; the bacteria can be subjected to UV stress, oxidative stress, competition with other bacteria, temperature, light, removing/adding minerals, etc. One promising approach to awake cryptic genes is to add soil extracts which have been shown to switch on cryptic antibiotic genes in other bacteria (Lincke et al., 2010), which is particularly interesting for us since all three strains are terrestrial cyanobacteria.

Another pressing matter is to confirm/disprove the expression patterns observed in the *AvaK* gene cluster in KVJ20, if new studies confirm our results, *AvaK* is not such a universal akinete marker as previously thought. In addition, further research on the *PilT* gene cluster in KVJ20 and KVJ2, and how the *PilT* plays a role in the regulation of the transition into motile stage is needed.

For the conduction of this study, one thing stood out as difficult, the analyzing of different spectra and MS data of the crude extracts. In further research I highly recommend to fraction these crude extracts so that a smaller amount of data is needed to be analyzed, and also optimize the settings of the mass spectrometry and the chromatography to get the best possible spectra's, as well as the best possible fragmentation patterns, since several cyanobacterial secondary metabolites have been characterized by their typical fragmentation. By doing so the undetected but predicted secondary metabolites (Nostoginin in KVJ10 and Anabaenopeptin in KVJ20) might be detected in further analysis.

Further isolation and characterization of the peptides previously not observed in these strains are very interesting, as well as the elucidation of identified secondary metabolites, where Hapalosin has the greatest bioactive potential, based on already known bioactivity. Further isolation and characterization are also important to enhance current knowledge about secondary metabolites from terrestrial cyanobacteria, hence guide the further discovery of novel cyanobacterial secondary metabolites.

Conclusions

The newly sequenced genomes of Three terrestrial *Nostoc* spp. KVJ20, KVJ2 and KVJ10 allowed us to predict secondary metabolite gene clusters with the bioinformatic AntiSMASH tool. We predicted 6 NRPS, 2 PKS and 11 RiPP gene clusters in KVJ20, and 7 NRPS, 3 PKS and 7 RiPP gene clusters in KVJ2, and 9 NRPS, 3 PKS and 6 RiPP gene clusters in KVJ10. *Nostoc* sp. KVJ20 and KVJ2 share similarities in their set of secondary metabolite gene clusters, while *Nostoc* sp. KVJ10 does not. From these predicted gene clusters, we successfully designed primers for qPCR by using PRIMER-BLAST, and further studied the gene expression of the predicted genes with reverse transcription-qPCR in response to different nutrient conditions and competition. In addition, UPLC-HR-MS profiles were established for all three strains in these different nutrient conditions, where several secondary metabolites were identified through extensive database and literature search.

This study has confirmed that altering cultivations conditions, results in great upregulation of several secondary metabolite gene cluster, also in gene clusters regarded as cryptic. Most notably several RiPP genes were higher expressed in response to competition and nutrient deprivation. This study also revealed that gene expression patterns do not necessarily correspond to the observed changes in identified secondary metabolite production. The gene expression data and results of UPLC-HR-MS analysis also allowed us to suggest suitable growth conditions for the enrichment of the identified compounds.

This thesis opens for several intriguing questions regarding the gene expression of secondary metabolites gene clusters, the production of secondary metabolites, and their role in allelopathic interactions and in free-living strains for *Nostoc* spp. KVJ20, KVJ2, and KVJ10.

References

Abed, R. M. M., Dobretsov, S., & Sudesh, K. (2009). Applications of cyanobacteria in biotechnology. *Journal of Applied Microbiology, 106*(1), 1-12. doi:10.1111/j.1365-2672.2008.03918.x

Adams, D. G., Bergman, B., Nierzwicki-Bauer, S. A., Duggan, P. S., Rai, A. N., & Schüßler, A. (2013). Cyanobacterial-Plant Symbioses. In E. Rosenberg, E. F. DeLong, S. Lory, E. Stackebrandt, & F. Thompson (Eds.), *The Prokaryotes: Prokaryotic Biology and Symbiotic Associations* (pp. 359-400). Berlin, Heidelberg: Springer Berlin Heidelberg. doi:10.1007/978-3-642-30194-0_17

Ansari, M. Z., Yadav, G., Gokhale, R. S., & Mohanty, D. (2004). NRPS-PKS: a knowledge-based resource for analysis of NRPS/PKS megasynthases. *Nucleic Acids Research, 32*(Web Server issue), W405-W413. doi:10.1093/nar/gkh359

Argueta, C., Yuksek, K., & Summers, M. (2004). Construction and use of GFP reporter vectors for analysis of cell-type-specific gene expression in Nostoc punctiforme. *Journal of Microbiological Methods, 59*(2), 181-188. doi:10.1016/j.mimet.2004.06.009.

Arnison, P. G., Bibb, M. J., Bierbaum, G., Bowers, A. A., Bugni, T. S., Bulaj, G., . . . van der Donk, W. A. (2013). Ribosomally synthesized and post-translationally modified peptide natural products: overview and recommendations for a universal nomenclature. *Natural Product Reports, 30*(1), 108-160. doi:10.1039/c2np20085f

Balunas, M. J., Linington, R. G., Tidgewell, K., Fenner, A. M., Ureña, L.-D., Togna, G. D., . . . Gerwick, W. H. (2010). Dragonamide E, a modified linear lipopeptide from Lyngbya majuscula with antileishmanial activity. *Journal of natural products, 73*(1), 60-66. doi:10.1021/np900622m

Becker, J. E., Moore, R. E., & Moore, B. S. (2004). Cloning, sequencing, and biochemical characterization of the nostocyclopeptide biosynthetic gene cluster: molecular basis for imine macrocyclization. *Gene, 325*, 35-42. doi:10.1016/j.gene.2003.09.034

Berry, J. P., Gantar, M., Perez, M. H., Berry, G., & Noriega, F. G. (2008). Cyanobacterial toxins as allelochemicals with potential applications as algaecides, herbicides and insecticides. *Marine Drugs, 6*(2), 117-146. doi:10.3390/md20080007

Bister, B., Keller, S., Baumann, H. I., Nicholson, G., Weist, S., Jung, G., . . . Jüttner, F. (2004). Cyanopeptolin 963A, a Chymotrypsin Inhibitor of Microcystis PCC 7806. *Journal of natural products, 67*(10), 1755-1757. doi:10.1021/np049828f

Blackhurst, R. L., Genge, M. J., Kearsley, A. T., & Grady, M. M. (2005). Cryptoendolithic alteration of Antarctic sandstones: Pioneers or opportunists? *Journal of Geophysical Research: Planets, 110*(E12). doi:10.1029/2005JE002463

Blin, K., Weber, T., Kim, H. U., Lee, S. Y., Medema, M. H., Duddela, S., . . . Breitling, R. (2015). antiSMASH 3.0—a comprehensive resource for the genome mining of biosynthetic gene clusters. *Nucleic Acids Research, 43*(W1), W237-W243. doi:10.1093/nar/gkv437

Briand, E., Bormans, M., Gugger, M., Dorrestein, P. C., & Gerwick, W. H. (2016). Changes in secondary metabolic profiles of Microcystis aeruginosa strains in response to intraspecific interactions. *Environmental Microbiology, 18*(2), 384-400. doi:10.1111/1462-2920.12904

Buikema, W. J., & Haselkorn, R. (1991). Characterization of a gene controlling heterocyst differentiation in the cyanobacterium Anabaena 7120. *Genes & Development, 5*(2), 321-330. doi:10.1101/gad.5.2.321

Burja, A. M., Banaigs, B., Abou-Mansour, E., Grant Burgess, J., & Wright, P. C. (2001). Marine cyanobacteria—a prolific source of natural products. *Tetrahedron, 57*(46), 9347-9377. doi:10.1016/S0040-4020(01)00931-0

Bustin, S. A. (2002). Quantification of mRNA using real-time reverse transcription PCR (RT-PCR): trends and problems. *Journal of Molecular Endocrinology, 29*(1), 23-39. doi:10.1677/jme.0.0290023

Castenholz, R. W. (2015). General Characteristics of the Cyanobacteria. In B. Whitman, F. Rainey, P. Kämpfer, M. Trujillo, J. Chun, P. DeVos, B. Hedlund, & S. Dedysh (Eds.), *Bergey's Manual of Systematics of Archaea and Bacteria*. doi:10.1002/9781118960608.cbm00019

Castenholz, R. W., & Waterbury, J. B. (1989). Oxygenic photosynthetic bacteria. Group I. Cyanobacteria. In *Bergey's manual of systematic bacteriology* (Vol. 3): Springer, New York, NY. doi:10.1002/9781118960608.pbm00010

Castenholz, R. W., Wilmotte, A., Herdman, M., Rippka, R., Waterbury, J. B., Iteman, I., & Hoffmann, L. (2001). Phylum BX. Cyanobacteria. In D. R. Boone, R. W. Castenholz, & G. M. Garrity (Eds.), *Bergey's Manual® of Systematic Bacteriology: Volume One : The Archaea and the Deeply Branching and Phototrophic Bacteria* (pp. 473-599). New York, NY: Springer New York. doi:10.1007/978-0-387-21609-6_27

Challis, G. L., & Naismith, J. H. (2004). Structural aspects of non-ribosomal peptide biosynthesis. *Current opinion in structural biology, 14*(6), 748-756. doi:10.1016/j.sbi.2004.10.005

Chang, Z., Flatt, P., Gerwick, W. H., Nguyen, V.-A., Willis, C. L., & Sherman, D. H. (2002). The barbamide biosynthetic gene cluster: a novel marine cyanobacterial system of mixed polyketide synthase (PKS)-

non-ribosomal peptide synthetase (NRPS) origin involving an unusual trichloroleucyl starter unit. *Gene, 296*(1), 235-247. doi:10.1016/S0378-1119(02)00860-0
Choi, H., Pereira, A. R., Cao, Z., Shuman, C. F., Engene, N., Byrum, T., . . . Gerwick, W. H. (2010). The hoiamides, structurally intriguing neurotoxic lipopeptides from Papua New Guinea marine cyanobacteria. *Journal of natural products, 73*(8), 1411-1421. doi:10.1021/np100468n
Chojnacka, K., & Noworyta, A. (2004). Evaluation of Spirulina sp. growth in photoautotrophic, heterotrophic and mixotrophic cultures. *Enzyme and Microbial Technology, 34*(5), 461-465. doi:10.1016/j.enzmictec.2003.12.002
Cohen-Bazire, G., Kunisawa, R., & Pfennig, N. (1969). Comparative study of the structure of gas vacuoles. *Journal of bacteriology, 100*(2), 1049-1061.
Conti, E., Stachelhaus, T., Marahiel, M. A., & Brick, P. (1997). Structural basis for the activation of phenylalanine in the non-ribosomal biosynthesis of gramicidin S. *The EMBO Journal, 16*(14), 4174-4183. doi:10.1093/emboj/16.14.4174
Costa, M., Costa-Rodrigues, J., Fernandes, M. H., Barros, P., Vasconcelos, V., & Martins, R. (2012). Marine cyanobacteria compounds with anticancer properties: a review on the implication of apoptosis. *Marine Drugs, 10*(10), 2181-2207. doi:10.3390/md10102181
Cubillos-Ruiz, A., Berta-Thompson, J. W., Becker, J. W., Van Der Donk, W. A., & Chisholm, S. W. (2017). Evolutionary radiation of lanthipeptides in marine cyanobacteria. *Proceedings of the National Academy of Sciences of the United States of America, 114*(27), E5424-E5433. doi:10.1073/pnas.1700990114
Damerval, T., Houmard, J., Guglielmi, G., Csiszàr, K., & de Marsac, N. T. (1987). A developmentally regulated gvpABC operon is involved in the formation of gas vesicles in the cyanobacterium Calothrix 7601. *Gene, 54*(1), 83-92. doi:10.1016/0378-1119(87)90350-7
de Figueiredo, D. R., Reboleira, A. S. S. P., Antunes, S. C., Abrantes, N., Azeiteiro, U., Gonçalves, F., & Pereira, M. J. (2006). The effect of environmental parameters and cyanobacterial blooms on phytoplankton dynamics of a Portuguese temperate Lake. *Hydrobiologia, 568*(1), 145-157. doi:10.1007/s10750-006-0196-y
Dittmann, E., Fewer, D. P., & Neilan, B. A. (2013). Cyanobacterial toxins: biosynthetic routes and evolutionary roots. *FEMS Microbiology Reviews, 37*(1), 23-43. doi:10.1111/j.1574-6976.2012.12000.x
Dittmann, E., Gugger, M., Sivonen, K., & Fewer, D. P. (2015). Natural Product Biosynthetic Diversity and Comparative Genomics of the Cyanobacteria. *Trends in Microbiology, 23*(10), 642-652. doi:10.1016/j.tim.2015.07.008
Dittmann, E., & Wiegand, C. (2006). Cyanobacterial toxins – occurrence, biosynthesis and impact on human affairs. *Molecular Nutrition & Food Research, 50*(1), 7-17. doi:10.1002/mnfr.200500162
Dodds, W. K., Gudder, D. A., & Mollenhauer, D. (1995). THE ECOLOGY OF NOSTOC. *Journal of Phycology, 31*(1), 2-18. doi:10.1111/j.0022-3646.1995.00002.x
Donia, M. S., Ravel, J., & Schmidt, E. W. (2008). A global assembly line for cyanobactins. *Nature chemical biology, 4*(6), 341-343. doi:10.1038/nchembio.84
Ducat, D. C., Way, J. C., & Silver, P. A. (2011). Engineering cyanobacteria to generate high-value products. *Trends in Biotechnology, 29*(2), 95-103. doi:10.1016/j.tibtech.2010.12.003
Duggan, P. S., & Adams, D. G. (2008). Cyanobacteria–bryophyte symbioses. *Journal of Experimental Botany, 59*(5), 1047-1058. doi:10.1093/jxb/ern005
Edwards, D. J., Marquez, B. L., Nogle, L. M., McPhail, K., Goeger, D. E., Roberts, M. A., & Gerwick, W. H. (2004). Structure and Biosynthesis of the Jamaicamides, New Mixed Polyketide-Peptide Neurotoxins from the Marine Cyanobacterium Lyngbya majuscula. *Chemistry & Biology, 11*(6), 817-833. doi:10.1016/j.chembiol.2004.03.030
Ersmark, K., Del Valle, J. R., & Hanessian, S. (2008). Chemistry and Biology of the Aeruginosin Family of Serine Protease Inhibitors. *Angewandte Chemie International Edition, 47*(7), 1202-1223. doi:10.1002/anie.200605219
Fastner, J., Erhard, M., & von Döhren, H. (2001). Determination of oligopeptide diversity within a natural population of Microcystis spp. (cyanobacteria) by typing single colonies by matrix-assisted laser desorption ionization-time of flight mass spectrometry. *Applied and Environmental Microbiology, 67*(11), 5069-5076. doi:10.1128/AEM.67.11.5069-5076.2001
Fewer, D. P., Rouhiainen, L., Jokela, J., Wahlsten, M., Laakso, K., Wang, H., & Sivonen, K. (2007). Recurrent adenylation domain replacement in the microcystin synthetase gene cluster. *BMC Evolutionary Biology, 7*(1), 183. doi:10.1186/1471-2148-7-183
Foster, R. A., Kuypers, M. M. M., Vagner, T., Paerl, R. W., Musat, N., & Zehr, J. P. (2011). Nitrogen fixation and transfer in open ocean diatom-cyanobacterial symbioses. *The ISME journal, 5*(9), 1484-1493. doi:10.1038/ismej.2011.26

Freeman, C. J., & Thacker, R. W. (2011). Complex interactions between marine sponges and their symbiotic microbial communities. *Limnology and Oceanography, 56*(5), 1577-1586. doi:10.4319/lo.2011.56.5.1577

Fu, X., Do, T., Schmitz, F. J., Andrusevich, V., & Engel, M. H. (1998). New Cyclic Peptides from the Ascidian Lissoclinum patella. *Journal of natural products, 61*(12), 1547-1551. doi:10.1021/np9802872

Fujii, K., Mayumi, T., Noguchi, K., Kashiwagi, T., Akashi, S., Sivonen, K., . . . Harada, K.-i. (2000). Mass Spectrometric Studies of Peptides from Cyanobacteria under FAB MS/MS Conditions. *Journal of the Mass Spectrometry Society of Japan, 48*(1), 56-64. doi:10.5702/massspec.48.56

Gatte-Picchi, D., Weiz, A., Ishida, K., Hertweck, C., & Dittmann, E. (2014). Functional Analysis of Environmental DNA-Derived Microviridins Provides New Insights into the Diversity of the Tricyclic Peptide Family. *Applied and Environmental Microbiology, 80*(4), 1380-1387. doi:10.1128/aem.03502-13

Gerwick, W. H., Proteau, P. J., Nagle, D. G., Hamel, E., Blokhin, A., & Slate, D. L. (1994). Structure of Curacin A, a Novel Antimitotic, Antiproliferative and Brine Shrimp Toxic Natural Product from the Marine Cyanobacterium Lyngbya majuscula. *The Journal of Organic Chemistry, 59*(6), 1243-1245. doi:10.1021/jo00085a006

Golakoti, T., Ogino, J., Heltzel, C. E., Le Husebo, T., Jensen, C. M., Larsen, L. K., . . . Valeriote, F. A. (1995). Structure determination, conformational analysis, chemical stability studies, and antitumor evaluation of the cryptophycins. Isolation of 18 new analogs from Nostoc sp. strain GSV 224. *Journal of the American Chemical Society, 117*(49), 12030-12049. doi:10.1021/ja00154a002

Golakoti, T., Yoshida, W. Y., Chaganty, S., & Moore, R. E. (2000). Isolation and Structures of Nostopeptolides A1, A2 and A3 from the Cyanobacterium Nostoc sp. GSV224. *Tetrahedron, 56*(46), 9093-9102. doi:10.1016/S0040-4020(00)00764-X

Golakoti, T., Yoshida, W. Y., Chaganty, S., & Moore, R. E. (2001). Isolation and Structure Determination of Nostocyclopeptides A1 and A2 from the Terrestrial Cyanobacterium Nostoc sp. ATCC53789. *Journal of natural products, 64*(1), 54-59. doi:10.1021/np000316k

Grata, E., Boccard, J., Guillarme, D., Glauser, G., Carrupt, P.-A., Farmer, E. E., . . . Rudaz, S. (2008). UPLC–TOF-MS for plant metabolomics: A sequential approach for wound marker analysis in Arabidopsis thaliana. *Journal of Chromatography B, 871*(2), 261-270. doi:10.1016/j.jchromb.2008.04.021

Gugger, M. F., & Hoffmann, L. (2004). Polyphyly of true branching cyanobacteria (Stigonematales). *International Journal of Systematic and Evolutionary Microbiology, 54*(2), 349-357. doi:doi:10.1099/ijs.0.02744-0

Guljamow, A., Kreische, M., Ishida, K., Liaimer, A., Altermark, B., Bähr, L., . . . Dittmann, E. (2017). High-Density Cultivation of Terrestrial Nostoc Strains Leads to Reprogramming of Secondary Metabolome. *Applied and Environmental Microbiology, 83*(23), e01510-01517. doi:10.1128/aem.01510-17

Harada, K.-i., Fujii, K., Shimada, T., Suzuki, M., Sano, H., Adachi, K., & Carmichael, W. W. (1995). Two cyclic peptides, anabaenopeptins, a third group of bioactive compounds from the cyanobacteriumAnabaena flos-aquae NRC 525-17. *Tetrahedron Letters, 36*(9), 1511-1514. doi:10.1016/0040-4039(95)00073-L

Harrigan, G. G., & Goetz, G. (2002). Symbiotic and dietary marine microalgae as a source of bioactive molecules–experience from natural products research. *Journal of Applied Phycology, 14*(2), 103-108. doi:10.1023/a:1019570122349

Heid, C. A., Stevens, J., Livak, K. J., & Williams, P. M. (1996). Real time quantitative PCR. *Genome Research, 6*(10), 986-994. doi:10.1101/gr.6.10.986

Heidrich, J., Thurotte, A., & Schneider, D. (2017). Specific interaction of IM30/Vipp1 with cyanobacterial and chloroplast membranes results in membrane remodeling and eventually in membrane fusion. *Biochimica et Biophysica Acta (BBA) - Biomembranes, 1859*(4), 537-549. doi:10.1016/j.bbamem.2016.09.025

Hess, W. R. (2011). Cyanobacterial genomics for ecology and biotechnology. *Current Opinion in Microbiology, 14*(5), 608-614. doi:10.1016/j.mib.2011.07.024

Hetrick, K. J., & van der Donk, W. A. (2017). Ribosomally synthesized and post-translationally modified peptide natural product discovery in the genomic era. *Current Opinion in Chemical Biology, 38*, 36-44. doi:10.1016/j.cbpa.2017.02.005

Hoffmann, D., Hevel, J. M., Moore, R. E., & Moore, B. S. (2003). Sequence analysis and biochemical characterization of the nostopeptolide A biosynthetic gene cluster from Nostoc sp. GSV224. *Gene, 311*, 171-180. doi:10.1016/S0378-1119(03)00587-0

Hopwood, D. A. (1997). Genetic Contributions to Understanding Polyketide Synthases. *Chemical Reviews, 97*(7), 2465-2498. doi:10.1021/cr960034i

Ingolfsson, H., & Yona, G. (2008). Protein Domain Prediction. In B. Kobe, M. Guss, & T. Huber (Eds.), *Structural Proteomics: High-Throughput Methods* (pp. 117-143). Totowa, NJ: Humana Press. doi:10.1007/978-1-60327-058-8_7

Ishida, K., Christiansen, G., Yoshida, W. Y., Kurmayer, R., Welker, M., Valls, N., . . . Dittmann, E. (2007). Biosynthesis and Structure of Aeruginoside 126A and 126B, Cyanobacterial Peptide Glycosides Bearing a 2-Carboxy-6-Hydroxyoctahydroindole Moiety. *Chemistry & Biology, 14*(5), 565-576. doi:10.1016/j.chembiol.2007.04.006

Ishida, K., Okita, Y., Matsuda, H., Okino, T., & Murakami, M. (1999). Aeruginosins, protease inhibitors from the cyanobacterium Microcystis aeruginosa. *Tetrahedron, 55*(36), 10971-10988. doi:10.1016/S0040-4020(99)00621-3

Ishitsuka, M. O., Kusumi, T., Kakisawa, H., Kaya, K., & Watanabe, M. M. (1990). Microviridin. A novel tricyclic depsipeptide from the toxic cyanobacterium Microcystis viridis. *Journal of the American Chemical Society, 112*(22), 8180-8182. doi:10.1021/ja00178a060

Jean-Luc, W., Guillaume, M., & Emerson Ferreira, Q. (2010). Advances in Techniques for Profiling Crude Extracts and for the Rapid Identificationof Natural Products: Dereplication, Quality Control and Metabolomics. *Current Organic Chemistry, 14*(16), 1808-1832. doi:10.2174/138527210792927645

Jeanjean, R., Talla, E., Latifi, A., Havaux, M., Janicki, A., & Zhang, C.-C. (2008). A large gene cluster encoding peptide synthetases and polyketide synthases is involved in production of siderophores and oxidative stress response in the cyanobacterium Anabaena sp. strain PCC 7120. *Environmental Microbiology, 10*(10), 2574-2585. doi:10.1111/j.1462-2920.2008.01680.x

Jenke-Kodama, H., Sandmann, A., Müller, R., & Dittmann, E. (2005). Evolutionary Implications of Bacterial Polyketide Synthases. *Molecular Biology and Evolution, 22*(10), 2027-2039. doi:10.1093/molbev/msi193

Jokela , J., Herfindal , L., Wahlsten, M., Permi, P., Selheim , F., Vasconçelos, V., . . . Sivonen, K. (2010). A Novel Cyanobacterial Nostocyclopeptide is a Potent Antitoxin against Microcystins. *ChemBioChem, 11*(11), 1594-1599. doi:10.1002/cbic.201000179

Jones, A. C., Gu, L., Sorrels, C. M., Sherman, D. H., & Gerwick, W. H. (2009). New tricks from ancient algae: natural products biosynthesis in marine cyanobacteria. *Current Opinion in Chemical Biology, 13*(2), 216-223. doi:10.1016/j.cbpa.2009.02.019

Kampa, A., Gagunashvili, A. N., Gulder, T. A. M., Morinaka, B. I., Daolio, C., Godejohann, M., . . . Andrésson, Ó. S. (2013). Metagenomic natural product discovery in lichen provides evidence for a family of biosynthetic pathways in diverse symbioses. *Proceedings of the National Academy of Sciences, 110*(33), E3129-E3137. doi:10.1073/pnas.1305867110

Kanekiyo, K., Lee, J.-B., Hayashi, K., Takenaka, H., Hayakawa, Y., Endo, S., & Hayashi, T. (2005). Isolation of an Antiviral Polysaccharide, Nostoflan, from a Terrestrial Cyanobacterium, Nostoc flagelliforme. *Journal of natural products, 68*(7), 1037-1041. doi:10.1021/np050056c

Kapuścik, A., Hrouzek, P., Kuzma, M., Bártová, S., Novák, P., Jokela, J., . . . Kopecký, J. (2013). Novel Aeruginosin-865 from Nostoc sp. as a Potent Anti-inflammatory Agent. *ChemBioChem, 14*(17), 2329-2337. doi:10.1002/cbic.201300246

Kashihara, N., To-E, S., Nakamura, K., Umezawa, K., Yamamura, S., & Nishiyama, S. (2000). Synthesis and biological activities of hapalosin derivatives with modification at the C12 position. *Bioorganic and Medicinal Chemistry Letters, 10*(2), 101-103. doi:10.1016/S0960-894X(99)00647-2

Kehr, J.-C., Gatte Picchi, D., & Dittmann, E. (2011). Natural product biosyntheses in cyanobacteria: A treasure trove of unique enzymes. *Beilstein journal of organic chemistry, 7*, 1622-1635. doi:10.3762/bjoc.7.191

Knerr, P. J., & Donk, W. A. v. d. (2012). Discovery, Biosynthesis, and Engineering of Lantipeptides. *Annual Review of Biochemistry, 81*(1), 479-505. doi:10.1146/annurev-biochem-060110-113521

Koglin, A., & Walsh, C. T. (2009). Structural insights into nonribosomal peptide enzymatic assembly lines. *Natural Product Reports, 26*(8), 987-1000. doi:10.1039/B904543K

Kohli, R. M., Trauger, J. W., Schwarzer, D., Marahiel, M. A., & Walsh, C. T. (2001). Generality of Peptide Cyclization Catalyzed by Isolated Thioesterase Domains of Nonribosomal Peptide Synthetases. *Biochemistry, 40*(24), 7099-7108. doi:10.1021/bi010036j

Kustka, A., Carpenter, E. J., & Sañudo-Wilhelmy, S. A. (2002). Iron and marine nitrogen fixation: progress and future directions. *Research in Microbiology, 153*(5), 255-262. doi:10.1016/S0923-2508(02)01325-6

Lautru, S., & Challis, G. L. (2004). Substrate recognition by nonribosomal peptide synthetase multi-enzymes. *Microbiology, 150*(6), 1629-1636. doi:10.1099/mic.0.26837-0

Leikoski, N., Fewer, D. P., Jokela, J., Wahlsten, M., Rouhiainen, L., & Sivonen, K. (2010). Highly diverse cyanobactins in strains of the genus Anabaena. *Applied and Environmental Microbiology, 76*(3), 701-709. doi:10.1128/AEM.01061-09

Leikoski, N., Fewer, D. P., & Sivonen, K. (2009). Widespread occurrence and lateral transfer of the cyanobactin biosynthesis gene cluster in cyanobacteria. *Applied and Environmental Microbiology, 75*(3), 853-857. doi:10.1128/AEM.02134-08

Li, B., Sher, D., Kelly, L., Shi, Y., Huang, K., Knerr, P. J., . . . van der Donk, W. A. (2010). Catalytic promiscuity in the biosynthesis of cyclic peptide secondary metabolites in planktonic marine

cyanobacteria. *Proceedings of the National Academy of Sciences of the United States of America, 107*(23), 10430-10435. doi:10.1073/pnas.0913677107
Liaimer, A., Helfrich, E. J. N., Hinrichs, K., Guljamow, A., Ishida, K., Hertweck, C., & Dittmann, E. (2015). Nostopeptolide plays a governing role during cellular differentiation of the symbiotic cyanobacterium Nostoc punctiforme. *Proceedings of the National Academy of Sciences of the United States of America, 112*(6), 1862-1867. doi:10.1073/pnas.1419543112
Liaimer, A., Jensen, J. B., & Dittmann, E. (2016). A Genetic and Chemical Perspective on Symbiotic Recruitment of Cyanobacteria of the Genus Nostoc into the Host Plant Blasia pusilla L. *Frontiers in microbiology, 7*, 1693-1693. doi:10.3389/fmicb.2016.01693
Liengen, T., & Olsen, R. A. (1997). Nitrogen Fixation by Free-living Cyanobacteria from Different Coastal Sites in a High Arctic Tundra, Spitsbergen. *Arctic and Alpine Research, 29*(4), 470-477. doi:10.1080/00040851.1997.12003267
Lincke, T., Behnken, S., Ishida, K., Roth, M., & Hertweck, C. (2010). Closthioamide: An Unprecedented Polythioamide Antibiotic from the Strictly Anaerobic Bacterium Clostridium cellulolyticum. *Angewandte Chemie International Edition, 49*(11), 2011-2013. doi:10.1002/anie.200906114
López-Gomollón, S., Hernández, J. A., Pellicer, S., Angarica, V. E., Peleato, M. L., & Fillat, M. F. (2007). Cross-talk Between Iron and Nitrogen Regulatory Networks in Anabaena (Nostoc) sp. PCC 7120: Identification of Overlapping Genes in FurA and NtcA Regulons. *Journal of Molecular Biology, 374*(1), 267-281. doi:10.1016/j.jmb.2007.09.010
Los, D. A., & Mironov, K. S. (2015). Modes of Fatty Acid desaturation in cyanobacteria: an update. *Life (Basel, Switzerland), 5*(1), 554-567. doi:10.3390/life5010554
Luesch, H., Hoffmann, D., Hevel, J. M., Becker, J. E., Golakoti, T., & Moore, R. E. (2003). Biosynthesis of 4-Methylproline in Cyanobacteria: Cloning of nosE and nosF Genes and Biochemical Characterization of the Encoded Dehydrogenase and Reductase Activities. *The Journal of Organic Chemistry, 68*(1), 83-91. doi:10.1021/jo026479q
Magarvey, N. A., Beck, Z. Q., Golakoti, T., Ding, Y., Huber, U., Hemscheidt, T. K., . . . Sherman, D. H. (2006). Biosynthetic Characterization and Chemoenzymatic Assembly of the Cryptophycins. Potent Anticancer Agents from Nostoc Cyanobionts. *ACS Chemical Biology, 1*(12), 766-779. doi:10.1021/cb6004307
Man-Aharonovich, D., Kress, N., Zeev, E. B., Berman-Frank, I., & Béjà, O. (2007). Molecular ecology of nifH genes and transcripts in the eastern Mediterranean Sea. *Environmental Microbiology, 9*(9), 2354-2363. doi:10.1111/j.1462-2920.2007.01353.x
Mandal, S., & Rath, J. (2015). Secondary Metabolites of Cyanobacteria and Drug Development. In *Extremophilic Cyanobacteria For Novel Drug Development* (pp. 23-43). Cham: Springer International Publishing. doi:10.1007/978-3-319-12009-6_2
Martin, W. F., Garg, S., & Zimorski, V. (2015). Endosymbiotic theories for eukaryote origin. *Philosophical transactions of the Royal Society of London. Series B, Biological sciences, 370*(1678), 20140330-20140330. doi:10.1098/rstb.2014.0330
Martins, A., & Vasconcelos, V. (2011). Use of qPCR for the study of hepatotoxic cyanobacteria population dynamics. *Archives of Microbiology, 193*(9), 615. doi:10.1007/s00203-011-0724-7
Medema, M. H., Blin, K., Cimermancic, P., de Jager, V., Zakrzewski, P., Fischbach, M. A., . . . Breitling, R. (2011). antiSMASH: rapid identification, annotation and analysis of secondary metabolite biosynthesis gene clusters in bacterial and fungal genome sequences. *Nucleic Acids Research, 39*(Web Server issue), W339-W346. doi:10.1093/nar/gkr466
Meeks, J. C. (1998). Symbiosis between Nitrogen-Fixing Cyanobacteria and Plants: The establishment of symbiosis causes dramatic morphological and physiological changes in the cyanobacterium. *BioScience, 48*(4), 266-276. doi:10.2307/1313353
Meeks, J. C., Campbell, E. L., Summers, M. L., & Wong, F. C. (2002). Cellular differentiation in the cyanobacterium Nostoc punctiforme. *Archives of Microbiology, 178*(6), 395-403. doi:10.1007/s00203-002-0476-5
Mitra, A., & Flynn, K. J. (2010). Modelling mixotrophy in harmful algal blooms: More or less the sum of the parts? *Journal of Marine Systems, 83*(3), 158-169. doi:10.1016/j.jmarsys.2010.04.006
Morel, F. M. M., Hudson, R. J. M., & Price, N. M. (1991). Limitation of productivity by trace metals in the sea. *Limnology and Oceanography, 36*(8), 1742-1755. doi:10.4319/lo.1991.36.8.1742
Murakami, M., Ishida, K., Okino, T., Okita, Y., Matsuda, H., & Yamaguchi, K. (1995). Aeruginosins 98-A and B, trypsin inhibitors from the blue-green alga Microcystis aeruginosa (NIES-98). *Tetrahedron Letters, 36*(16), 2785-2788. doi:10.1016/0040-4039(95)00396-T
Murakami, M., Sun, Q., Ishida, K., Matsuda, H., Okino, T., & Yamaguchi, K. (1997). Microviridins, elastase inhibitors from the cyanobacterium Nostoc minutum (NIES-26). *Phytochemistry, 45*(6), 1197-1202. doi:10.1016/S0031-9422(97)00131-3

Murakami, M., Suzuki, S., Itou, Y., Kodani, S., & Ishida, K. (2000). New Anabaenopeptins, Potent Carboxypeptidase-A Inhibitors from the Cyanobacterium Aphanizomenon flos-aquae. *Journal of natural products, 63*(9), 1280-1282. doi:10.1021/np000120k

Nishizawa, T., Ueda, A., Asayama, M., Fujii, K., Harada, K.-i., Ochi, K., & Shirai, M. (2000). Polyketide Synthase Gene Coupled to the Peptide Synthetase Module Involved in the Biosynthesis of the Cyclic Heptapeptide Microcystin. *The Journal of Biochemistry, 127*(5), 779-789. doi:10.1093/oxfordjournals.jbchem.a022670

Nowruzi, B., Khavari-Nejad, R.-A., Sivonen, K., Kazemi, B., Najafi, F., & Nejadsattari, T. (2012). Identification and toxigenic potential of a Nostoc sp. *ALGAE, 27*(4), 303-313. doi:10.4490/algae.2012.27.4.303

Nunnery, J. K., Mevers, E., & Gerwick, W. H. (2010). Biologically active secondary metabolites from marine cyanobacteria. *Current Opinion in Biotechnology, 21*(6), 787-793. doi:10.1016/j.copbio.2010.09.019

O'Carra, P., Murphy, R. F., & Killilea, S. D. (1980). The native forms of the phycobilin chromophores of algal biliproteins. A clarification. *The Biochemical journal, 187*(2), 303-309. doi:10.1042/bj1870303

O'Connell, C. E., Salvato, K. A., Meng, Z., Littlefield, B. A., & Schwartz, C. E. (1999). Synthesis and evaluation of hapalosin and analogs as MDR-reversing agents. *Bioorganic & Medicinal Chemistry Letters, 9*(11), 1541-1546. doi:10.1016/S0960-894X(99)00243-7

Okamoto, S., & Ohmori, M. (2002). The Cyanobacterial PilT Protein Responsible for Cell Motility and Transformation Hydrolyzes ATP. *Plant and Cell Physiology, 43*(10), 1127-1136. doi:10.1093/pcp/pcf128

Oman, T. J., & van der Donk, W. A. (2010). Follow the leader: the use of leader peptides to guide natural product biosynthesis. *Nature chemical biology, 6*(1), 9-18. doi:10.1038/nchembio.286

Pattanaik, B., & Lindberg, P. (2015). Terpenoids and their biosynthesis in cyanobacteria. *Life (Basel, Switzerland), 5*(1), 269-293. doi:10.3390/life5010269

Perez, R., Forchhammer, K., Salerno, G., & Maldener, I. (2016). Clear differences in metabolic and morphological adaptations of akinetes of two Nostocales living in different habitats. *Microbiology, 162*(2), 214-223. doi:10.1099/mic.0.000230

Potts, M., & Friedmann, E. I. (1981). Effects of water stress on cryptoendolithic cyanobacteria from hot desert rocks. *Archives of Microbiology, 130*(4), 267-271. doi:10.1007/BF00425938

Punta, M., & Ofran, Y. (2008). The rough guide to in silico function prediction, or how to use sequence and structure information to predict protein function. *PLoS computational biology, 4*(10), e1000160-e1000160. doi:10.1371/journal.pcbi.1000160

Pupin, M., Esmaeel, Q., Flissi, A., Dufresne, Y., Jacques, P., & Leclère, V. (2015). Norine: A powerful resource for novel nonribosomal peptide discovery. *Synthetic and systems biotechnology, 1*(2), 89-94. doi:10.1016/j.synbio.2015.11.001

Pushkareva, E., Pessi, I. S., Namsaraev, Z., Mano, M.-J., Elster, J., & Wilmotte, A. (2018). Cyanobacteria inhabiting biological soil crusts of a polar desert: Sør Rondane Mountains, Antarctica. *Systematic and Applied Microbiology, 41*(4), 363-373. doi:10.1016/j.syapm.2018.01.006

Rai, A. N., Söderbäck, E., & Bergman, B. (2000). Tansley Review No. 116. *New Phytologist, 147*(3), 449-481. doi:10.1046/j.1469-8137.2000.00720.x

Rasmussen, B., Fletcher, I. R., Brocks, J. J., & Kilburn, M. R. (2008). Reassessing the first appearance of eukaryotes and cyanobacteria. *Nature, 455*, 1101. doi:10.1038/nature07381

Raven, J. A. (1988). The iron and molybdenum use efficiencies of plant growth with different energy, carbon and nitrogen sources. *New Phytologist, 109*(3), 279-287. doi:10.1111/j.1469-8137.1988.tb04196.x

Reinhold, B. B., Hauer, C. R., Plummer, T. H., & Reinhold, V. N. (1995). Detailed Structural Analysis of a Novel, Specific O-Linked Glycan from the Prokaryote Flavobacterium meningosepticum. *Journal of Biological Chemistry, 270*(22), 13197-13203. doi:10.1074/jbc.270.22.13197

Repka, S., Koivula, M., Harjunpä, V., Rouhiainen, L., & Sivonen, K. (2004). Effects of phosphate and light on growth of and bioactive peptide production by the Cyanobacterium anabaena strain 90 and its anabaenopeptilide mutant. *Applied and Environmental Microbiology, 70*(8), 4551-4560. doi:10.1128/AEM.70.8.4551-4560.2004

Rippka, R., Deruelles, J., Waterbury, J. B., Herdman, M., & Stanier, R. Y. (1979). Generic Assignments, Strain Histories and Properties of Pure Cultures of Cyanobacteria. *Microbiology, 111*(1), 1-61. doi:10.1099/00221287-111-1-1

Rodgers, G. A., & Stewart, W. D. P. (1977). THE CYANOPHYTE-HEPATIC SYMBIOSIS I. MORPHOLOGY AND PHYSIOLOGY. *New Phytologist, 78*(2), 441-458. doi:10.1111/j.1469-8137.1977.tb04851.x

Röttig, M., Medema, M. H., Blin, K., Weber, T., Rausch, C., & Kohlbacher, O. (2011). NRPSpredictor2--a web server for predicting NRPS adenylation domain specificity. *Nucleic Acids Research, 39*(Web Server issue), W362-W367. doi:10.1093/nar/gkr323

Sano, T., Usui, T., Ueda, K., Osada, H., & Kaya, K. (2001). Isolation of New Protein Phosphatase Inhibitors from Two Cyanobacteria Species, Planktothrix spp. *Journal of natural products, 64*(8), 1052-1055. doi:10.1021/np0005356

Santi, C., Bogusz, D., & Franche, C. (2013). Biological nitrogen fixation in non-legume plants. *Annals of Botany, 111*(5), 743-767. doi:10.1093/aob/mct048

Sarma, T. A., Ahuja, G., & Khattar, J. I. S. (2004). Nutrient stress causes akinete differentiation in cyanobacteriumAnabaena torulosa with concomitant increase in nitrogen reserve substances. *Folia Microbiologica, 49*(5), 557. doi:10.1007/bf02931533

Saw, J. H. W., Schatz, M., Brown, M. V., Kunkel, D. D., Foster, J. S., Shick, H., . . . Donachie, S. P. (2013). Cultivation and complete genome sequencing of Gloeobacter kilaueensis sp. nov., from a lava cave in Kīlauea Caldera, Hawai'i. *PloS one, 8*(10), e76376-e76376. doi:10.1371/journal.pone.0076376

Schindler, C. S., Bertschi, L., & Carreira, E. M. (2010). Total Synthesis of Nominal Banyaside B: Structural Revision of the Glycosylation Site. *Angewandte Chemie International Edition, 49*(48), 9229-9232. doi:10.1002/anie.201004047

Schirrmeister, B. E., Antonelli, A., & Bagheri, H. C. (2011). The origin of multicellularity in cyanobacteria. *BMC Evolutionary Biology, 11*(1), 45. doi:10.1186/1471-2148-11-45

Schmidt, E. W. (2010). The hidden diversity of ribosomal peptide natural products. *BMC Biology, 8*(1), 83. doi:10.1186/1741-7007-8-83

Schmidt, E. W., Nelson, J. T., Rasko, D. A., Sudek, S., Eisen, J. A., Haygood, M. G., & Ravel, J. (2005). Patellamide A and C biosynthesis by a microcin-like pathway in Prochloron didemni, the cyanobacterial symbiont of Lissoclinum patella. *Proceedings of the National Academy of Sciences of the United States of America, 102*(20), 7315-7320. doi:10.1073/pnas.0501424102

Schoffman, H., Lis, H., Shaked, Y., & Keren, N. (2016). Iron-Nutrient Interactions within Phytoplankton. *Frontiers in plant science, 7*, 1223-1223. doi:10.3389/fpls.2016.01223

Shapiro, S. D. (2002). Proteinases in chronic obstructive pulmonary disease. *Biochemical Society Transactions, 30*(2), 98-102. doi:10.1042/bst0300098

Singh, R. K., Tiwari, S. P., Rai, A. K., & Mohapatra, T. M. (2011). Cyanobacteria: an emerging source for drug discovery. *The Journal Of Antibiotics, 64*, 401. doi:10.1038/ja.2011.21

Sivonen, K., Leikoski, N., Fewer, D. P., & Jokela, J. (2010). Cyanobactins-ribosomal cyclic peptides produced by cyanobacteria. *Applied microbiology and biotechnology, 86*(5), 1213-1225. doi:10.1007/s00253-010-2482-x

Soo, R. M., Hemp, J., Parks, D. H., Fischer, W. W., & Hugenholtz, P. (2017). On the origins of oxygenic photosynthesis and aerobic respiration in Cyanobacteria. *Science, 355*(6332), 1436. doi:10.1126/science.aal3794

Stachelhaus, T., Mootz, H. D., & Marahiel, M. A. (1999). The specificity-conferring code of adenylation domains in nonribosomal peptide synthetases. *Chemistry & Biology, 6*(8), 493-505. doi:10.1016/S1074-5521(99)80082-9

Stanier, R. Y., Kunisawa, R., Mandel, M., & Cohen-Bazire, G. (1971). Purification and properties of unicellular blue-green algae (order Chroococcales). *Bacteriological reviews, 35*(2), 171-205.

Staunton, J., & Weissman, K. J. (2001). Polyketide biosynthesis: a millennium review. *Natural Product Reports, 18*(4), 380-416. doi:10.1039/A909079G

Steunou, A.-S., Bhaya, D., Bateson, M. M., Melendrez, M. C., Ward, D. M., Brecht, E., . . . Grossman, A. R. (2006). In situ analysis of nitrogen fixation and metabolic switching in unicellular thermophilic cyanobacteria inhabiting hot spring microbial mats. *Proceedings of the National Academy of Sciences of the United States of America, 103*(7), 2398-2403. doi:10.1073/pnas.0507513103

Stratmann, K., Burgoyne, D. L., Moore, R. E., Patterson, G. M. L., & Smith, C. D. (1994). Hapalosin, a Cyanobacterial Cyclic Depsipeptide with Multidrug-Resistance Reversing Activity. *The Journal of Organic Chemistry, 59*(24), 7219-7226. doi:10.1021/jo00103a011

Taylor, M. S., Stahl-Timmins, W., Redshaw, C. H., & Osborne, N. J. (2014). Toxic alkaloids in Lyngbya majuscula and related tropical marine cyanobacteria. *Harmful Algae, 31*, 1-8. doi:10.1016/j.hal.2013.09.003

Tillett, D., Dittmann, E., Erhard, M., von Döhren, H., Börner, T., & Neilan, B. A. (2000). Structural organization of microcystin biosynthesis in Microcystis aeruginosa PCC7806: an integrated peptide–polyketide synthetase system. *Chemistry & Biology, 7*(10), 753-764. doi:10.1016/S1074-5521(00)00021-1

Tzubari, Y., Magnezi, L., Be'er, A., & Berman-Frank, I. (2018). Iron and phosphorus deprivation induce sociality in the marine bloom-forming cyanobacterium Trichodesmium. *The ISME journal, 12*(7), 1682-1693. doi:10.1038/s41396-018-0073-5

van Heel, A. J., de Jong, A., Montalbán-López, M., Kok, J., & Kuipers, O. P. (2013). BAGEL3: Automated identification of genes encoding bacteriocins and (non-)bactericidal posttranslationally modified peptides. *Nucleic Acids Research, 41*(Web Server issue), W448-W453. doi:10.1093/nar/gkt391

Villa, F. A., Lieske, K., & Gerwick, L. (2010). Selective MyD88-dependent pathway inhibition by the cyanobacterial natural product malyngamide F acetate. *European Journal of Pharmacology, 629*(1), 140-146. doi:10.1016/j.ejphar.2009.12.002

Walsh, C. T., O'Brien, R. V., & Khosla, C. (2013). Nonproteinogenic amino acid building blocks for nonribosomal peptide and hybrid polyketide scaffolds. *Angewandte Chemie (International ed. in English), 52*(28), 7098-7124. doi:10.1002/anie.201208344

Wang, L., Yu, Z., Yang, J., & Zhou, J. (2015). Diazotrophic bacterial community variability in a subtropical deep reservoir is correlated with seasonal changes in nitrogen. *Environmental Science and Pollution Research, 22*(24), 19695-19705. doi:10.1007/s11356-015-5144-9

Waterbury, J. B. (2006). The Cyanobacteria—Isolation, Purification and Identification. In M. Dworkin, S. Falkow, E. Rosenberg, K.-H. Schleifer, & E. Stackebrandt (Eds.), *The Prokaryotes: Volume 4: Bacteria: Firmicutes, Cyanobacteria* (pp. 1053-1073). New York, NY: Springer US. doi:10.1007/0-387-30744-3_38

Weber, T. (2014). In silico tools for the analysis of antibiotic biosynthetic pathways. *International Journal of Medical Microbiology, 304*(3), 230-235. doi:10.1016/j.ijmm.2014.02.001

Welker, M., & Von Döhren, H. (2006). Cyanobacterial peptides – Nature's own combinatorial biosynthesis. *FEMS Microbiology Reviews, 30*(4), 530-563. doi:10.1111/j.1574-6976.2006.00022.x

Wilde, A., & Mullineaux, C. W. (2015). Motility in cyanobacteria: polysaccharide tracks and Type IV pilus motors. *Molecular Microbiology, 98*(6), 998-1001. doi:10.1111/mmi.13242

Williams, A. B., & Jacobs, R. S. (1993). A marine natural product, patellamide D, reverses multidrug resistance in a human leukemic cell line. *Cancer Letters, 71*(1), 97-102. doi:10.1016/0304-3835(93)90103-G

Wohlleben, W., Stegmann, E., & Süssmuth, R. D. (2009). Chapter 18 Molecular Genetic Approaches to Analyze Glycopeptide Biosynthesis. In *Methods in Enzymology* (Vol. 458, pp. 459-486): Academic Press. doi:10.1016/S0076-6879(09)04818-6

Wolk, C. P., Ernst, A., & Elhai, J. (1994). Heterocyst Metabolism and Development. In D. A. Bryant (Ed.), *The Molecular Biology of Cyanobacteria* (pp. 769-823). Dordrecht: Springer Netherlands. doi:10.1007/978-94-011-0227-8_27

Wolk, C. P., & Simon, R. D. (1969). Pigments and lipids of heterocysts. *Planta, 86*(1), 92-97. doi:10.1007/bf00385308

Yang, Y., Qiu, Z., Hou, X., & Sun, L. (2017). Ultrasonic Characteristics and Cellular Properties of Anabaena Gas Vesicles. *Ultrasound in Medicine & Biology, 43*(12), 2862-2870. doi:10.1016/j.ultrasmedbio.2017.08.004

Ye, J., Coulouris, G., Zaretskaya, I., Cutcutache, I., Rozen, S., & Madden, T. L. (2012). Primer-BLAST: A tool to design target-specific primers for polymerase chain reaction. *BMC Bioinformatics, 13*(1), 134. doi:10.1186/1471-2105-13-134

Yoon, V., & Nodwell, J. R. (2014). Activating secondary metabolism with stress and chemicals. *Journal of Industrial Microbiology & Biotechnology, 41*(2), 415-424. doi:10.1007/s10295-013-1387-y

Yoshihara, S., Geng, X., Okamoto, S., Yura, K., Murata, T., Go, M., . . . Ikeuchi, M. (2001). Mutational Analysis of Genes Involved in Pilus Structure, Motilityand Transformation Competency in the Unicellular Motile CyanobacteriumSynechocystis sp. PCC6803. *Plant and Cell Physiology, 42*(1), 63-73. doi:10.1093/pcp/pce007

Zhang, C., Naman, C. B., Engene, N., & Gerwick, W. H. (2017). Laucysteinamide A, a Hybrid PKS/NRPS Metabolite from a Saipan Cyanobacterium, cf. Caldora penicillata. *Marine Drugs, 15*(4), 121. doi:10.3390/md15040121

Zhou, R., & Wolk, C. P. (2002). Identification of an Akinete Marker Gene in Anabaena variabilis. *Journal of bacteriology, 184*(9), 2529-2532. doi:10.1128/jb.184.9.2529-2532.2002

Ziegler, K., Diener, A., Herpin, C., Richter, R., Deutzmann, R., & Lockau, W. (1998). Molecular characterization of cyanophycin synthetase, the enzyme catalyzing the biosynthesis of the cyanobacterial reserve material multi- L-arginyl-poly- L-aspartate (cyanophycin). *European Journal of Biochemistry, 254*(1), 154-159. doi:10.1046/j.1432-1327.1998.2540154.x

Ziemert, N., Ishida, K., Liaimer, A., Hertweck, C., & Dittmann, E. (2008). Ribosomal Synthesis of Tricyclic Depsipeptides in Bloom-Forming Cyanobacteria. *Angewandte Chemie International Edition, 47*(40), 7756-7759. doi:10.1002/anie.200802730

Ziemert, N., Ishida, K., Weiz, A., Hertweck, C., & Dittmann, E. (2010). Exploiting the natural diversity of microviridin gene clusters for discovery of novel tricyclic depsipeptides. *Applied and Environmental Microbiology, 76*(11), 3568-3574. doi:10.1128/AEM.02858-09

Appendix

Appendix 1: BG11 recipe

Table 25: BG11 stock recipe, first described in Stanier et al. (1971).

Stock	***Chemicals***	***g/L in medium***	***In stock solution (final volume x 1000)(g/l)***
I.	K_2HPO_4 x $3H_2O$	0,04	40
II.	$MgSO_4$ x $7H_2O$	0,075	75
III.	$CaCl_2$ x $2H_2O$	0,036	36
	Citric acid	06	6
IV.	Ferric ammonium citrate	06	6
	Na_2Mg EDTA	01	1
V.	Na_2CO_3	0,04	40
VI.	Trace elements (1ml/liter)		
	H_3BO_3	2,86	
	$MnCl_2$ x $4H_2O$	1,81	
	$ZnSO_4$ 4 x $7H_2O$	0,222	
	Na_2MoO_4 x $2H_2O$	0,39	
	$CuSO_4$ x $5H_2O$	0,079	
	$Co(NO_3)_2$ x $6H_2O$	0,0404	
VII.	NaNO3	1,5	1500

For solid plates; 1% agar was added.

Appendix 2: primers and locus.

Primers for KVJ20

Table 26: Primers designed for Nostoc KVJ20 from gene predictions from AntiSMASH using Primer-BLAST. The table shows cluster, cluster type, possible product and reverse/forward primer.

Primer	Cluster type	Product/function	NCBI accession and coordinates	Reverse primer sequence	Forward primer sequence
20-RnpB	Householding, reference gene	Ribonuclease III	LSSA01000318.1: 20771-20958	ATCCTAGCTTGGTTCCGTGC	GCTCTTGGCTAGATCCCCAC
20-NifH	Nitrogen fixation	Nitrogenase	LSSA01000069.1: 8617-8801	GAGCGATGTTGTTAGCAGCG	CCAGAACCCGGTGTAGGTTG
20-GvpC	Motility, buoyancy	Gas vesicle	LSSA01000004.1: 11984-12207	CAAGAATACCGCCAACAGCG	ATCGTATTGGCGGAAGGACG
20-AvaK	Akinete marker gene	Membrane bound barrel	LSSA01000133.1: 14032-14209	GGCGTCGTTTACTGGCAATC	ACGGGTGCGTGGTGTATAT
20-PilT	Motility	Twitching motility protein	LSSA01000126.1: 5922-6097	TTGCATCCTGTTCGTCACCA	GCGGGAAGACCCAGATTTG
20-N1 (S/B like)	NRPS	S/B like	LSSA01000176.1: 6892-9906	TCCAGCTTGATTGGCTCTGG	ACGCCCAATGGCAAAGTAGA
20-N2 (Apt)	NRPS	Apt	LSSA01000425.1: 19463-22459	ATTGGGGTGGATTGCAGAGG	GCGATGAATTTTGGCGGTGT
20-N3	NRPS	Unknown	LSSA01000197.1: 146-6064	CAGCAAACTGTCGTCACAGC	GGGTTAGGGGTAGGGTGTCT
20-N4 (Ncp)	NRPS	Ncp	LSSA01000164.1: 29725-32772	GCAACTAGAGCAGACAGCCA	TCTTCAATAGGAGTGCGCGG
20-NP1 (Val-Val)	NRPS/PKS	Val-Val	LSSA01000013.1: 23704-28650	AAAGCAAGTTTGCCGCAGAG	TTCATGTTCCCCGGACAAGG
20-NP2 (Sid)	NRPS/PKS	Sideophore	LSSA01000336.1: 21785-28384	AACCGCTGGGTGTTGGTTTA	TAATCGCCCAGAATCGACCG
20-P1 (Hgl)	PKS	Heterocyst glycolipids	LSSA01000165.1: 23368-28743	TGTCCAAATTGCTGCCTTGC	CAGCCATTGCTTGACCCCTA
20-P2	PKS	Unknown	LSSA01000184.1: 29769-32819	GGCGGATTTATCCCGGATGT	TTCTCGCAGTCAGTGGAACC
20-RiPP1	RiPP	Unknown	LSSA01000401.1: 45825-47084	CAAGCCAACTGGACTGGCTA	TCAGAACGCTGTACCACCAC
20-RiPP2	RiPP	Unknown	LSSA01000352.1: 15209-16471	AGTGGTGCATCCCTAAAGGC	GTTGACCAAGAGCGGGATCA
20-RiPP3	RiPP	Unknown	LSSA01000102.1: 5744-8062	CCTGAGCAAAGGCTGGTACA	CGGGTGTTGTGCTGACAATG
20-RiPP4	RiPP	Unknown	LSSA01000383.1: 1971-5093	TGGATGAGGCAACCAGTCAC	CGTGAGTACCGCTTTCGACT
20-RiPP5	RiPP	Unknown	LSSA01000098.1: 8076-10244	CGGGGATTGCTGAGTCAAGT	TTGCAATGCTTGCAGACCAC
20-RiPP6	RiPP	Unknown	LSSA01000337.1: 181966-183417	CTTAGGCGCACCACAGGTTA	TGGTCACAATGGCTCTTGCT
20-RiPP7	RiPP	Unknown	LSSA01000346.1: 285-2513	TAGGTGCATGACGATGACGG	GTTTTGGAGGCTTTCTGCGG
20-RiPP8 (Mvd)	RiPP, Microviridin	Unknown	LSSA01000045.1: 26899-27903	CCCAAGAATGTGAGCAGGGT	GCAATTCAAGGGCTTTGGGG
20-RiPP9 (Mvd)	RiPP, Microviridin	Unknown	LSSA01000164.1: 41782-42756	GACCAACTTTGCGTGCAACT	TCCTCAGTTTGGTATCGGCG
20-RiPP10 (Lan)	RiPP, Lantibiotics	Unknown	LSSA01000386.1: 2980-6204	ATCCAGTTGATGCGGCAGAA	GTCGGAGTCAGACTGGAACG
20-RiPP11 (Lan)	RiPP, Lantibiotics	Unknown	LSSA01000045.1: 18651-21953	CGAATTCGGCTGCTCTTTCG	CCATCTGCACCATTGAACGC

Primers for KVJ2

Table 27: Primers designed for Nostoc KVJ20 from gene predictions from AntiSMASH using Primer-BLAST. The table shows cluster, cluster type, possible product and reverse/forward primer

Primer	Cluster type	Product/function	NCBI accession and coordinates	Reverse primer sequence	Forward primer sequence
2-RnpB	Housekeeping gene	Ribonuclease III	NNBU01000047.1: 36227-36943	TAAAGTGCGCCCAAAACTGC	TGTCGGCCGTTGTCTTATGG
2-NifH	Nitrogenase	Nitrogenase subunit H	NNBU01000053.1: 7720-8589	ACCGTTTTGCCAAGGTTTCG	TATCCGCGAAGGTAAGGCAC
2-AvaK	Akinete induced	Membrane protein	NNBU01000036.1: 88650-89522	CGCCATTAGATACGACCCCC	TTCCACCGGTACTGCAACTC
2-PilT	Hormogonium induced formation	Twitching motility protein	NNBU01000171.1: 10229-11518	ACCTCCCGCAACCAATTCAT	CGCCAATACCTAGTTCCGCT
2-P1	PKS	Unknown	NNBU01000005.1: 7397-10405	ACCAGAAATACCCACAGCCG	GCCTGTTGTCGTCCAACCTA
2-P2	PKS	Similar to heterocyst glycolipid	NNBU01000076.1: 31940-34939	TGGGCAAGGTTCGCAATACT	CTGCAACGCATTCATCTGGG
2-P3 (Hgl)	PKS	Heterocyst glycolipid	NNBU01000168.1: 7155-12551	GCAAATCGCCACAGATTCCC	TTTCCGCCCAACTCCATACC
2-N1	NRPS	Unknown	NNBU01000007.1: 35227-41145	ATTACCAACCGACCGACCAC	TCTTCTTGCCCAGTGTAGCG
2-N2a (Aer)	NRPS	Aeruginosin	NNBU01000009.1: 58572-63866	CACGATGCTTTACGACTGCG	CACGATGCTTTACGACTGCG
2-N2b	NRPS	Unknown	NNBU01000009.1: 99209-102196	GCCTATCTTGTCCCAGTCGG	AGAGAACCCTGGAAATGGCG
2-N3	NRPS/PKS	Unknown	NNBU01000017.1: 49407-54734	ACGGATGATGACCTTGCTGG	AACTGTCCTGACTGAAGGCG
2-N4	NRPS	Unknown	NNBU01000032.1: 83029-87963	CCAACTAAGGGAGTCTGCGG	TCGTAGCGTCTCGTTCATCG
2-N5 (Ncp)	NRPS	Nostocyclopeptide	NNBU01000089.1: 80073-83123	ATTGGCGACCAGAGAAGGTG	GCGATCGCTCTAGCAACTCT
2-N6 (Apt)	NRPS	Anabaenopeptin	NNBU01000114.1: 11445-14438	GCCAAATGCTCGATGGTGTC	CTACCCCAAGCACAGGTGAG
2-RIPP1	RiPP	Unknown	NNBU01000039.1: 75753-78806	TATGCTCAACAAAGCGCAGC	AGAGTGGCTTTCACAGGACG
2-RIPP2	RiPP	Microviridin	NNBU01000121.1: 11889-12890	CTCGGTGTTGAGGGAGCAAT	ACCTTGAGCGTGATGTGGTT
2-RIPP3	RiPP	Lanthipeptide	NNBU01000135.1: 6265-9585	AAGCGCACCTGCTGATTTTG	GAGCCTGTAACCTTGCCGAT
2-RiPP4	RiPP	Unknown	NNBU01000219.1: 3587-6877	ATCGCAGGTAGGGGTTGTTG	CTGACTGTGGGGCATCTTGT
2-RiPP5	RiPP	Unknown	NNBU01000061.1: 7769-10495	TCTGGCTCCACATCCAACAC	TTGCTGTGGTTTGGGGCTTA
2-RiPP6	RiPP	Unknown	NNBU01000106.1: 42735-44903	ACCTGGATCGGCAACAACAT	CGAGAAGCGGTAGGAACTGG
2-RiPP7	RiPP	Unknown	NNBU01000127.1: 3094-5241	ACTACCTGCTGACGCAAACA	CACTATGCTGGTCGGCTTGA

Primers for KVJ10

Table 28: Primers designed for Nostoc KVJ20 from gene predictions from AntiSMASH using Primer-BLAST. The table shows cluster, cluster type, possible product and reverse/forward primer

Primer	Cluster type	Product/function	NCBI accession and coordinates	Reverse primer sequence	Forward primer sequence
10-RnpB	Housekeeping, reference gene	Ribonuclease III	NNBT01000352.1: 4989-5180	TACCGCCGATAAAGTTGGTC	GTCCATTCTTGGAGAGCAGC
10-NifH	Nitrogen fixation	Nitrogenase	NNBT01008035.1: 140-304	TTGCGACCCTAAAGCTGACT	TCTGGCCCACCAGATTCTAC
10-GvpC	Motility, buoyancy	Gas vesicles	NNBT01000542.1: 5968-6157	GGAACTCACAACAGCAGCAA	CTGTAATCGCCCCAAACACT
10-AvaK	Akinete marker gene	Membrane bound barrel	NNBT01000211.1: 2213-2422	TTTAGGAGCGCCTGTAGCAT	ATCCGTGCGGTATCAGTTTC
10-P1 (Hgl)	PKS	Heterocyst envelope	NNBT01000273.1: 1339-1514	ATCACAAAGTTTTACCGCCG	AACGTGATAGTTGGTTCCGC
10-P2	PKS	Unknown	NNBT01007897.1: 112-282	TTTGTATCTAGCTGCGGGCT	GCCAAAGCTAAGGCACACTC
10-P3	PKS	Unknown	NNBT01000465.1: 131-322	GCCCCCTCATGTTTAGACCC	TCTGCCGATTCCTGCAAGTT
10-N1	NRPS	Unknown	NNBT01000019.1: 1785-1975	TGCATACAGTTCCTTCGCTG	TGCCAAAGTTGTCTCTGTCG
10-N2 (Ngn)	NRPS	Possible Nostoginin	NNBT01000934.1: 1489-1723	AGTTTTGGGTGTCCAACGAG	AGAGAGGCGGTGACGAACTA
10-N3	NRPS	Unknown	NNBT01000546.1: 5276-5502	ATTACCCGCAGGTGTTTCTG	CTAGCTCAATACGGAAGCCG
10-N4	NRPS	Unknown	NNBT01001356.1: 733-898	TGCTGACTGGAATTGTAGCG	GGCGTTTTTCTGACTTGCTC
10-NP1	NRPS/PKS	Unknown	NNBT01000015.1: 6795-7015	ACGGCGGTAATTCTGACAAC	CCATGATTGAGCATCACACC
10-NP2 (Hap)	NRPS/PKS	Hapalosin	NNBT01000031.1: 34609-34834	CTTCCGAAGAAATTTGCGAG	TGCATTAGCCTCGAGTGTTG
10-NP3 (Nsp)	NRPS/PKS	Nosperin	NNBT01000568.1: 162-358	ATCACGTAGCGTCCAAAACC	ATGCATGGACGTGGACTACA
10-NP4	NRPS/PKS	Unknown	NNBT01000173.1: 16148-16347	AATTTAGCAACGCGCCTTTAT	TCACCTGCTTCATCTTGACG
10-NP5	NRPS/PKS	Unknown	NNBT01001947.1: 449-672	CAATATATCGGTATGGGGCG	TGCCATAGCTCAGACAATGC
10-RiPP1	RiPP	Unknown	NNBT01000192.1 28923-29153	CCCTTCATGATGCAACTCCT	ACTGCGTCGTCCTTCAAAGT
10-RiPP2	RiPP	Unknown	NNBT01000265.1: 3166-3354	GGGAGATACCCAACTGCTGA	CTGCGACGTGCTTCAAAATA
10-RiPP3	RiPP	Unknown	NNBT01000358.1: 60371-60545	ACCACCATTCTTTTTGCTGG	TAACTCCTCCCAATGCCAAC
10-RiPP4	RiPP	Unknown	NNBT01001217.1: 1267-1491	TTATCAACCCAAAAGTCGGC	CACCCGGAATAAAGCACAGT
10-RIPP5	RiPP	Unknown	NNBT01000550.1: 1649-1803	GCATACAATCACCCGCTTTT	TGGCAGCAACAGCAGAATAC
10-Ripp6 (Lan)	RiPP	Lanthipeptide	NNBT01000526.1: 2364-2572	AAAAAGCGCGTCTACCTCAA	AACCCAGCTAGCAAGCAAAA

Appendix 3: Relative peak intensity in percentage.

Relative peak intensity in percentage for KVJ20

Table 29: Relative peak intensity in different cultivations in percentage for compounds found in KVJ20. Relative peak intensity > 20% is highlighted in bold.

OM	*NM*	*Extract*	*O*	*O-Fe*	*O-P*	*N*	*N-Fe*	*N-P*	*OS*	*NS*	*20vs2*	*20vs10*
353,27	**352,26**	Cells	1	6	**26**	1	**26**	19	**24**	**27**	18	**23**
		Media	0	0	0	0	0	0	-	-	-	-
365,16	**364,15**	Cells	0	0	0	0	0	0	0	0	0	0
		Media	**22**	16	17	17	12	13	-	-	-	-
379,17	**378,17**	Cells	0	0	0	0	0	0	0	0	0	0
		Media	**100**	**100**	**100**	**100**	**100**	**100**	-	-	-	-
387,18	**386,17**	Cells	8	10	**34**	2	17	19	**30**	**36**	**40**	2
		Media	5	5	8	5	5	5	-	-	-	-
415,21	**414,20**	Cells	**38**	9	**70**	1	**34**	**29**	**97**	**100**	**100**	**35**
		Media	0	0	0	0	0	0	-	-	-	-
447,20	**446,19**	Cells	0	0	0	0	0	0	0	0	0	0
		Media	**36**	**25**	**24**	**25**	**24**	**25**	-	-	-	-
471,37	**470,36**	Cells	0	0	0	0	0	0	0	0	0	0
		Media	7	18	**21**	2	15	10	-	-	-	-
513,30	**512,30**	Cells	**30**	**49**	**20**	9	**72**	14	**32**	**68**	**44**	**68**
		Media	0	0	0	0	0	0	-	-	-	-
515,32	**514,31**	Cells	19	**30**	5	4	**40**	4	14	**44**	**21**	**39**
		Media	0	0	0	0	0	0	-	-	-	-
549,27	**548,26**	Cells	0	0	0	0	0	0	0	0	0	0
		Media	16	14	11	14	13	14	-	-	-	-
614,39	**613,38**	Cells	**31**	**49**	0	15	**35**	0	**44**	10	**23**	**57**
		Media	3	1	0	2	1	0	-	-	-	-
670,40	**669,40**	Cells	14	11	17	4	**22**	0	15	18	17	16
		Media	0	0	0	0	0	0	-	-	-	-
694,40	**693,39**	Cells	10	9	**28**	1	**28**	0	19	**24**	16	**20**
		Media	0	0	0	0	0	0	-	-	-	-
696,44	**695,43**	Cells	**39**	**25**	**100**	**39**	**55**	**100**	**93**	**80**	**63**	**46**
		Media	0	10	0	0	5	0	-	-	-	-
Ncp 757,42	**756,42**	Cell	0	3	0	8	0	0	4	0	0	3
		media	5	2	3	5	2	4	-	-	-	-
Ncp 775,44	**774,43**	Cells	**50**	**48**	0	**94**	**33**	0	**44**	4	**22**	**62**
		Media	17	5	2	7	6	6	-	-	-	-
Ncp 809,42	**808,41**	Cells	**63**	**36**	5	**91**	**30**	0	**60**	9	**22**	**80**
		Media	11	5	7	4	5	8	-	-	-	-
836,63	**835,62**	Cells	3	11	0	5	5	0	5	4	0	5
		Media	0	0	0	0	0	0	-	-	-	-
899,43	**898,43**	Cells	**22**	18	0	**24**	**24**	0	6	4	0	6
		Media	1	0	4	0	0	1	-	-	-	-
S/B 927,47	**926,46**	Cells	**46**	**42**	4	**45**	**47**	0	**61**	16	**20**	**62**
		Media	15	7	11	9	10	15	-	-	-	-
S/B 1007,42	**927,42**	Cells	**43**	**39**	4	**42**	**43**	0	**54**	15	19	**52**
		Media	13	8	11	8	10	13	-	-	-	-
S/B 969,48	**968,47**	Cells	18	15	4	19	13	0	4	6	0	4
		Media	0	0	5	0	0	1	-	-	-	-
S/B 1049,43	**969,43**	Cells	16	15	4	18	12	0	0	5	0	4
		Media	0	0	4	0	0	1	-	-	-	-
S/B 997,51	**996,50**	Cells	**100**	**100**	**40**	**100**	**100**	14	**100**	**57**	**44**	**100**
		Media	7	1	26	3	1	15	-	-	-	-
S/B 1077,46	**997,46**	Cells	**80**	**74**	**40**	**65**	**90**	15	**81**	**52**	**47**	**83**
		Media	8	2	22	3	2	13	-	-	-	-
1025,54	**1024,53**	Cells	9	7	0	8	4	0	5	0	0	5
		Media	0	0	0	0	0	0	-	-	-	-

Relative peak intensity in percentage for KVJ2

Table 30: Relative peak intensity in different cultivations in percentage for compounds found in KVJ2. Relative peak intensity > 20% is highlighted in bold.

OM	*NM*	*Extract*	*O*	*O-Fe*	*O-P*	*N*	*N-Fe*	*N-P*	*OS*	*NS*	*2vs20*	*2vs10*
365,16	**364,15**	Cells	0	0	0	0	0	0	0	0	0	0
		Media	9	12	10	11	10	10	-	-	-	-
379,17	**378,17**	Cells	0	0	0	0	0	0	0	0	0	0
		Media	**100**	**100**	**100**	**100**	**100**	**100**	-	-	-	-
402,36	**401,35**	Cells	2	3	5	1	5	4	7	11	8	5
		Media	4	2	3	3	3	3	-	-	-	-
412,22	**411,21**	Cells	**30**	**21**	**24**	14	10	8	15	13	6	4
		Media	4	11	4	8	7	2	-	-	-	-
415,21	**414,20**	Cells	0	0	0	6	18	0	0	0	0	1
		Media	0	0	0	0	0	0	-	-	-	-
447,20	**446,19**	Cells	0	0	0	0	0	0	0	0	0	0
		Media	18	**21**	17	**21**	**20**	14	-	-	-	-
471,37	**470,36**	Cells	1	0	0	0	0	0	0	0	0	0
		Media	13	10	**29**	10	**22**	**22**	-	-	-	-
513,30	**512,30**	Cells	4	4	5	2	6	5	6	7	13	8
		Media	0	0	0	0	0	0	-	-	-	-
515,32	**514,31**	Cells	2	1	3	1	3	3	4	7	10	5
		Media	0	0	0	0	0	0	-	-	-	-
549,27	**548,26**	Cells	0	0	0	0	0	0	0	0	0	0
		Media	8	11	9	11	10	8	-	-	-	-
564,36	**563,35**	Cells	**53**	**58**	**43**	**36**	**100**	**74**	**100**	**100**	**100**	**100**
		Media	1	**29**	3	1	10	2	-	-	-	-
608,38	**607,38**	Cells	**51**	**54**	**38**	**34**	**96**	**69**	**90**	**82**	**86**	**89**
		Media	1	**31**	2	1	11	1	-	-	-	-
652,41	**651,40**	Cells	**38**	**39**	**24**	17	**67**	**46**	1	**51**	**56**	**60**
		Media	0	24	1	0	8	1	-	-	-	-
696,44	**695,43**	Cells	17	17	9	10	**29**	19	**23**	19	**21**	**25**
		Media	0	11	0	0	3	0	-	-	-	-
Ncp 757,42	**756,42**	Cells	4	4	5	5	4	5	1	2	1	1
		Media	6	10	7	**20**	**22**	10	-	-	-	-
Ncp 775,44	**774,43**	Cells	**86**	**79**	**100**	**100**	**62**	**100**	**37**	**77**	**37**	19
		Media	17	21	17	72	54	16	-	-	-	-
Ncp 791,41	**790,40**	Cells	5	6	4	1	8	5	1	0	0	1
		Media	9	16	6	6	**26**	6	-	-	-	-
Ncp 805,42	**804,42**	Cells	6	6	6	4	7	6	3	1	3	3
		Media	15	**23**	10	**27**	**36**	11	-	-	-	-
Ncp 809,42	**808,41**	Cells	13	18	**57**	**22**	**90**	**25**	13	0	9	16
		Media	**25**	**26**	6	12	**43**	2	-	-	-	-
Apt 812,44	**811,43**	Cells	1	0	4	0	0	7	0	0	0	0
		Media	0	0	0	0	0	0	-	-	-	-
Ncp 823,44	**822,43**	Cells	**100**	**100**	**88**	**85**	**23**	**80**	**52**	**38**	**37**	**39**
		Media	**40**	**36**	16	**75**	**51**	18	-	-	-	-
Apt 828,43	**827,42**	Cells	5	3	16	2	4	**28**	1	0	0	1
		Media	0	1	0	1	1	4	-	-	-	-
Apt 842,44	**841,44**	Cells	2	1	4	1	2	**7**	0	0	0	0
		Media	0	0	0	0	0	0	-	-	-	-
Aer 889,46	**888,45**	Cells	**41**	**47**	**29**	**45**	**56**	**29**	**21**	14	**23**	16
		Media	10	16	12	**37**	**26**	10	-	-	-	-

Relative peak intensity in percentage for KVJ10

Table 31: Relative peak intensity in different cultivations in percentage for compounds found in KVJ10. Relative peak intensity > 20% is highlighted in bold.

OM	*NM*	*Extracts*	*O*	*O-Fe*	*O-P*	*N*	*N-Fe*	*N-P*	*OS*	*NS*	*10vs2*	*10vs20*
365,16	**364,15**	Cells	0	0	0	0	0	0	0	0	0	0
		Media	**28**	**28**	**27**	**24**	18	1	-	-	-	-
379,17	**378,17**	Cells	0	0	0	0	0	0	0	0	0	0
		Media	**99**	**100**	**100**	**100**	**100**	**100**				
387,19	**386,19**	Cells	3	4	3	6	5	4	7	6	0	0
		Media	3	3	3	3	3	3				
440,41	**439,40**	Cells	3	4	4	8	8	4	**22**	7	0	0
		Media	1	2	1	2	3	2				
447,20	**446,19**	Cells	0	0	0	0	0	0	0	0	0	0
		Media	**46**	**44**	**44**	**39**	**40**	**46**				
476,30	**475,29**	Cells	7	13	7	5	5	6	2	4	0	0
		Media	0	0	1	0	0	1				
486,32	**485,31**	Cells	**25**	**61**	**43**	**69**	**66**	**52**	**60**	**62**	6	7
		Media	9	1	**23**	2	4	6				
Hap 490,32	**489,31**	Cells	**21**	**34**	**24**	**31**	**27**	**27**	**46**	**29**	8	8
		Media	7	1	15	3	4	6				
Hap 512,30	**489,31**	Cells	**100**	**80**	**100**	**67**	**50**	**100**	**62**	**60**	4	5
		Media	6	1	14	3	3	6				
494,31	**493,30**	Cells	1	1	0	0	0	0	0	0	0	0
		Media	13	9	9	3	3	5				
500,30	**499,29**	Cells	1	3	1	0	0	0	0	0	0	0
		Media	19	10	11	3	2	6				
502,32	**501,31**	Cells	**23**	**34**	**28**	**59**	**57**	**31**	**64**	**42**	14	14
		Media	0	0	7	1	1	1				
524,30	**501,31**	Cells	**72**	**100**	**72**	**76**	**46**	**65**	**76**	**82**	12	13
		Media	0	0	6	1	1	1				
504,33	**503,32**	Cells	**23**	**35**	**26**	**40**	**42**	**28**	**47**	6	**100**	**100**
		Media	**32**	11	**44**	**25**	**32**	**35**				
526,31	**503,32**	Cells	**55**	**87**	**60**	**100**	**100**	**74**	**100**	**100**	**28**	**27**
		Media	**39**	8	**84**	17	**23**	**31**				
507,22	**506,21**	Cells	0	0	0	0	0	0	0	0	0	0
		Media	**25**	**22**	**23**	17	19	**21**				
542,31	**519,32**	Cells	4	7	2	1	1	2	0	0	0	0
		Media	**59**	**35**	**51**	**24**	**26**	**28**				
520,33	**519,32**	Cells	19	**20**	11	18	17	14	7	14	0	1
		Media	10	**26**	18	**24**	**23**	19				
522,34	**521,34**	Cells	7	14	6	3	4	4	1	1	0	0
		Media	11	**30**	14	**43**	**44**	**41**				
544,32	**521,36**	Cells	10	16	6	3	3	4	0	1	0	0
		Media	**100**	**65**	**91**	**38**	**46**	**63**				
556,29	**533,30**	Cells	6	8	2	1	2	2	0	0	0	0
		Media	**58**	36	**51**	**53**	**61**	**46**				
534,31	**533,30**	Cells	10	15	4	4	5	4	1	1	0	0
		Media	**45**	**39**	**47**	**59**	**61**	**49**				
538,34	**537,33**	Cells	1	1	0	0	0	0	0	0	0	0
		Media	14	5	7	8	12	7				
Nsp 564,29	**563,28**	Cells	5	6	3	11	10	8	4	4	0	0
		Media	**21**	4	19	6	13	8				
597,43	**596,43**	Cells	8	9	7	10	8	4	**22**	5	0	0
		Media	0	0	0	0	0	0				
599,45	**598,44**	Cells	15	19	14	**28**	**26**	13	**38**	19	3	5
		Media	2	0	10	0	0	0				
610,41	**609,40**	Cells	5	3	7	11	12	11	6	12	0	0
		Media	0	0	0	0	0	0				
701,39	**700,39**	Cells	15	19	11	9	6	9	14	9	1	1
		Media	**23**	**33**	**27**	**21**	16	**23**				
734,46	**733,45**	Cells	10	7	13	**25**	**28**	**21**	19	**28**	0	0
		Media	0	0	0	0	0	0				
745,42	**744,41**	Cells	10	12	7	5	3	5	8	5	0	0
		Media	13	22	17	12	10	13				

Appendix 4: Fragmentation pattern examples.

Examples of fragmentation profiles of identified compounds recorded in this study obtained by UPLC-HR-MS analysis. A: Aeruginosin, B: Anabenopeptin, C-D: Nostocyclopeptide, E: Suomilide/Banyaside-like, F: Nosperin. The ions matching reference/diagnostic ions of known compounds are marked by *.

A **Aeruginosin m/z 889**

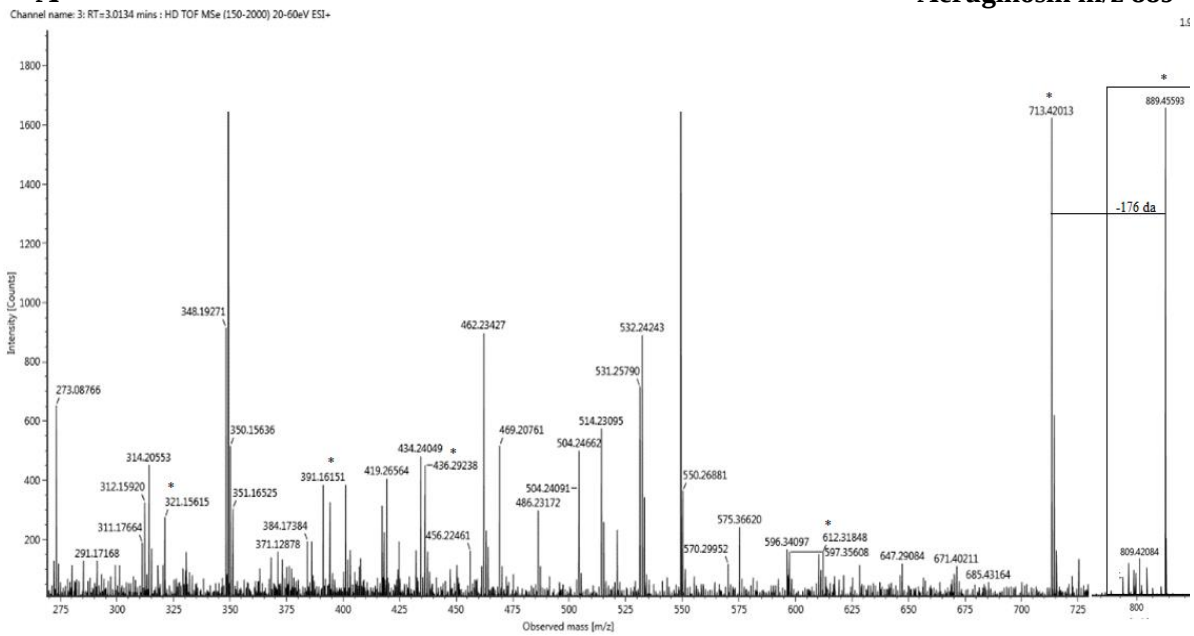

Reference Aeruginosin in Liaimer et al. (2016)

B **Anabaenopeptin m/z 828**

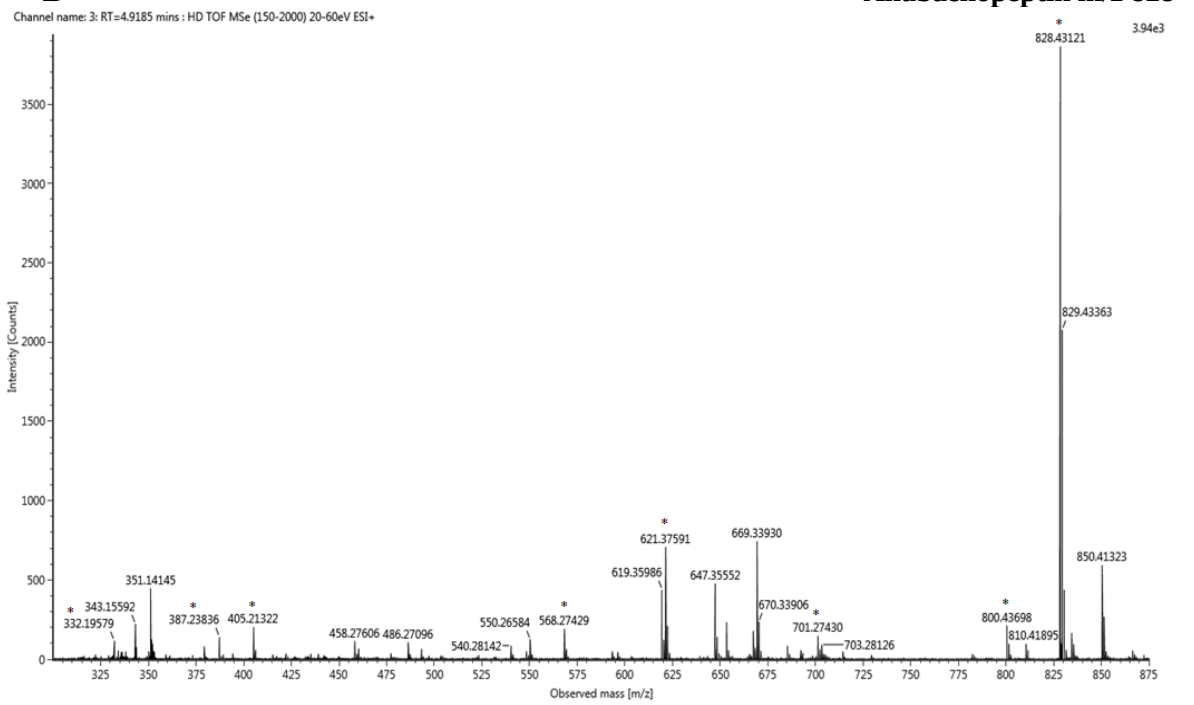

Reference Anabaenopeptin in Guljamow et al. (2017)

C **Nostocyclopeptide m/z 775**

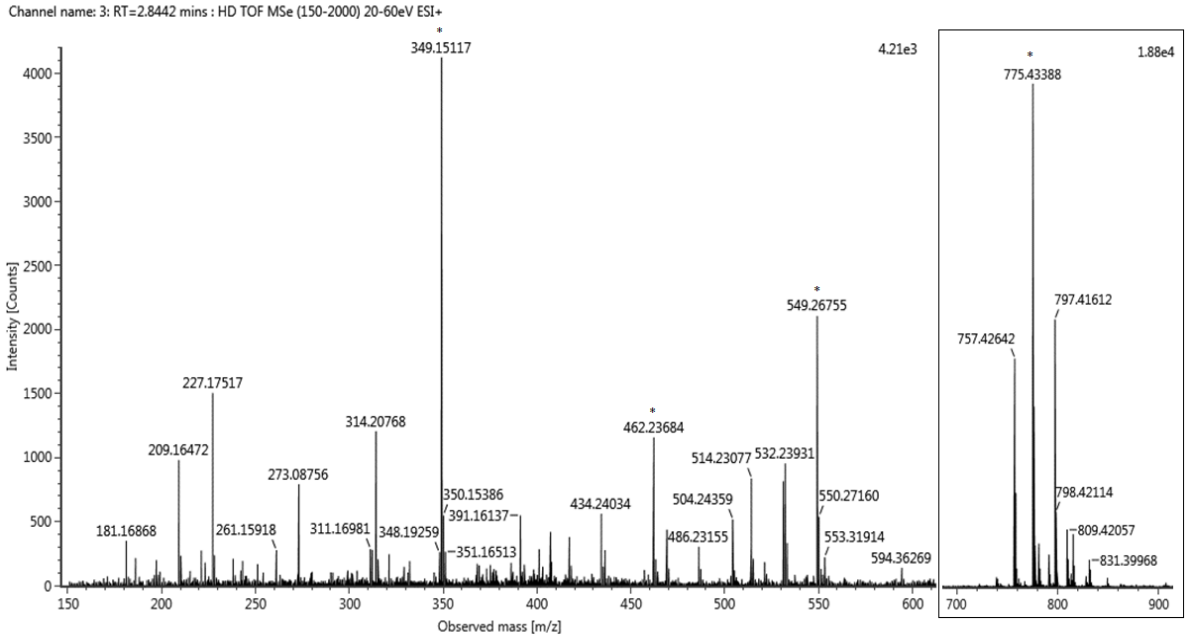

Reference Nostocyclopeptide in Nowruzi et al. (2012)

D **Nostocyclopeptide m/z 809**

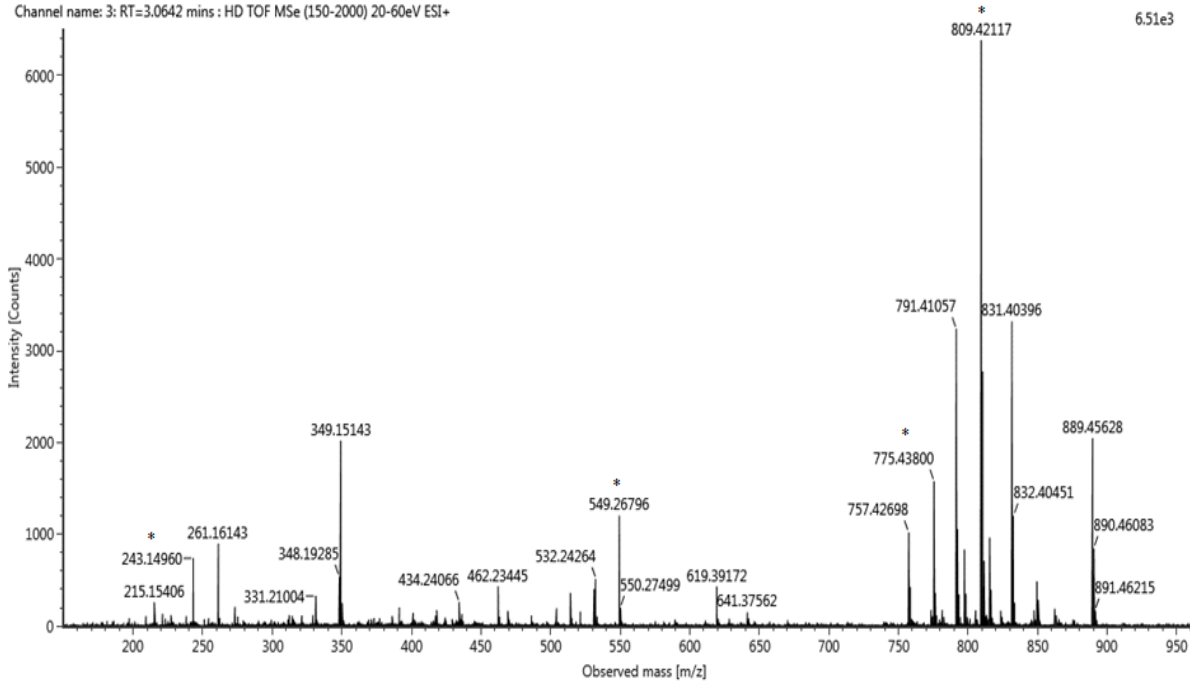

Reference Nostocyclopeptide in Nowruzi et al. (2012)

E **Suomilide*/Banyaside**-like m/z 927**

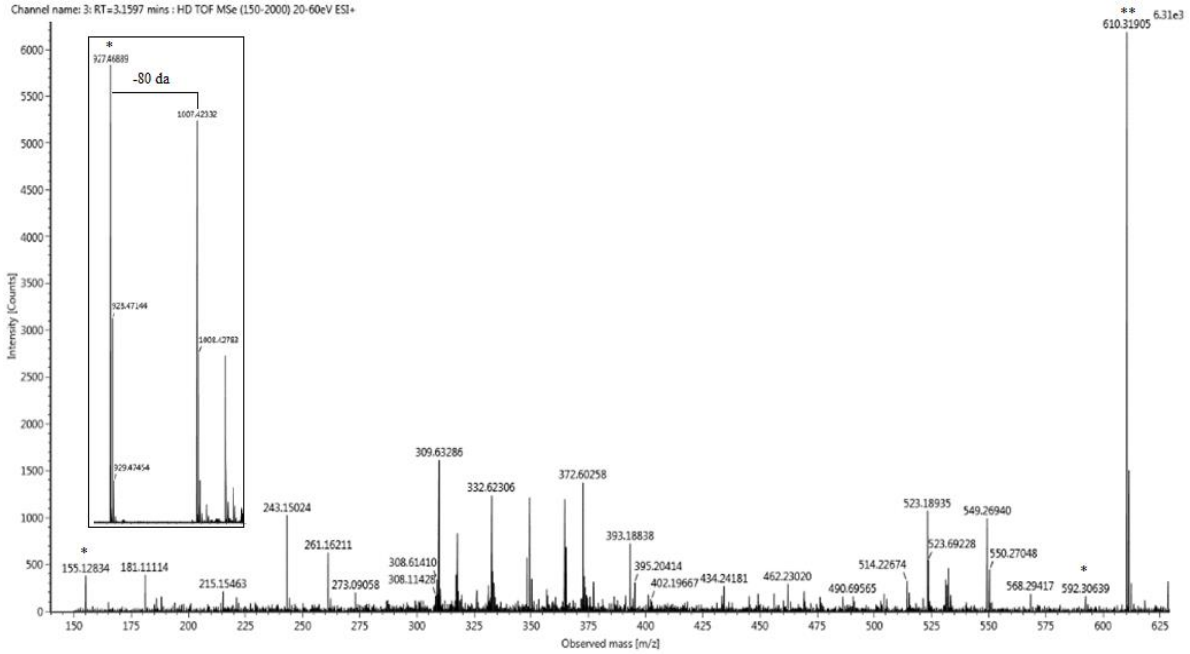

Reference Suomilide in Fujii et al. (2000) and Banyasides in Liaimer et al. (2016); Schindler et al. (2010)

F **Nosperin m/z 564**

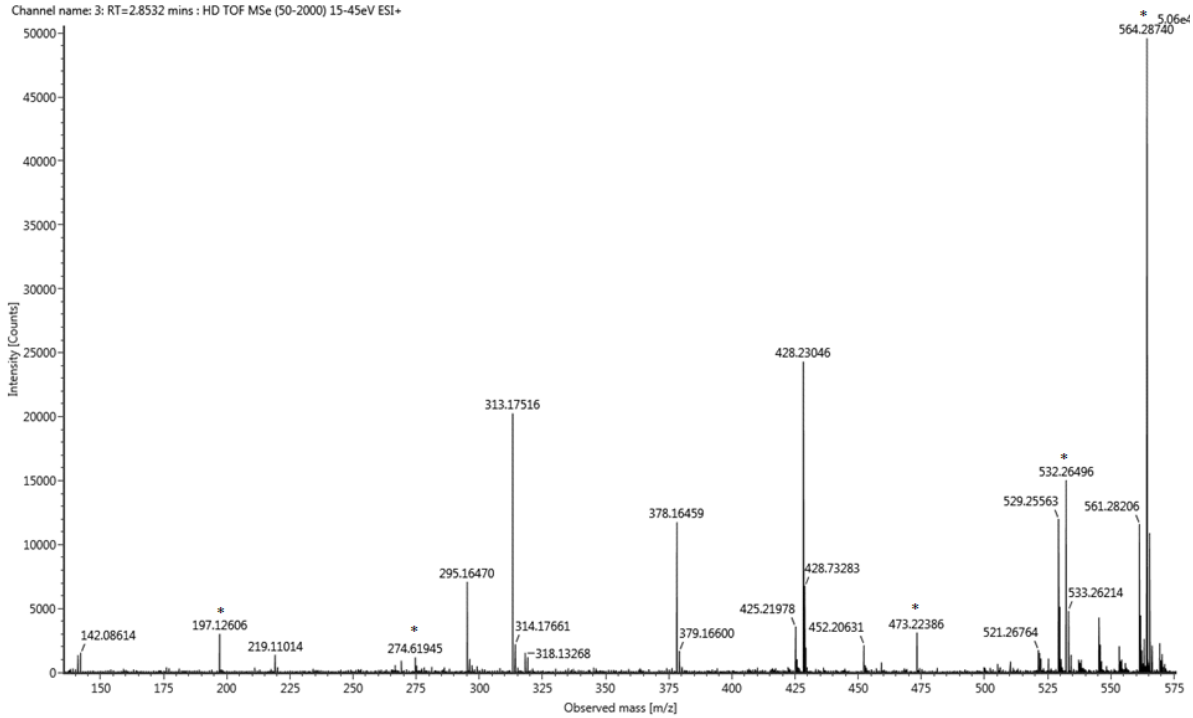

Reference Nosperin in Kampa et al. (2013)